FEDERAL UNIVERSITY OF SANTA CATARINA - UFSC
CHEMICAL ENGINEERING GRADUATE PROGRAM - PÓSENQ
DEPARTMENT OF CHEMICAL AND FOOD ENGINEERING - EQA

José Octávio da Silva Sierra Fernandez

MODELING AND SIMULATION OF THE INDUSTRIAL ACID PICKLING PROCESS WITH HCl: A CHEMICAL REACTOR PHENOMENOLOGICAL APPROACH

Florianópolis
2023

José Octávio da Silva Sierra Fernandez

MODELING AND SIMULATION OF THE INDUSTRIAL ACID PICKLING PROCESS WITH HCl: A CHEMICAL REACTOR PHENOMENOLOGICAL APPROACH

Doctorate thesis for the degree of Doctor in Chemical Engineering presented to the Graduate Program in Chemical Engineering at Federal University of Santa Catarina.
Advisor: Prof. Agenor De Noni Jr., Dr.
Co-advisor: Prof. Luismar Marques Porto, Dr.

Florianópolis

2023

Ficha de identificação da obra elaborada pelo autor,
através do Programa de Geração Automática da Biblioteca Universitária da UFSC.

Fernandez, José Octávio da Silva Sierra
MODELING AND SIMULATION OF THE INDUSTRIAL ACID PICKLING PROCESS WITH HCl: A CHEMICAL REACTOR PHENOMENOLOGICAL APPROACH / José Octávio da Silva Sierra Fernandez ; orientador, Agenor De Noni Jr., coorientador, Luismar Marques Porto, 2023.
167 p.

Tese (doutorado) - Universidade Federal de Santa Catarina, Centro Tecnológico, Programa de Pós-Graduação em Engenharia Química, Florianópolis, 2023.

Inclui referências.

1. Engenharia Química. 2. Steel pickling process. 3. Pickling process simulation. 4. Chemical reactor modelling. 5. Pickling number. I. De Noni Jr., Agenor. II. Porto, Luismar Marques. III. Universidade Federal de Santa Catarina. Programa de Pós-Graduação em Engenharia Química. IV. Título.

José Octávio da Silva Sierra Fernandez

MODELING AND SIMULATION OF THE INDUSTRIAL ACID PICKLING PROCESS WITH HCl: A CHEMICAL REACTOR PHENOMENOLOGICAL APPROACH

This thesis was considered adequate for the degree of Doctor in Chemical Engineering and was approved in its final form by the Graduate Program in Chemical Engineering at Federal University of Santa Catarina.

Examination Board:

Prof.Eduardo Junca, Dr.
University of the Extreme South of Santa Catarina - UNESC

Prof. Natan Padoin, Dr.
Federal University of Santa Catarina - UFSC

Prof. Felipe Fardin Grillo, Dr.
Federal Institute of Espírito Santo - IFES

We certify that this is the **original and final version** of this thesis that was judged adequate to obtain the title of Doctor in Chemical Engineering.

Documento assinado digitalmente
Debora de Oliveira
Data: 10/11/2023 11:19:45-0300
CPF: ***.453.929-**
Verifique as assinaturas em https://v.ufsc.br

Prof. Débora de Oliveira, Dr.
Coordinator of the Graduate Program in Chemical Engineering - PósENQ

Documento assinado digitalmente
Agenor de Noni Junior
Data: 10/11/2023 16:56:58-0300
CPF: ***.980.349-**
Verifique as assinaturas em https://v.ufsc.br

Prof. Agenor De Noni Jr., Dr.
Advisor

Prof. Luismar Marques Porto, Dr.
Co-advisor
Florianópolis, August 15th 2023.

To Camila and Filomena...

Acknowledgements

First, I would like to dedicate this thesis to my wife Camila, for her unconditional, constant support and relaxed way of dealing with life.

I also dedicate this work to my advisors and friends Prof. Dr. Agenor De Noni Jr. and Prof. Dr. Luismar Marques Porto, for their trust, patience, encouragement and excellent guidance. Without their support, this work would not have been possible. To them, my many, many thanks.

I would also like to thank the Graduate Program in Chemical Engineering - PósENQ, for the privilege of attending a program of excellence and internationally recognized.

I am also thankful to GreyLogix Brasil for their support throughout these years of research, especially the colleagues and friends who are part of this journey: Rafael Gonçalves d'Ávila da Silva, Renato Leal, Anderson Ernesto Gonçalves, Bruno Kiyoshi, Leonardo Abreu, Tales Gaspar, Rafaela Bodaneze, Diogo Guebert, Gabriel Ludwig and Renato Pedron Jr. To them and other colleagues who directly or indirectly helped me on this journey, thank you very much.

Special thanks to my fellow chemical engineers and steel pickling specialists Jeferson Rocio de Oliveira and Leonardo Pinez. The technical support and explanations regarding the industrial specificities of this complex physical-chemical operation were enormous. Thank you very much!

Thanks to CAPES - Coordination for the Improvement of Higher Education Personnel, for the financial support granted to me.

Finally, I would like to thank my parents Fernandez and Luzia, and my brothers Victor and João Eduardo, for their encouragement on my journey. I couldn't end this section without thanking Filomena, an *english bulldog* who, even involuntarily, offered me excellent leisure time.

Abstract

Industrial acid pickling process removes iron oxide from steel surfaces. The technique ensures good material finishing to satisfy the most diversified industrial segments. The presence of oxide layers on metal surfaces is caused by hot rolling, a steel manufacturing process performed at 500-900°C. The hot rolling process is followed by atmospheric air cooling. Oxygen and metallic iron combine to generate scale, oxide layers on the material's surface. Acidic solutions are utilized to start a surface reaction that converts oxide to salt and removes these micrometric layers. Due to its fast reaction speed, bath regeneration capacity, and good finishing, hydrochloric acid is the most often utilized chemical agent. Pickling equipment has different designs, but turbulent counter-current has been the most used for 30 years. The technique is to promote hydrochloric acid interaction with a scale-enriched surface, resulting in the generation of $FeCl_2$ and $FeCl_3$. The pickling bath reduces potential when iron II and III ions rise in the solution during the surface reaction. Scientific advancement of this process has been missing in this industry. Steel corporations prioritize the advancement of steel production, restricting chemical processes such as acid pickling to a secondary role. This thesis aims to contribute to the field of chemical engineering by developing equations to compute physicochemical properties of pickling baths, chemical kinetics of pickling, and modeling and simulation of the acid pickling system. This thesis aimed to create a phenomenological mathematical model utilizing a chemical reactor approach to simulate a southern Brazilian plant's industrial process. To obtain information for the industrial process, research was conducted to 1) understand the physicochemical properties of pickling baths as a function of composition and temperature, and 2) create a rate law to represent the dissolution of oxide in acidic environments. To achieve secondary aims, this study presents techniques for computing seven physical parameters of pickling baths: density, vapor pressure, heat of vaporization, specific heat, viscosity, thermal conductivity, and HCl diffusion coefficient. Furthermore, a methodology was employed to evaluate the variation of these characteristics in relation to the composition and temperature across several pickling solutions. Surface maps were created for different operating scenarios and a criterion was designed to simplify concentration and temperature effects. In this research, a phenomenological rate law for solid-liquid chemical pickling kinetics was studied and proposed. The shrinking core model (SCM) was used to build a kinetic expression. Experimental data from the literature was used to determine model parameters. The kinetic rate was validated by comparing it to empirical equations from the literature. Lastly, this thesis presents a phenomenological model of heterogeneous chemical reactors that simulates hydrochloric acid and scale behavior in industrial pickling lines. Regarding the original contributions made by this thesis, the following aspects are particularly notable: 1) A mathematical model of partial differential equations that provides the capability to accurately replicate a turbulent pickling line; 2) The determination of a dimensionless parameter, referred to as the Pickling Number, which serves to quantify the descaling rate; 3) The development of a heterogeneous rate law that can effectively modelling the pickling rate across a pickling tank.

Keywords: Steel pickling process. Pickling process simulation. Chemical reactor modelling. Pickling Number.

Resumo Estendido

O processo industrial de decapagem ácida é uma técnica utilizada com o objetivo de remover camadas de óxido de ferro presentes nas superfícies de aço. A intenção do processo é garantir que o material apresente boas condições de acabamento a fim de atender os mais diversos segmentos industriais. A existência das camadas de óxido na superfície metálica é resultante de um processo de conformação do aço, denominada laminação a quente, realizada com temperaturas entre 500 a 900 °C. Após a operação de laminação uma etapa de resfriamento ocorre através do ar atmosférico. Como resultado da interação entre o oxigênio e ferro metálico, camadas de óxido são formadas na superfície do material as quais são denominadas como carepa. Para a remoção destas camadas micrométricas, geralmente, se faz uso de soluções ácidas com o intuito de promover uma reação de superfície convertendo o óxido a um sal. Industrialmente o agente químico mais utilizado é o ácido clorídrico em função do bom nível de acabamento, elevada velocidade de reação e alta capacidade de regeneração do banho. Do ponto de vista do equipamento de decapagem, muitas são as configurações, todavia a abordagem turbulenta em contra-corrente é a mais adotada nos últimos trinta anos. Em termos operacionais, o processo ocorre promovendo o contato do ácido clorídrico com a superfície enriquecida em carepa; uma reação química de superfície ocorre resultando na formação de $FeCl_2$ e $FeCl_3$. Conforme a reação ocorre sobre a superfície, o banho de decapagem perde seu potencial em função do incremento da concentração de íons de ferro II e III na solução. Por ser contracorrente, os banhos com maior concentração de ácido entram em contato com a superfície que deixa o sistema, *i.e.*, o último tanque. Já a solução com baixa concentração entra em contato com o material novo, o qual é inserido no primeiro tanque do sistema. Ao longo dos tanques, um cascateamento é feito transferindo os banhos entre os estágios. Sempre do mais concentrado em termos de HCl para o menor. Com respeito as configurações térmicas dos diferentes tanques, industrialmente, opera-se com temperaturas variando de 65 a 85 °C. Em função da composição química dos banhos e das temperaturas de operação, a operação torna-se um ambiente propício à evaporação. Com respeito ao desenvolvimento científico deste processo, este segmento industrial é bastante carente. Haja vista que as indústrias siderúrgicas focam no desenvolvindo do aço - produto principal; em outras palavras, processos químicos como a decapagem ácida são tratadas em segundo plano. Motivado pelo pouco desenvolvimento deste setor esta tese foi desenvolvida com o objetivo de agregar contribuições da área de engenharia química, a saber: *desenvolvimento de equações consitutivas para computar propriedades físico-químicas dos banhos de decapagem*, *cinética química de decapagem* e *modelagem e simulação do sistema de decapagem ácida*. O objetivo central desta tese foi o de desenvolver um modelo matemático fenomenológico utilizando uma abordagem de reatores químicos para simular o processo industrial de uma planta sediada no sul do Brasil. Para tal, foi requerido desenvolver pesquisas com o objetivo de obter informações relavantes ao processo industrial, *i.e.*, 1) conhecer o comportamento das principais propriedades físico-químicas dos banhos de decapagem como função de composição e temperatura e 2) desenvolver uma lei de velocidade capaz de representar a taxa com que o óxido é degrado em meio ácido. Em função destes objetivos secundários este trabalho contempla um capítulo dedicado a apresentar métodos para computar sete principais propriedades físicas dos banhos de decapagem, a saber: massa específica, pressão de vapor, calor de evaporação, calor específico, viscosidade, condustividade térmica e difusão mássica de HCl. Além disso, incluíu-se uma abordagem para analisar o nível de variação destas propriedades em relação a composição e temperatura ao longo dos diferentes banhos de decapagem. Como resultado mapas de

superfície foram gerados para diferentes condições operacionais e um critério foi estabelecido a fim de permitir simplificações das infuências da concentração e temperatura. Com respeito a cinética química de decapagem, um capítulo desta tese foi dedicado ao estudo e proposição de uma lei de velocidade fenomenológica capaz de relacionar a fase sólida e líquida. O método do núcleo não reagido foi adotado a fim de construir uma lei de velocidade. Dados experimentais disponíveis na literatura foram utilizados para obter parâmetros do modelo proposto. Uma validação foi feita comparando a expressão cinética desenvolvida com equações empíricas disponíveis na literatura. Por fim, o terceiro e principal capítulo desta tese é dedicado a apresentar um modelo fenomenológico, típico de reatores químicos heterogêneos, a fim de simular o comportamento do ácido clorídrico e carepa ao longo de uma série de quatro tanques de decapagem. A ideia foi reproduzir a operação de uma unidade industrial sediada no sul do Brasil. O modelo levou em conta o efeito da evaporação ao longo dos banhos, bem como o efeito da recirculação individual de banhos em cada tanque. Com base no modelo, uma validação preliminar foi realizada comparando as velocidades máximas de operação simuladas com a velocidade de projeto do equipamento industrial. Em termos de contribuições originais desta tese destacam-se: 1) Modelo matemático de equações diferenciais parciais capaz de reproduzir uma linha de decapagem turbulenta; 2) Identificação de um grupo adimensional que caracteriza a velocidade de decapagem ácida, denominado como Número de Decapagem, 3) Desenvolvimento de uma lei de velocidade heterogêna capaz de simular a velocidade de decapagem ao longo de um sistema físico. As contribuições desenvolvidas nesta tese, consistem em contribuições na área de conhecimento da engenharia química aplicada a um processo industrial típico da metalurgia. Apesar das contribuições, é importante salientar que o trabalho desenvolvido foi teórico, *i.e.*, não foi desenvolvido experimentos em laboratório a fim de validar as leis de velocidade, bem como a consistência das equações constitutivas das propriedades físico-químicas. Apesar disso, o trabalho fez uso de informações industriais de projeto e operação de uma planta real e, baseada em condições de entrada bem definidas, verificou-se a consistência das informações calculadas pela ferramenta de cálculo. Em especial: Composições ao longo dos banhos, velocidades nominais de operação e temperaturas ao longo dos banhos. Todas os resultados demonstraram um excelente nível de consistência do simulador com as faixas praticadas e reportadas em manuais de operação desta indústria.
Palavras-chave: Processo de decapagem do aço. Simulação do processo de decapagem. Modelagem de reator químico. Número de Decapagem.

List of Figures

List of Tables

List of abbreviations and acronyms

ARP	Acid Regeneration Plant
BFD	Block Flow Diagram
CFD	Computational Fluid Dynamics
CV	Coefficient of Variation
DCS	Distributed Control System
FTCS	Forward Time-Centered Space
HCT	High Coil Temperature
IEC	International Electrotechnical Commission
JMA	Johnson-Mehl-Avrami
LCT	Low Coil Temperature
MV	Material Variation
NFPA	National Fire Protection Agency
OSHA	Organization Safety and Health Administration
PDE	Partial Differential Equation
PFR	Plug Flow Reactor
R&D	Research & Development
SBU	Stretch Bending Unit
SCM	Shrinking Core Model
TV	Temperature Variation

LIST OF SYMBOLS

$\overline{v}_{app,i}$	Specific volume of generic "i" water-soluble electrolyte, $m^3 \cdot kg^{-1}$
x_i	Generic "i" water-soluble electrolyte component mass fraction, –
T	Temperature, °C
c_0	Laliberte & Cooper (2004) first empiral constant, $kg \cdot m^{-3}$
c_1	Laliberte & Cooper (2004) second empiral constant, $kg \cdot m^{-3}$
c_2	Laliberte & Cooper (2004) third empiral constant, –
c_3	Laliberte & Cooper (2004) fourth empiral constant, $°C^{-1}$
c_4	Laliberte & Cooper (2004) fifth empiral constant, °C
ρ	Pickling solution density, $kg \cdot m^{-3}$
$P_{vap,HCl}$	HCl vapor pressure, Pa
M_{HCl}	HCl molar mass, $kg \cdot mol^{-1}$
R	Ideal gas constant, $Pa \cdot m^3 \cdot (kmol \cdot K)^{-1}$
x_{HCl}	HCl mass fraction, –
x_{FeCl_2}	$FeCl_2$ mass fraction, –
P_{vap,H_2O}	H_2O vapor pressure, Pa
$\Delta H_{v,i}$	Evaporation heat of a generic compound "i", $J \cdot mol^{-1}$
$P_{vap,i}$	Vapor pressure of a generic compound "i", Pa
ΔH_v	Pickling solution evaporation heat, $J \cdot mol^{-1}$
$\Delta H_{v,HCl}$	HCl evaporation heat, $J \cdot mol^{-1}$
$\Delta H_{v,H_2O}$	H_2O evaporation heat, $J \cdot mol^{-1}$
z_{HCl}	HCl molar fraction, -
z_{FeCl_2}	$FeCl_2$ molar fraction, -
c_p	Pickling solution specific heat, $kJ \cdot (kg \cdot K)^{-1}$
x_{H_2O}	H_2O mass fraction, -
c^*_{p,H_2O}	Liquid H_2O molar specific heat, $J \cdot (mol \cdot K)^{-1}$
a_1	Laliberte (2009) first empirical constant, $kJ \cdot (kg \cdot K)^{-1}$
a_2	Laliberte (2009) second empirical constant, $°C^{-1}$
a_3	Laliberte (2009) third empirical constant, -
a_4	Laliberte (2009) fourth empirical constant, -
a_5	Laliberte (2009) fifth empirical constant, $kJ \cdot (kg \cdot K)^{-1}$
a_6	Laliberte (2009) sixth empirical constant , -
$c_{p,i}$	Specific heat of water-soluble electrolyte, $kJ \cdot (kg \cdot K)^{-1}$
η_{H_2O}	Liquid water viscosity, mPa·s
η_i	Water-soluble electrolyteviscosity, mPa·s
$v_{1,i}$	Laliberte (2007) first empirical constant, -
$v_{2,i}$	Laliberte (2007) second empirical constant, -
$v_{3,i}$	Laliberte (2007) third empirical constant, -
$v_{4,i}$	Laliberte (2007) fourth empirical constant, $°C^{-1}$
$v_{5,i}$	Laliberte (2007) fifth empirical constant, $(mPa \cdot s)^{-1}$
$v_{6,i}$	Laliberte (2007) sixth empirical constant, -
k	Pickling solution thermal conductivity, $W \cdot (m \cdot K)^{-1}$
f	Water thermal conductivity ratio, -
α_i	McLaughlin (1964) constant for generic "i" ion, $W \cdot (m \cdot K)^{-1} \cdot (L \cdot mol^{-1})$
C_i	Molar concentration for generic "i" ion, $mol \cdot L^{-1}$
$\mathcal{D}_\infty$	HCl diffusion coefficient in water infinite solution, $cm^2 \cdot s \cdot^{-1}$
λ_+	Equivalent cationic conductivities, $ohm \cdot eq. \cdot^{-1}$
λ_-	Equivalent anionic conductivities, $ohm \cdot eq. \cdot^{-1}$
z_+	Cationic charge of dissociated electrolyte , -
z_-	Anionic charge of dissociated electrolyte , -

m_{HCl}	HCl molar concentration per water weight, mol·kg^{-1}
Γ	HCl thermodynamic coefficient, -
γ_{HCl}	HCl activity coefficient, -
I	Ionic strength , mol·kg^{-1}
t	Time , s
ρ^*_{FeO}	Scale molar density , mol·m^{-3}
V	Scale control volume , m^3
r_{FeO}	FeO descaling rate , mol·(m^3·s)$^{-1}$
S	Surface area of scale cross section , m^2
e	Scale thickness , m
e_0	Initial scale thickness , m
r_{HCl}	HCl pickling rate , mol·(m^3·s)$^{-1}$
Ea	Activation energy , J·mol^{-1}
C_{HCl}	HCl molar concentration in liquid phase , mol·m^{-3}
m	Exponent of the pickling rate law , –
k_0	Pickling rate frequency factor , mol$^{0.14}$·(m$^{0.42}$·s)$^{-1}$
X	Pickled fraction , –
N_{HCl}	HCl molar flux , mol·(m^2·s)$^{-1}$
r'_{HCl}	HCl pickling rate per surface area , mol·(m^2·s)$^{-1}$
u	Pickling line speed , m·s^{-1}
$\Theta_{\frac{FeO}{HCl}}$	HCl and FeO Stoichiometric ratio , –
e_{in}	Scale thickness at the pickling tank inlet , m
e_s	Steel strip thickness , m
z	Axial position towards the steel strip , m
ρ_s	Steel density, kg·m^{-3}
$c_{p,s}$	Steel specific heat , kJ·(kg·K)$^{-1}$
T_b	Liquid phase temperature , K
T_s	Strip temperature , K
$T_{s,in}$	Strip temperature at the pickling tank inlet , K
$T_{s,0}$	Strip temperature at time zero , K
$\Delta H_{rx.}$	Heat of reaction , kJ·mol^{-1}
λ	Liquid-solid convective heat transfer coefficient , W·(m^2·K)$^{-1}$
τ	Dimensionless time , –
ζ	Dimensionless length , –
ψ	Dimensionless concentration , –
θ	Dimensionless temperature , –
L	Pickling tank length , m
$C_{HCl,tk}$	HCl molar concentration in liquid phase at tank's inlet , mol·m^{-3}
Da	Modified Damkohler number , –
Da_T	Thermal Damkohler number , –
Arr	Arrhenius number , –
St	Stanton number , –
γ	Dimensionless relationship between pickling bath and steel volumetric heat capacity , –
s	Dimensionless relationship between scale and steel thickness , –
Φ	Dimensionless relationship between reactor length and steel thickness , –
ρ_{tk}	Tank's pickling density, kg·m^{-3}
$c_{p,tk}$	Tank's pickling specific heat , kJ·(kg·K)$^{-1}$
μ_{tk}	Tank's pickling viscosity , mPa·s^{-1}
$C_{HCl,tk}$	Tank's pickling HCl molar concentration in liquid phase , mol·m^{-3}
k_{tk}	Tank's pickling solution thermal conductivity , W·(m·K)$^{-1}$
W	Scale amount , kg·m^{-2}
Re	Reynolds number , –
Pr	Prandtl number , –

Nu	Nusselt number , –
T	Temperature, °C
$\Delta H_{v,i}$	Heat of vaporization of a generic compound "i", J·mol^{-1}
T	Temperature in liquid phase, K
R	Ideal gas constant, Pa·m^3·(mol·K)$^{-1}$
$\Delta H_{v,i}$	Pickling solution evaporation heat, J·mol^{-1}
c_p	Pickling solution specific heat , kJ·(kg·K)$^{-1}$
x_{H_2O}	H_2O mass fraction , -
c^*_{p,H_2O}	Liquid H_2O molar specific heat , J·(mol·K)$^{-1}$
a_1	Laliberte (2009) first empirical constant , kJ·(kg·K)$^{-1}$
a_2	Laliberte (2009) second empirical constant , °C^{-1}
a_3	Laliberte (2009) third empirical constant , -
a_4	Laliberte (2009) fourth empirical constant , -
a_5	Laliberte (2009) fifth empirical constant , kJ·(kg·K)$^{-1}$
$c_{p,i}$	Specific heat of water-soluble electrolyte , kJ·(kg·K)$^{-1}$
η_{H_2O}	Liquid water viscosity , mPa·s
η_i	Water-soluble electrolyte viscosity , mPa·s
$v_{1,i}$	Laliberte (2007) first empirical constant , -
$v_{2,i}$	Laliberte (2007) second empirical constant , -
$v_{3,i}$	Laliberte (2007) third empirical constant , -
$v_{4,i}$	Laliberte (2007) fourth empirical constant , °C^{-1}
$v_{5,i}$	Laliberte (2007) fifth empirical constant , (mPa·s)$^{-1}$
$v_{6,i}$	Laliberte (2007) sixth empirical constant , -
k	Pickling solution thermal conductivity , W·(m·K)$^{-1}$
f	Water thermal conductivity ratio , -
C_i	Molar concentration for generic "i" ion , mol·L^{-1}
X_i	Initial pickled fraction at time zero , –
X_0	Inlet pickled fraction , –
u_z	Pickling line speed , m·s^{-1}
$u_{z,design}$	Design pickling line speed , m·s^{-1}
e_L	Liquid film thickness , m
T_i	Liquid phase temperature at time zero , K
T_0	Liquid phase temperature at pickling tank inlet , K
ψ	Dimensionless concentration in bulk phase , –
θ	Dimensionless temperature in liquid phase , –
θ_s	Dimensionless temperature in solid phase, –
C_{HCl}	HCl molar concentration in liquid phase , mol·m^{-3}
$C_{HCl,0}$	HCl molar concentration in liquid phase at tank's inlet , mol·m^{-3}
$C_{HCl,i}$	Initial HCl molar concentration in liquid phase , mol·m^{-3}
St	Thermal Stanton number , –
Φ	Dimensionless relationship between liquid film and steel thickness , –
ρ	Tank's pickling density, kg·m^{-3}
ρ_{ARP}	Acid regenerated density from ARP, kg·m^{-3}
c_p	Tank's pickling specific heat , kJ·(kg·K)$^{-1}$
W	Strip width , m
Pe	Peclet number , –
Pe_T	Thermal Peclet number , –
Q_r	Recirculating acid flowrate in each pickling tank , m^3·s^{-1}
$\mathcal{D}_{eff.}$	Dispersion coefficient , m^2·s^{-1}
D_{HCl}	HCl diffusion coefficient ionic solution , m^2·s^{-1}
α	Thermal diffusion coefficient in liquid phase , m^2·s^{-1}
$\dot{q}_{04N}$	Generic recycling volumetric flow rate in pickling stage "N" , m^3·s^{-1}

$\dot{q}_{ARP}$ Volumetric flow rate from Acid Regeneration Plant (ARP) , $m^3 \cdot s^{-1}$
R Recycling ratio for each pickling tank , -
η_{design} HCl global efficiency in pickling process , -
$\dot{m}_{ARP}$ Mass flow rate from Acid Regeneration Plant (ARP) , $kg \cdot s^{-1}$
$\dot{m}_{07N}$ Stationary evaporated mass flow rate from a generic stage "N" , $kg \cdot s^{-1}$
$\dot{m}_{ev.,i}$ Generic mass flow-rate evaporated , $kg \cdot s^{-1}$
$P_{VAP.,I}$ Vapor pressure of a generic solute "i" , Pa
P_i Partial pressure of a generic solute "i" , Pa
$\dot{n}_{ev.,i}$ Generic molar flow-rate evaporated , $mol \cdot s^{-1}$
$k_{ev.,i}$ Convective mass transfer coefficient of generic solute "i" between the liquid and gas phase , $m \cdot s^{-1}$
$k_{ev.,HCl}$ Convective mass transfer coefficient of HCl between the liquid and gas phase , $m \cdot s^{-1}$
$k_{ev.,H_2O}$ Convective mass transfer coefficient of H_2O between the liquid and gas phase , $m \cdot s^{-1}$
$A_{sprk.}$ Sprinklers' surface area , m^2
x_i Generic solute "i" molar fraction in liquid phase , -
y_i Generic solute "i" molar fraction in gas phase , -
M_i Generic solute "i" molar mass , $kg \cdot mol^{-1}$
M_{H_2O} Water molar mass , $kg \cdot mol^{-1}$
$V_{chamber}$ Pickling tank chamber volume , m^3
$y_{HCl,3}$ HCl molar fraction in gas phase , -
$P_{VAP.,HCl,1}$ HCl vapor pressure in liquid phase , Pa
$x_{HCl,1}$ HCl molar fraction in liquid phase , -
$\dot{n}_1$ Liquid molar flow in a sprinkler , $mol \cdot s^{-1}$
$y_{H_2O,3}$ H_2O molar fraction in gas phase , -
$P_{VAP.,H_2O,1}$ H_2O vapor pressure in liquid phase , Pa
$x_{H_2O,1}$ H_2O molar fraction in liquid phase , -
$y_{H_2O,2}$ H_2O molar fraction in atmospheric condition , -
P_2 Atmospheric pressure , Pa
P_3 Chamber suction pressure , Pa
T_2 Ambient temperature , K
T_3 Chamber temperature , K
$\varphi_{ev.}$ Liquid evaporated fraction , -
γ_2 Air permeability through the equipment gasket , $kg \cdot (m^2 \cdot s)^{-1}$
γ_2^* Modified air permeability through the equipment gasket , $kg \cdot (m^2 \cdot s \cdot Pa^{0.5})^{-1}$
$y_{O_2,2}$ O_2 molar fraction in atmospheric condition , -
$y_{O_2,3}$ O_2 molar fraction in gas phase , -
$y_{N_2,2}$ N_2 molar fraction in atmospheric condition , -
$y_{N_2,3}$ N_2 molar fraction in gas phase , -
V_t Pickling tank volume , m^3
$\dot{q}_3$ Outlet gas volumetric flow , $m^3 \cdot s^{-1}$
V_L Discharged liquid volume , m^3
ρ_l^* Liquid molar density , $mol \cdot m^{-3}$
$c_{p,l}$ Liquid specific heat , $kJ \cdot (mol \cdot K)^{-1}$
ΔH_v Liquid evaporation heat , $kJ \cdot mol^{-1}$
C_V Gas flow hydraulic constant , $m^3 \cdot (s \cdot Pa^{0.5})^{-1}$
d_3 Gas duct internal diameter , m
K Head loss kinetic fitting constant , -
P_{vent} Absolute pressure in the gas outlet duct , Pa
$N_{sprk.}$ Sprinklers number in a pickling tank , -

$A^{*}_{sprk.}$	Triangular surface area from one sprinkler , m^2
a	Perpendicular distance between the sprinkler jet outlet and the metallic surface of the surface. , m
b	Parallel distance between the liquid attack point on the surface and the shower exit point , m
c	Hypotenuse between distances a and b. , m
l	Length of the base of the right triangle , m
$\hat{B}$	Angle formed between a and b. , -
$\hat{C}$	Angle formed between l and c. Assuming a right triangle. , -
μ	Pickling solution viscosity , Pa·s
κ	Molar ratio between the scale amount and the molar concentration of HCl, -
T	Temperature in liquid phase, K
R	Ideal gas constant, $Pa \cdot m^3 \cdot (mol \cdot K)^{-1}$
$\Delta H_{v,i}$	Pickling solution evaporation heat, $J \cdot mol^{-1}$
a_5	Laliberte (2009) fifth empirical constant , $kJ \cdot (kg \cdot K)^{-1}$
$c_{p,i}$	Specific heat of water-soluble electrolyte , $kJ \cdot (kg \cdot K)^{-1}$

Contents

1 INTRODUCTION: WHAT IS THIS THESIS ABOUT?

Typically in industrial steel rolling processing plants, a series of mechanical and chemical operations are required to ensure that the materials, for example a steel flat coil, conform to technical standards and market requirements.

Despite mechanical transformation operations being the majority, chemical unit operations have an important role in the material's production process. In particular, the pickling operation stands out.

The pickling operation consists of a process of removing layers of iron oxide, known as scale, from the surface of the metallic material. This operation is necessary depending upon the hot rolling process, in which metal is shaped at elevated temperatures in an open environment. The result of high surface temperatures and direct contact with the atmospheric environment results in micro-metric layers of iron oxide.

There are many processes capable of removing scale from the surface of steel, namely: mechanical pickling (sandblasting), acid or alkaline pickling, electrochemical, and even the reduction of oxide by reaction with gaseous H_2. Despite so many options, industrially the acid pickling processes using HCl and H_2SO_4 stand out.

Shreve (1997) reports that for a long time, especially in the 1970s and 1980s, consumption of HCl and H_2SO_4 was considered an indicator of a country's development as they are directly related to steel production, in this case, acid pickling. Even today this indicator is relevant; after all, steel continues to be a widely used raw material and is the basis of industrialization in any country. In this context, the search of more efficient solutions for steel production with reduced input consumption is a pertinent area of study within the current Brazilian industrial scenario.

Steel conglomerates prioritize Research & Development (R&D) in areas closely associated with Material Engineering due to their production of steel as their main product. That is, areas that aim to improve the intrinsic properties of the product. On the other hand, the physicochemical process that involves the acid pickling of steel is treated as a secondary activity, in terms of investments in R&D. Thus, the development of this area of knowledge is somewhat dependent on centuries-old process technology companies. Which are not always interested in publishing their *know-how*.

Due to this limitation, this study was developed with the aim of applying some process engineering applications to the industrial process of pickling steel using HCl. Throughout the literature review stage, it became somewhat clear that this segment had no contributions from the chemical engineering knowledge area. In particular in:

- *Thermodynamics*: constitutive equations to evaluate the behavior of ionic pickling solutions as function of temperature and concentration;
- *Chemical Kinetics*: velocity laws able to relate the influences of the liquid and solid

phase. Non-catalytic heterogeneous reactions;

- *Phenomenological Modelling*: in particular, with regard to mathematical models of chemical reactors.

Throughout the research it was noted that the chemical reaction approach is somewhat applicable to the acid pickling operation. Some adaptations and abstractions were necessary. However, it was observed that models of heterogeneous dispersion reactors can represent and predict the physics of the process. A topic of significant importance within the industrial sector. Whether in the early stages of conceptual design or in the improvement of existing plants.

Through this assessment, it becomes feasible to contemplate the potentiality of making a scientific contribution to this field of understanding by suggesting a chemical reactor model that is tailored to suit the acid pickling process. In order to effectively navigate this journey, it is important to have a comprehensive understanding on the physicochemical properties and reaction behavior associated with scale dissolution in HCl.

Due to the aforementioned necessity, this research was undertaken to provide significant contributions in various fields, namely: 1) Thermodynamics of solutions; 2) Chemical kinetics; and 3) Modelling and Simulation of Chemical Processes. The entire work was developed theoretically, without the use of experiments. A case study was developed using industrial information from a manufacturing plant located in southern Brazil.

1.1 Aims of this study

Based on the current problem involving the industrial process of acid pickling using HCl, this thesis aims to make a contribution to this particular field by addressing a series of concerns that are categorized into three distinct areas. 1) Constitutive models of physicochemical properties of pickling baths; 2) Non-catalytic heterogeneous chemical kinetics; and 3) Phenomenological mathematical modelling . The following questions are presented below:

1. Pickling baths are characterized as ionic solutions with a high level of complexity in terms of their thermophysical behavior. Regarding to the physicochemical properties of pickling solutions:

    a) How does the temperature and concentration of $FeCl_2$ and HCl interfere with the main physicochemical properties of pickling baths?

    b) Based on the dependency level, is it possible to create a criterion to define which of the parameters are more prevalent in relation to the other?

2. In steelmaking, empirical expressions are used to estimate the time required for a material to be pickled. Typically, it is not possible to identify the relationship of these parameters with thermodynamic, phenomenological, physical-chemical and kinetic properties. Regarding the rate law applied to pickling lines:

a) Is there any number or group of dimensionless numbers capable of characterizing the rate law or pickling kinetic of different materials?

b) Could the models that have been developed as a function of these dimensionless groups demonstrate reliability in accordance with the existing literature?

3. Industrial pickling plants are designed and built based on know-how from previous projects and pilot plants. Phenomenological models, typical of Chemical Engineering, have not yet been applied to this type of process. Regarding the use of Differential Equations models applied to Turbulent Stripping Lines:

a) Can a PDE system be applied, and is it consistent with the operating conditions of an industrial pickling line using HCl as a pickling agent?

b) Based on the mathematical model, what is the level of interference of the evaporation of HCl on the performance of the maximum operating speed of an industrial line?

1.2 Structure of this thesis

This thesis was structured in five chapters. The first of them, titled Chapter 1, presents the general context of the work, bringing out the main objectives/questions of research that we seek to answer. The next three chapters are structured in the format of three different scientific papers.

Chapter 2 presents a methodological approach to compute different physicochemical properties of acid pickling baths with HCl. This chapter is based on the article entitled: "Semi-quantitative method for categorizing the effect of composition and temperature on HCl solutions used in acid pickling processes", which will be submitted to specialized journals in the field of chemical engineering, by José Octávio Fernandez, Diogo Guebert, Luismar M. Porto and Agenor De Noni Jr. The main intention of this paper is to contribute with theoretical methods to evaluate the influence of composition (HCl and $FeCl_2$) and temperature of acid pickling baths for the following physicochemical properties: density, vapor pressure, heat of evaporation, specific heat, viscosity, thermal conductivity and mass diffusion of HCl. In addition to the calculation method, a semi-quantitative approach based on IEC 61508 and 61511 risk matrices was developed to classify the influence of the composition and temperature of the pickling baths along the different process tanks.

In Chapter 3, a kinetic study of the pickling process based on information from the literature was developed. As a rule, the phenomenological approach of the shrinking core model (SCM) was used to present a heterogeneous rate law - characteristic of Chemical Reaction Engineering. This chapter is based on the paper entitled: "Kinetic and phenomenological modelling to estimate maximum speeds of pickling lines using dimensionless numbers: a typical chemical reactor engineering approach", which will be submitted to specialized journals in the field of chemical engineering, by José Octávio Fernandez, Diogo Guebert, Luismar M.

Porto and Agenor De Noni Jr. The idea of the paper is to fill a gap present in the scientific literature regarding the speed law of pickling lines. Predominantly, empirical equations are adopted to solve this demand. Furthermore, a model of Partial Differential Equations was applied to the solid phase in order to evaluate the consistency of the obtained rate law. Dimensionless numbers have been identified, for example the Pickling Number. The developed kinetic expression was compared with other equations found in the scientific literature.

Chapter 4 was developed with the intention of contributing scientifically with a phenomenological model, chemical reaction engineering approach, applied to the turbulent acid pickling process. This chapter is based on the paper entitled: "Modelling and simulation of the industrial acid pickling process with HCl: a chemical reactor phenomenological approach", which will be submitted to specialized journals in the field of chemical engineering, by José Octávio Fernandez, Diogo Guebert, Luismar M. Porto and Agenor De Noni Jr. It is important to mention that this article, its title in particular, names the thesis and best characterizes the work developed. Regarding the article, the idea was to propose a model of Partial Differential Equations applied in the different control volumes, *i.e.*, solid, liquid and gas phase of a pickling system with the objective of: 1) designing new industrial units pickling process and 2) evaluating different operating scenarios. This paper uses all the tools developed in previous papers, and thus directly presents the interconnection between the chapters of this work.

Chapter 5 presents the essence of this document, that is, a concise analysis of what was discussed in chapters 2-4 and what to expect from future work. This section aims to concatenate the ideas developed in previous chapters and provide the reader with a global view of the research, *i.e.*, the real meaning of the proposed contributions.

Finally, a section with the bibliographic references used in this is presented at the end. In addition, three Appendices A, B and C contain supplementary material related to Chapter 2 and 3.

It is important to point out that the bibliographic revisions required for each of the researches carried out are presented in their respective chapters.

2 Semi-quantitative method for categorizing the effect of composition and temperature on HCl solutions used in acid pickling processes

General note

This chapter will serve as the basis for the paper entitled "Semi-quantitative method for categorizing the effect of composition and temperature on HCl solutions used in acid pickling processes", which will be submitted to specialized journals in the field of chemical engineering, by José Octávio Sierra Fernandez, Diogo Guebert, Luismar M. Porto and Agenor De Noni Jr. Abstract, keywords, acknowledgements and references were omitted. It should be noticed that some minor amendments were performed in the text presented herein, but the methodology, results and conclusions reported in the original paper submitted were not essentially affected.

2.1 Introduction

Pickling baths are acidic or basic solutions formulated to remove, via chemical reaction, layers of iron oxides (scale) from metallic surfaces, primarily steel (MAANONEN, 2014). Industrially, acidic pickling solutions, including H_2SO_4, H_3PO_4, HNO_3, HF and HCl, are used for their shorter residence times (LI et al., 2005). The carbon steel pickling process generally utilizes sulfuric and hydrochloric acids as the predominant acid solutions, despite the availability of other acid options.

Kladnig (2008) reported several advantages associated with the utilization of hydrochloric acid (HCl) solutions in comparison to sulfuric acid (H_2SO_4): 1) faster iron oxide dissolution; 2) smoother surfaces with superior finishing; 3) reaction rate roughly 10 times faster when compared under the same thermodynamic conditions; and 4) regeneration capability of approximately 99%. In contrast, Hudson (1994) identified excessive acid fume production as the primary disadvantage of hydrogen chloride application. Regardless, hydrochloric acid solutions are the most used in industrial pickling operations.

Given the extensive utilization of hydrochloric acid (HCl), the aim of this work is to propose a computational approach to evaluating and categorizing (in terms of concentration and temperature dependency) its physicochemical properties that are relevant to industrial processes, namely density, vapor pressure, heat of vaporization, specific heat capacity, viscosity, thermal conductivity, and HCl diffusion coefficient. The mathematical methodology employed for determining these properties was developed based on information obtained from existing literature. It is assumed that each property is dependent on both the composition of the system, namely the presence of hydrochloric acid (HCl) and ferrous chloride ($FeCl_2$), as well as the temperature. Table 1 provides engineering applications for each of the investigated properties.

The concentration of HCl and $FeCl_2$ affects the properties of acid pickling solutions. The countercurrent arrangment of industrial steel pickling process exposes the surface with

Table 1 – Some physicochemical properties of hydrochloric acid pickling solution have engineering applications.

Physicochemical properties	**Engineering applications**
Density	Design parameter for handling, storage and transportation facilities
Vapor pressure	Design parameter for fume system and operation limits for pumping system
Heat of vaporization	Material and Energy Balance; design parameter for fume system
Specific heat capacity	Material and energy balance parameter; design heat exchanger system
Viscosity	Design parameter for handling, storage and transportation facilities
Thermal conductivity	Design heat exchanger system
HCl diffusion coefficient	Calculations of mass transfers coefficients applied to gas-liquid systems

lower scale density to chemically more aggressive solutions, and the opposite occurs in the steel strip inlet side. Industrially, these two extremes are known as regenerated acid (with a high content of HCl, approximately 18%) and wasted acid (with a high content of $FeCl_2$, approximately 23%). Figure 1 illustrates a ternary diagram consisting of water, hydrogen chloride, and iron chloride. This graph depicts the application of distinct pickling solution concentrations to four operating tanks. Tank 0 refer to the wasted acid, whereas Tank 3 the regenerated acid.

A typical production plant has a configuration that consists of a pickling line, a tank farm and an Acid Regeneration Plant (ARP). Figure 2 depicts the configuration of the pickling bath solutions. This chemical process employs a cyclical structure for economic reasons. The regenerated acid stream is delivered from the ARP to the buffer tank (located at the tank farm). As needed by the pickling line, regenerated acid is transferred from this tank to the final pickling working tank (TK03). As the regenerated acid goes through the tanks, HCl is consumed and iron II in solution increases. The wasted acid moves from Tank 0 to the buffer tanks and ultimately to the ARP. Oxidation occurs in the oxidation chamber of the acid regeneration plant, usually employing a Ruthner Process (MCKINLEY; GHAHREMAN, 2018). The rinse water used to clean the pickled steel strip is returned to the ARP to ensure operational efficiency, where packed bed absorption towers recover acid.

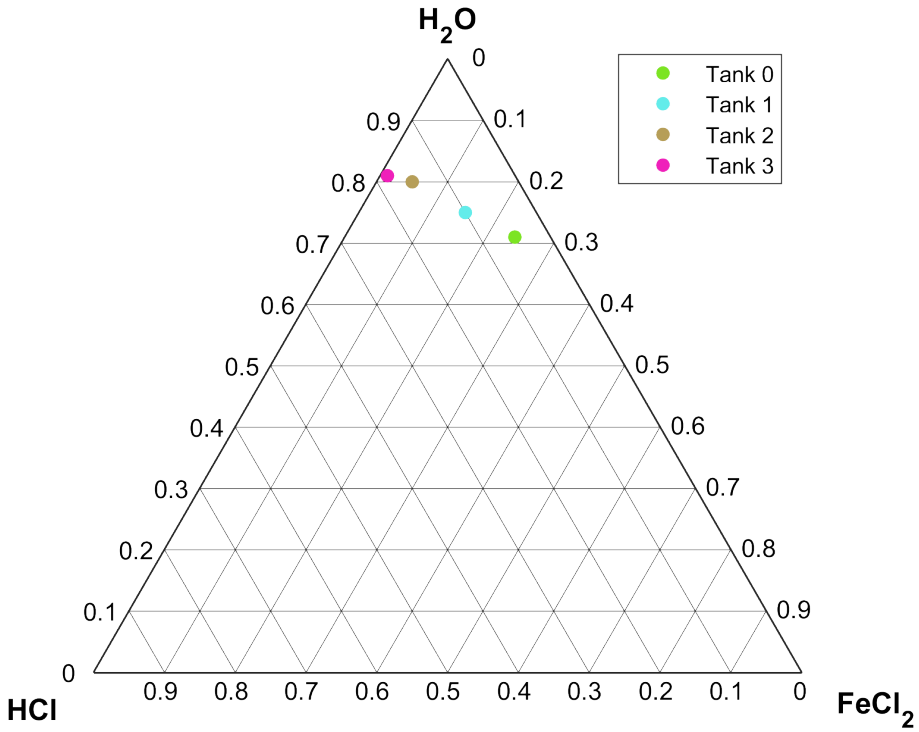

Figure 1 – Ternary diagram of HCl pickling solutions over four sequential working tanks. Tank 0 holds the wasted acid, which has the lowest concentration of free acid. Tank 3 solution has the highest concentration of HCl, referred to as regenerated acid. Other tanks have amounts of acid and $FeCl_2$ that fall between the extremes. The work tanks are named in ascending order relative to the steel strip inlet. Therefore, according to the countercurrent construction, concentrated acid enters Tank 3 and exits the process in Tank 0.

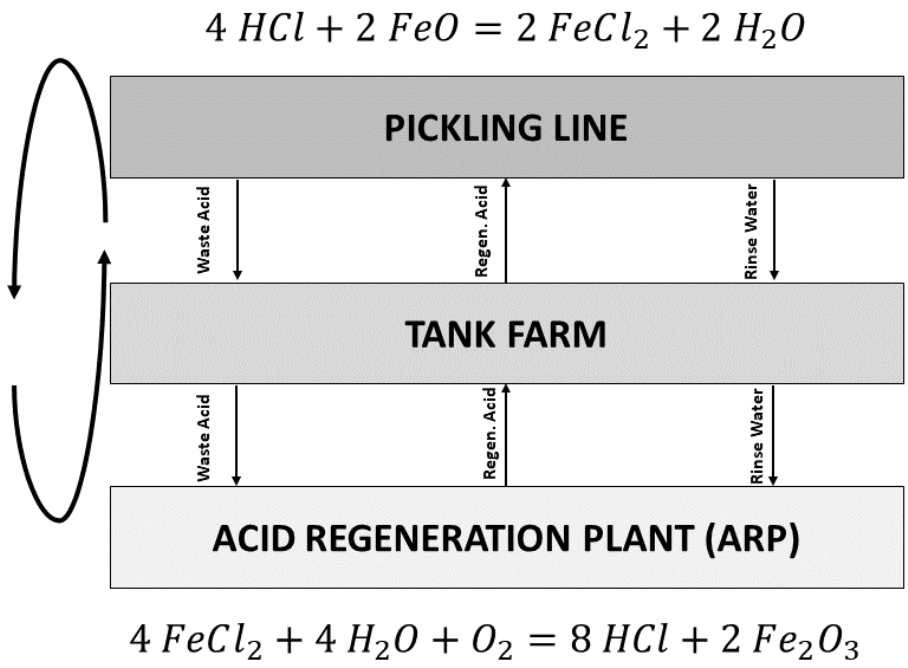

Figure 2 – Diagram of a typical acid pickling process, consisting of Pickling Line, Tank Farm, and a Acid Regeneration Plant (ARP). ARP usually provides regenerated acid (rich in HCl) to the pickling line. After wasted, the acid returns to the ARP. Rinse water is produced during the steel strip washing process and is transferred to the ARP absorption tower. The Tank Farm, an intermediate section, serves as a process buffer.

Due to environmental concerns, it is evident from the process design that the pickling lines operation requires regeneration units or an adequate commercial recovery technique (REGEL-ROSOCKA, 2010) (ÖZDEMIR; ÖZTIN; KINCAL, 2006). That indicates the importance of process engineering in steel production facilities. Consequently, it is essential to understand the physicochemical behavior of properties extensively utilized in operation and process design tools, such as process simulators (BASCONE et al., 2016). The comprehension of these characteristics allows the mitigation of engineering mistakes and the resolution of issues such as: 1) Is it possible to assume, for instance, that the physical property is constant throughout the pickling tanks? 2) Is it always necessary to adjust the property according to its composition? 3) Is it necessary to adjust the property regarding temperature? In order to achieve this objective, a semi-quantitative approach is introduced, which uses a risk analysis matrix according to the standards International Electrotechnical Commission (IEC) 61508 and 61511. The seven chosen properties were categorized as Classes I through IV. The higher the class, the more corrections are needed to estimate the property.

The main intention of this research is to present a methodology for calculating the most important physicochemical properties in terms of mass, heat, and momentum transfer phenomena. Typically, for complex solutions, such as this one, property calculations are simplified and performed with little rigor. Underestimating the effects of key components, or even temperature dependence, can lead to engineering mistakes. When process analyses are performed in commercial simulators, it is not always clear how the physicochemical properties are computed. Improperly selecting a thermodynamic package can lead to significant errors. To close these gaps, the aim of this paper is not only to demonstrate a method for calculating these physicochemical properties, but to assist engineers and scientists in their daily work. A semi-quantitative method is proposed for the classification of the dependence of characteristics on temperature and composition. This approach enables the assessment of properties in mass and energy balance applications, as well as in more sophisticated computer models, such as Computational Fluid Dynamics (CFD).

2.2 Physicochemical Properties

2.2.1 Density

The data available from Laliberte (2004) is used to estimate the liquid density. The given calculation method is an empirical equation capable of estimating the specific volume of various water-soluble electrolytes, including $FeCl_2$, $FeCl_3$, and HCl. The general equation, applicable to all electrolytes, is:

$$\overline{v}_{app,i} = \frac{x_i + c_2 + c_3 T}{(c_0 x_i + c_1) e^{(0{,}000001(T+c_4)^2)}} \tag{1}$$

In Equation (1) $\overline{v}_{app,i}$ represents the apparent specific volume of an electrolytic component $m^3 \cdot kg^{-1}$; x_i represents the mass fraction of the electrolytic component; T represents the solution temperature °C; c_0, c_1, c_2,c_3 and c_4 are empirical constants. Table 2 presents

the constants extracted from Laliberte (2004).

Table 2 – Empirical parameters for $FeCl_2$, $FeCl_3$, and HCl extracted from Laliberte (2004) for electrolytes in aqueous solution.

Compound	c_0 (kg·m^{-3})	c_1 (kg·m^{-3})	c_2	c_3 (°C^{-1})	c_4 (°C)
$FeCl_2$	98.654	199.51	0.33639	0.00386444	13650.1
$FeCl_3$	-1333.8	4369.2	1.5298	0.007099	829.21
HCl	-80.061	255.42	118.42	1.0164	2619.5

Equation (1) calculates the specific volume for a single component. In order to compute the density of an electrolyte solution, all components must be accounted for. The concept is based on Amagat's law:

$$\rho = \frac{1}{\frac{x_{H_2O}}{\rho_{H_2O}} + \Sigma_{i=1}^{c} x_i \overline{v}_{app,i}} \tag{2}$$

The density of an electrolyte solution is calculated considering the average apparent specific volume of all water soluble electrolytes, weighted by mass, according to Equation (2). Even though Laliberte (2004) have not verified the concept for a multi-component system, this work proposes applying the data to estimate the density of hydrochloric acid pickling solutions (ρ) according to Equation (2).

Kell (1975) correlation is used to calculate the density of pure water:

$$\rho_{H_2O} = \frac{(((((aT + b)T + c)T + d)T + e)T + f)}{1 + gT} \tag{3}$$

In Equation (3), T is the temperature, in Celsius degrees, and the coefficients a, b, c, d, e, f and g are model constants, respectively: -2.8054253·10^{-10}; 1.0556302·10^{-7}; -4.6170461·10^{-5}; -0.0079870401; 16.945176; 999.83952 and 0.01687985.

2.2.2 Vapor pressure

To compute the vapor pressure of hydrochloric acid in pickling bath solutions, the following correlation was adapted from Hudson *et al.* (1967):

$$\ln P_{vap,HCl} = -\ln\left(\frac{M_{HCl} \cdot 0.0283168}{R \cdot T}\right) + A \cdot T + B \cdot x_{FeCl_2} + C \cdot x_{HCl} + D \tag{4}$$

In Equation (4), HCl vapor pressure ($P_{vap,HCl}$) is in Pa; HCl molar mass (M_{HCl}) in kg·mol^{-1}; Ideal gas constant (R) in Pa·m^3·(kmol·K)$^{-1}$; T is in K; HCl mass fraction (x_{HCl}) and $FeCl_2$ mass fraction (x_{FeCl_2}) are the components mass fraction; A, B, C and D are equations constants, respectively: 0.0711; 16.8388; 46.6964 and -33.0406.

In order to calculate the vapor pressure of the pickling bath solution, it was assumed that iron chloride does not evaporate. In addition, Raoult's law was used to determine liquid-vapor equilibrium. These premises result in the following equation:

$$P = x_{\mathrm{HCl}} \cdot P_{vap,HCl} + (1 - x_{\mathrm{HCl}} - x_{\mathrm{FeCl_2}}) \cdot P_{vap,\mathrm{H_2O}} \tag{5}$$

Equation (5) requires evaluating pure water vapor pressure as a function temperature. Antoine's equation is applied:

$$\ln P_{vap,\mathrm{H_2O}} = A - \frac{B}{C + T} \tag{6}$$

In Equation (6), $P_{vap,\mathrm{H_2O}}$ is the vapor pressure of water, in Pa; T is the system temperature, in K; and A, B and C are the equation constants: 23.23703, 3841.20929 and -45.15, respectively. The equation is valid in the range of 60°C to 150°C, according to Felder *et al.* (2010).

2.2.3 Heat of vaporization

For determining the evaporation heat, the Clausius-Clapeyron equation was employed (FELDER; ROUSSEAU; BULLARD, 2010). For a generic compound "i":

$$\Delta H_{v,i} = R \cdot T^2 \left[\frac{d}{dT} (\ln P_{vap,i}) \right] \tag{7}$$

In Equation (7), note that the Heat of vaporization of a generic compound "i" ($\Delta H_{v,i}$) is a function of vapor pressure ($P_{vap,i}$). To compute the heat of vaporization of the pickling solution, the following rule is used, in molar basis:

$$\Delta H_v = \Sigma_{i=1}^{c} z_i \cdot \Delta H_{v,i} \tag{8}$$

Considering that $FeCl_2$ does not evaporate under operating conditions, Equation (8) may be written as:

$$\Delta H_v = z_{\mathrm{HCl}} \cdot \Delta H_{v,\mathrm{HCl}} + (1 - z_{\mathrm{HCl}} - z_{\mathrm{FeCl_2}}) \cdot \Delta H_{v,\mathrm{H_2O}} \tag{9}$$

In Equation (9), $\Delta H_{v,i}$ is the heat of vaporization of the solution, given in $\mathrm{J \cdot mol^{-1}}$; $\Delta H_{v,\mathrm{HCl}}$ and $\Delta H_{v,\mathrm{H_2O}}$ are the evaporation heats of HCl and H_2O; z_{HCl} and $z_{\mathrm{FeCl_2}}$ are the HCl and $FeCl_2$ mole fractions in the pickling solution.

Substituting the vapor pressure, Equation (4) and Equation (6), temperature derivative in Equation (7), the molar evaporation heat for each component is:

$$\Delta H_{v,\mathrm{HCl}} = R \cdot T^2 \left[A + \frac{1}{T} \right] \tag{10}$$

$$\Delta H_{v,\mathrm{H_2O}} = R \cdot T^2 \left[\frac{B}{(T + C)^2} \right] \tag{11}$$

The constants present in Equations (10) and (11) were presented in the above subsection.

2.2.4 Specific heat capacity

As demonstrated in Laliberté (2009) and Felder *et al.* (2010), the following rule is applied to compute the mixture specific heat capacity:

$$c_p = x_{H_2O} c_{pH_2O} + \Sigma_{i=1}^{c} x_i c_{pi} \tag{12}$$

In Equation (12), c_p is the pickling solution specific heat, in kJ·(kg·K)$^{-1}$; x_{H_2O} is the mass fraction of water and x_i is the fraction of any generic "i" solute.

From Green (2007), the following correlation is used for pure water:

$$c^*_{pH_2O} = 276{,}370 - 2090.1 \cdot T + 8.125 \cdot T^2 - 0.014116 \cdot T^3 + 9.3701 \cdot 10^{-6} \cdot T^4 \tag{13}$$

In the above equation, c^*_{p,H_2O} is the the molar specific heat of liquid water, valid for the range of 273.16 K to 533.15 K. For solutes specific heat calculations, the following correlation, proposed by Laliberté (2009), is used:

$$c_{p,i} = a_1 \cdot e^{\alpha} + a_5 \cdot (1 - x_{H_2O})^{a_6} \tag{14}$$

$$\alpha = a_2 \cdot T + a_3 \cdot e^{0{,}01 \cdot T} + a_4 \cdot (1 - x_{H_2O}) \tag{15}$$

In Equations (14) and (15), a_1, a_2, a_3, a_4, a_5 and a_6 are empirical coefficients; T is the temperature, in °C; x_{H_2O} is the mass fraction of water, assuming a binary system (water and solute); $c_{p,i}$ is the specific heat of water-soluble electrolyte, in kJ·(kg· K)$^{-1}$.

Due to the lack of data for $FeCl_3$, it is assumed, for calculation purposes, that all iron in solution is in the form of $FeCl_2$. Table 3 provides the empirical coefficients for calculating the solutes specific heats.

Table 3 – Laliberté (2009) provides empirical coefficients for estimating the specific heat of electrolytic solutes.

Coefficients	$FeCl_2$	HCl
a_1	-7.58	-1.44
a_2	-0.22	-0.02
a_3	0.39	0.76
a_4	-2.05	-0.25
a_5	-1.45	-0.09
a_6	1.63	-0.37

2.2.5 Viscosity

In order to calculate the electrolyte solution viscosity, the following mixing rule, from Laliberté (2007), is used:

$$\eta = \eta_{H_2O}^{x_{H_2O}} \cdot \eta_i^{x_i} \tag{16}$$

In Equation (16), η is the mixture viscosity, in mPa·s; η_{H_2O} is the pure water viscosity; η_i is the viscosity of an electrolytic solute; x_{H_2O} is the mass fraction of water and x_i is the mass fraction of any electrolytic solute.

As presented in Laliberté (2009), the following equations allow for the calculation of both solute and pure water:

$$\eta_i = \frac{e^{\left[\frac{v_{1,i}(1-x_{H_2O})^{v_{2,i}}+v_{3,i}}{v_{4,i}\cdot T+1}\right]}}{v_{5,i}\cdot(1-x_{H_2O})^{v_{6,i}}+1} \tag{17}$$

$$\eta_{H_2O} = \frac{T+246}{(0{,}05594\cdot T+5{,}2842)\cdot T+137{,}7} \tag{18}$$

In Equations (17) and (18), η_i and η_{H_2O} are given in mPa·s; T is the temperature, given in °C; x_{H_2O} is the water mass fraction. The coefficients $v_{1,i}$, $v_{2,i}$, $v_{3,i}$, $v_{4,i}$, $v_{5,i}$ and $v_{6,i}$ are empirical constants for each solute.

Table 4 presents the empirical coefficients used in the viscosity calculation of electrolytic solutions of ferrous chloride and hydrochloric acid in water.

Table 4 – Empirical coefficients for calculating the viscosity of electrolytic solutes, from Laliberté (2007).

Coefficients	**$FeCl_2$**	**HCl**
v_1	-0.29592	7.124
v_2	18.533	1.1919
v_3	8.8165	1.6648
v_4	0.021966	0.0096271
v_5	385.52	22.185
v_6	0.23964	1.479

It is assumed, for calculation purposes, that all iron in solution is in the form of $FeCl_2$. The final expression for the viscosity calculation is presented below:

$$\eta = \eta_{H_2O}^{(1-x_{FeCl_2}-x_{HCl})} \cdot \eta_{FeCl_2}^{x_{FeCl_2}} \cdot \eta_{HCl}^{x_{HCl}} \tag{19}$$

2.2.6 Thermal conductivity

The approach used to calculate the thermal conductivity is based on McLaughlin (1964):

$$k = f \cdot (0{,}515 + \Sigma_{i=1}^{c} \alpha_i \cdot C_i) \cdot 86.042^{-1} \tag{20}$$

In Equation (20), k is the thermal conductivity, in $W \cdot (m \cdot K)^{-1}$; α is the constant for the ion "i"; C_i is the molar concentration of the generic ion "i", in $mol \cdot L^{-1}$; f is defined as a ratio for water thermal conductivity, as follows:

$$f = \frac{k_w}{k_w(20°C)} \tag{21}$$

In the above equation, $k_w(20°C)$ is the thermal conductivity of water at 20°C and k_w is the thermal conductivity of water at the desired temperature. To determine the thermal conductivity of water, Equation (22) from Green (2007) is used.

$$k_w = -0.432 + 5.73 \cdot 10^{-3} \cdot T - 8.08 \cdot 10^{-6} \cdot T^2 + 1.86 \cdot 10^{-9} \cdot T^3 \tag{22}$$

In Equation (22), temperature T is given in K, and it is valid for the range of 273.16 K to 633.15 K.

Regarding calculations of ion molar concentration, the following equations are used, according to the target ionic compound:

$$C_{Fe^{2+}} = \frac{x_{FeCl_2} \cdot \rho}{M_{FeCl_2}} \tag{23}$$

$$C_{Fe^{3+}} = \frac{x_{FeCl_3} \cdot \rho}{M_{FeCl_3}} \tag{24}$$

$$C_{H^+} = \frac{x_{HCl} \cdot \rho}{M_{HCl}} \tag{25}$$

$$C_{Cl^-} = C_{Fe^{2+}} \cdot 2 + C_{Fe^{3+}} \cdot 3 + \frac{x_{HCl} \cdot \rho}{M_{HCl}} \tag{26}$$

In order to evaluate the thermal conductivity of pickling solutions, α values for each individual ion present in descaling solutions are necessary. According to McLaughlin (1964), the values for the anion H^+ and cation Cl^- are $-78 \cdot 10^{-4}$ and $-47 \cdot 10^{-4}$, respectively. Regarding the Iron II and Iron III ions, due to lack of data, the following values are assumed for each: $-100 \cdot 10^{-4}$ and $-280 \cdot 10^{-4}$. These values correspond to the Co^{+2} and Al^{+3} ions, and were chosen based on the ionic charge similarity between the ions. All α values were employed at 20°C.

2.2.7 HCl diffusion coefficient

The computation of the HCl diffusion coefficient is based on the work of Robinson (1957). The entire mathematical development is expressed in Cremasco (2019). Equation (27) presents an expression for the calculation of diffusion coefficient for an infinite ionic aqueous solution.

$$\mathcal{D}_{\infty} = 8{,}931 \times 10^{-10} \cdot T \cdot \left(\frac{|\lambda_+| \cdot |\lambda_-|}{\lambda_+| + |\lambda_-|}\right) \cdot \left(\frac{|z_+| + |z_-|}{|z_+| \cdot |z_-|}\right) \tag{27}$$

In Equation (27), T is the temperature, in K; λ_+ and λ_- are the equivalent ionic conductivities (anion and cation, respectively) at infinite dilution in H_2O at 25 °C, given in ohm·eq^{-1}; z_+ and z_- consist of the ionic charges of the dissociated electrolytes. For the HCl, the anion is H^+ and the cation Cl^-. Note that the diffusion coefficient $\mathcal{D}_{\infty}$ is expressed in cm^2·s^{-1}. For HCl application, λ_+ and λ_- consists, respectively, of 349.80 and 76.35 ohm·eq^{-1}. The charges z_+ and z_- are +1 and -1.

Based on the presented parameters, it is then possible to calculate the HCl diffusion coefficient in diluted water solutions. However, for the application considered here, the fraction of acid present in the bath does not correspond to a diluted solution. Thus, it is necessary to evaluate other parameters required for operating with concentrated baths.

2.2.7.1 Diffusion coefficient of electrolytes in concentrated liquids

As suggested by Cremasco (2019), the electrolyte diffusion coefficient can be adjusted for concentrated baths by multiplying the activity coefficient γ, as follows:

$$\mathcal{D}_{\mathrm{HCl}} = \mathcal{D}_{\infty} \cdot \Gamma^{p} \tag{28}$$

To estimate γ for a HCl solution, the equation below can be used:

$$\Gamma = 1 + \mathbf{m}_{\mathrm{HCl}} \cdot \frac{d \ln \gamma_{\mathrm{HCl}}}{d\mathbf{m}_{\mathrm{HCl}}} \tag{29}$$

In the above equation, γ_{HCl} is the activity coefficient of hydrochloric acid and m_{HCl} is the molal concentration, in mol of HCl·(kg of H_2O)$^{-1}$. To compute the activity coefficient, Cremasco (2019) suggests two approaches: 1) For solutions that have a molar concentration less than or equal to 1 mol·kg^{-1}, use the Debye-Hückel model proposed by Oliveira (2014); 2) For cases of higher concentrations, the Bromley-Zemaitis model extracted from Jaworski *et al.* (2011) is suggested.

For low molality situations (case 1):

$$\ln \gamma_{\mathrm{HCl}} = -\frac{A \cdot |z_{H^+} \cdot z_{Cl^-}| \cdot I^{1/2}}{1 + a \cdot B \cdot I^{1/2}} \tag{30}$$

For molality greater than 1 (case 2):

$$\ln \gamma_{\mathrm{HCl}} = -\frac{A \cdot |z_{H^+} \cdot z_{Cl^-}| \cdot I^{1/2}}{1 + I^{1/2}} + \frac{(0{,}06 + 0{,}6 \cdot B)|z_+ \cdot z_-| \cdot I}{\left(1 + \frac{1{,}5}{|z_{H^+} \cdot z_{Cl^-}|} \cdot I\right)^2} + B \cdot I + C \cdot I^2 + D \cdot I^3 \tag{31}$$

The parameter *I*, present in both cases, is defined as the ionic strength on a molal basis. It expresses the electric field intensity due to the presence of ions in solution. From its mathematical definition:

$$I = \frac{1}{2} \cdot \mathbf{m}_{HCl} \cdot |z_{H^+}| \cdot |z_{Cl^-}| \tag{32}$$

In Equations (30) and (69), coefficients A, B, C and D are experimental parameters, function of temperature and the type of ions present in the solution. Due to difficulty of obtaining these vales, it is proposed the use of the following parameters, valid to NaCl: 1; 1.1759; 0.1407; -4.9881·10^{-3} and 6.559·10^{-4}, respectively. It is important to take into account that for HCl diffusion calculations, it is assumed no influence from Iron II and III; The coefficient *p*, present in Equation (28), is assumed to be equal to 1.

2.3 Material and methods

2.3.1 Operating ranges

To develop the present work, it was necessary to determine and analyze the common operating limits in the steel pickling industry. From plant operation manuals and published literature (see Hudson *et al.* (1967), Yamaguchi *et al.* (1994) and Gines *et al.* (2002)), an operating range for material mass fractions (HCl and $FeCl_2$) and temperature was obtained and are shown in Table 5.

Table 5 – Typical operational conditions for a industrial pickling line using hydrochloric acid as pickling solution. The available data were provided by a plant based in southern Brazil.

Tank	**HCl**(wt.%)		**$FeCl_2$**(wt.%)		**Temperature** (°C)	
	Min.	**Max.**	**Min.**	**Max.**	**Min.**	**Max.**
0	1%	9%	20%	25%	65	85
1	5%	13%	14%	18%	65	85
2	10%	19%	3%	9%	65	85
3	16%	21%	0%	1%	65	85

The operating ranges for an industrial plant with four turbulent pickling tanks and indirect heat supply were determined. It was assumed a constant concentration of HCl in each tank, and the conservation of chlorine across the tanks, *i.e.* no evaporation occurs. These hypotheses allow a relationship between HCl and $FeCl_2$, according to Equation (33):

$$y^n_{HCl} = y^{n-1}_{HCl} - (x^n_{FeCl_2} - x^{n-1}_{FeCl_2}) \cdot \theta_{\frac{Cl}{FeCl_2}} \cdot \frac{M_{HCl}}{M_{FeCl_2}} \tag{33}$$

In Equation (33), the superscript "n" refers to the tank; $\theta_{\frac{Cl}{FeCl_2}}$ is the stoichiometric coefficient between chlorine and iron chloride II; and *M* is the molar mass of each component of interest. This equation represents a evaporation-free system, allowing the estimation of the theoretical concentration of HCl in each tank, given the inlet material condition.

2.3.2 Physical boundaries for a pickling system

To enrich the information on each physicochemical surface plot, it is necessary to restrict the operational range. For instance, it is not recommended to feed pickling tanks at bubble stage. The solubility limit of $FeCl_2$ is another factor that must be considered. On this basis, two surface plot limits are determined: 1) maximum feasible operational limit and 2) the minimal design operational limit.

2.3.2.1 Maximum feasible operational limit

The concept behind proposing this graphic line is to specify the upper boundary based on the maximum feasible operational limit. The surface plot above this line is irrelevant. Two points must be defined: one point is specified along the Y-axis (at HCl mass fraction with no $FeCl_2$) and the other along the X-axis (HCl-free).

To define the second point, we assume the extreme condition that all HCl have been consumed and the iron chloride II is at the solubility limit. Because the solubility limit is a function of temperature, information from the literature Green (2007) was used to create a linear function in Microsoft Excel using the Data Analysis Toolbox.

The other extreme condition, regarding the maximum HCl concentration, depends of three parameters: HCl mass fraction in pure water; operational temperature and inlet tank head space pressure. The main idea is to avoid a scenario where pure acid solution have been fed at bubble point in the tank. HCl vapor pressure as a function of temperature and HCl mass fraction data (extracted from Green (2007)) was fitted to a 5th degree polynomial in x and in y. A surface fit was performed using the MATLAB `Curve Fitter toolbox`, using an iterative reweighted least squares method, and the variables were normalized by mean and standard deviation. The resulting fit was a polynomial of 5th degree with 21 coefficients and R-square of 0.9975. MATLAB Symbolic Math Toolbox was used to solve the polynomial for HCl mass fraction as a function of temperature and vapor pressure. The equation has 5 solutions, but only one of them is feasible, representing the HCl mass fraction.

2.3.2.2 Minimum design operational limit

The Minimum design operational limit was defined considering a scenario where the HCl solution have 50% of the minimum HCl concentration in rich acid solutions, defined in Table 5, is $FeCl_2$ free and has the same inclination as the maximum limit line.

2.3.3 Physicochemical properties plot

A contour plot of each physicochemical properties as a function of HCl (Y-Axis) and $FeCl_2$ (X-Axis) was made for each temperature (65, 70, 75, 80 and 85 °C) using MATLAB `contourf` function. The Y-axis grid is a linear space from 0 to HCl mass fraction at the bubble point, calculated using the function of temperature and vapor pressure. The X-axis is a linear space from 0 to the $FeCl_2$ saturation. The physical properties are calculated for each point in the grid, and the points inside the operation limits are plotted.

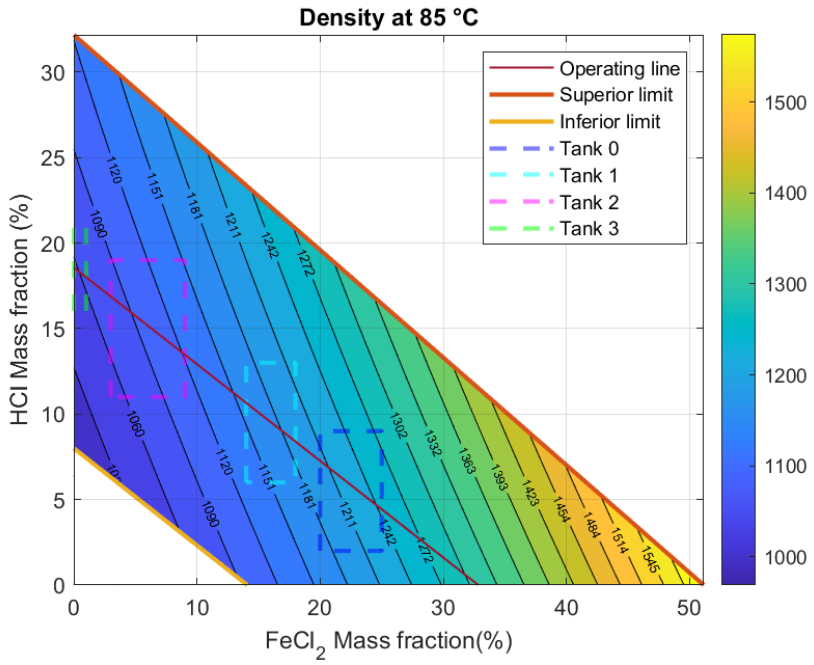

Figure 3 – Surface plot for density in feasible operational region for HCl pickling solution at 85°C. The operating line is based on a regenerated pickling solution with 18% of HCl and 1% of $FeCl_2$. Each pickling tank region is represented by rectangles delimited by the concentration ranges. The values range from 1300 to 1050 $kg{\cdot}m^{-3}$.

Table 6 – Average density and coefficient of variation at each pickling tank and temperature. The density unit is in $kg{\cdot}m^{-3}$ and temperature in °C. CV refers to coefficient of variation. TK 00 through TK03 consist of each operational tank.

Temperature	TK00		TK01		TK02		TK03	
	Average	CV	Average	CV	Average	CV	Average	CV
65	1238	1.8%	1188	1.6%	1111	2.0%	1073	0.7%
70	1235	1.8%	1185	1.6%	1108	2.0%	1070	0.7%
75	1231	1.8%	1181	1.5%	1105	2.0%	1067	0.7%
80	1227	1.9%	1178	1.6%	1102	2.0%	1064	0.7%
85	1223	1.9%	1174	1.6%	1099	2.0%	1061	0.7%

2.4 Results and discussions

2.4.1 Density

Figure 3 displays the data at 85°C. Within the operating ranges, the displayed surface contains only physically possible regions of occurrence. The operation line was determined by applying Equation (33) to a regenerated pickling solution containing 18% HCl and 1% $FeCl_2$. The tanks operational region, delimited by the admitted concentration range, is illustrated.

In addition to the surface plot, the table 6 is provided to aid in the analysis of the results. This table presents the property average and coefficient of variation (CV) values in each concentration region for each evaluated temperature.

The dispersion of density values, as determined by the coefficient of variation, varied from 0.7% to 2.0%. The range of property values was observed to be between 1238 and

Table 7 – The average vapor pressure and coefficient of variation observed in each pickling tank. The vapor pressure unit is at kPa and temperature is in °C. CV refers to coefficient of variation. TK 00 through TK03 consist of each operational tank.

Temperature	TK00		TK01		TK02		TK03	
	Average	CV	Average	CV	Average	CV	Average	CV
65	18.0	3.3%	18.7	2.8%	20.1	2.4%	20.8	0.6%
70	22.5	3.3%	23.3	2.7%	25.1	2.3%	26.0	0.7%
75	27.8	3.3%	28.9	2.6%	31.1	2.1%	32.3	0.9%
80	34.2	3.3%	35.5	2.6%	38.4	2.1%	39.9	1.2%
85	41.7	3.2%	43.4	2.5%	47.0	2.1%	49.0	1.7%

1061 $kg \cdot m^{-3}$. The area of coverage characterized by the lowest recorded temperature (65°C) and the highest concentration of Iron II salt had the most significant density values. This is a common tendency of ionic solutions, where density increases with salt content and decreases with temperature. The analysis focused on the relationship between temperature and density, specifically examining the ratio of average density variance to temperature fluctuation. The outcome yielded a matrix consisting of 16 data points, each with an average value of 0.65 $kg \cdot m^{-3} \cdot °C^{-1}$.

2.4.2 Vapor pressure

In order to evaluate the behavior of pickling solution vapor pressure, Figures 4a and 4b display the surface plot for vapor pressure at 65 and 85°C, respectively. The effect of temperature on the property can be observed by examining each figure. A 20°C increase roughly doubled the vapor pressure in each tank region. As expected, it shows that vapor pressure is extremely temperature sensitive.

Table 7 displays the average vapor pressure values for the studied operating range. A significant temperature effect is observed, in which the vapor pressure rises with temperature. Regarding the concentration of iron(II) chloride ($FeCl_2$), an inverse relationship is seen. The coefficient of variation (CV) ranges from 0.6% to 3.3%, meaning a low level of dispersion around the average value. The pickling tank's operational range has a influence in the coefficient of variation. The TK03 has the smallest range, and as a result, the CV values are the lowest. The highest and lowest average values were 18 and 49 kPa, respectively, a range of 31 kPa. The average ratio between vapor pressure variation and temperature variation is 1.29 $kPa \cdot °C^{-1}$. This is to be expected given that the underlying equations for these calculations are exponential functions of temperature.

2.4.3 Heat of vaporization

Figure 5 displays the evaporation heat surface plot at 85°C. It was not observed a significant effect of temperature on the evaporation heat. The values range from 1700 to 2300 $kJ \cdot kg^{-1}$. The evaporation heat tends to decrease as the concentration of $FeCl_2$ increases due to the fact that iron salts do not evaporate.

Table 8 shows the average heat of vaporization and Coefficient of Variation (CV)

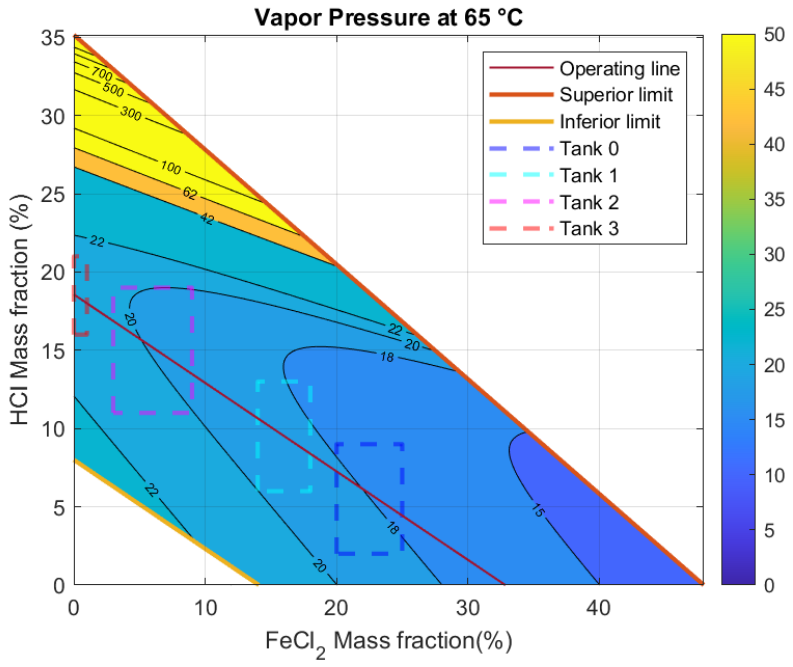

(a)

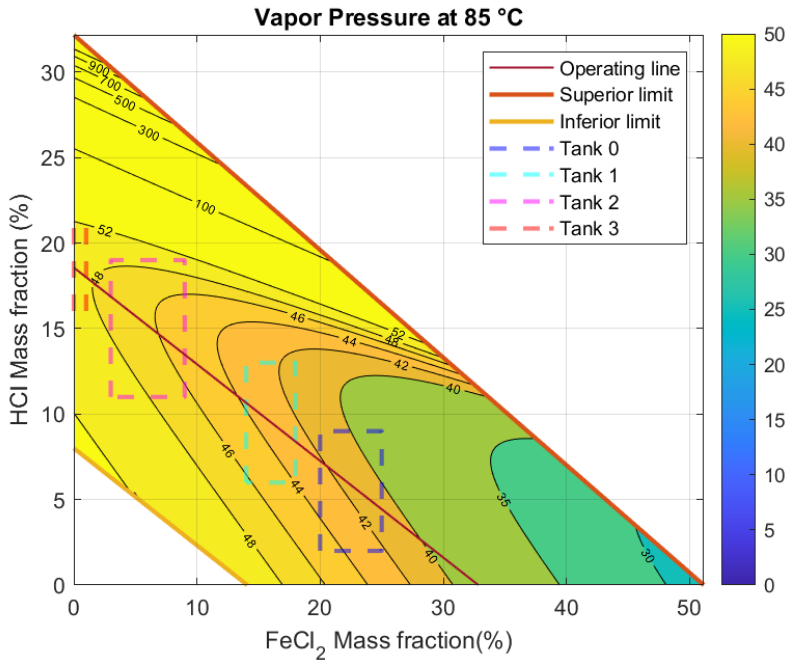

(b)

Figure 4 – Surface plots for HCl pickling solutions vapor pressure at 65°C (Figure 4a) and 85°C (Figure 4b). The operating line is based on a composition of 18% HCl and 1% $FeCl_2$. Each pickling tank region is represented by rectangles delimited by the concentration ranges.

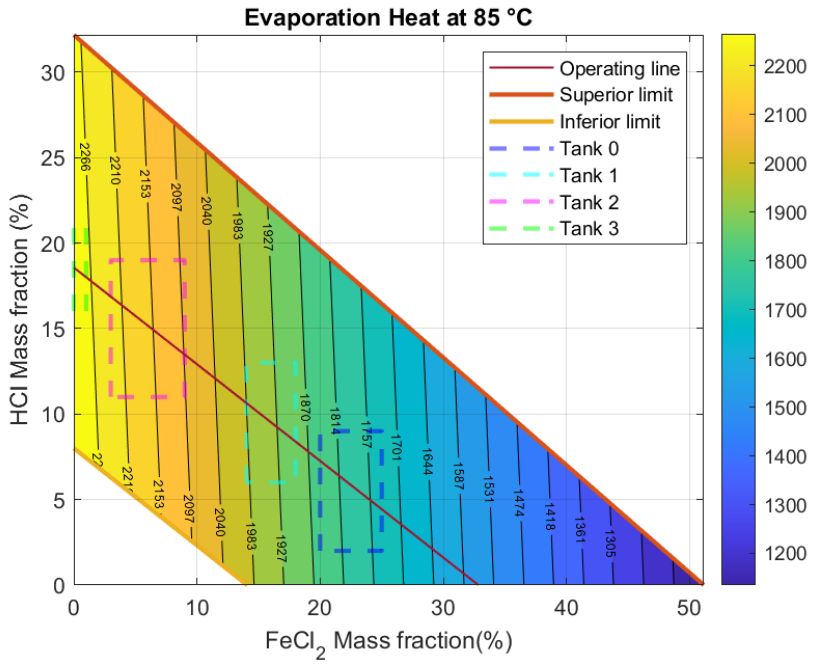

Figure 5 – Evaporation heat surface plot in feasible operational region for HCl pickling solution at 85°C. The operating line is based on a regenerated pickling solution with 18% of HCl and 1% of $FeCl_2$. Each pickling tank region is represented by rectangles delimited by the concentration ranges. The values range from 1700 to 2300 $kJ \cdot kg^{-1}$.

Table 8 – The average heat of vaporization and coefficient of variation observed in each pickling tank. The heat of vaporization unit it is at $kJ \cdot kg^{-1}$ and temperature in °C. CV refers to coefficient of variation. TK 00 through TK03 consist of each operational tank.

Temperature	TK00		TK01		TK02		TK03	
	Average	CV	Average	CV	Average	CV	Average	CV
65	1809	1.9%	1946	1.5%	2160	1.9%	2276	0.4%
70	1804	1.9%	1944	1.4%	2160	1.9%	2278	0.4%
75	1800	1.9%	1942	1.4%	2161	1.9%	2280	0.4%
80	1796	1.9%	1940	1.4%	2162	1.9%	2283	0.3%
85	1793	1.9%	1938	1.4%	2163	1.9%	2286	0.3%

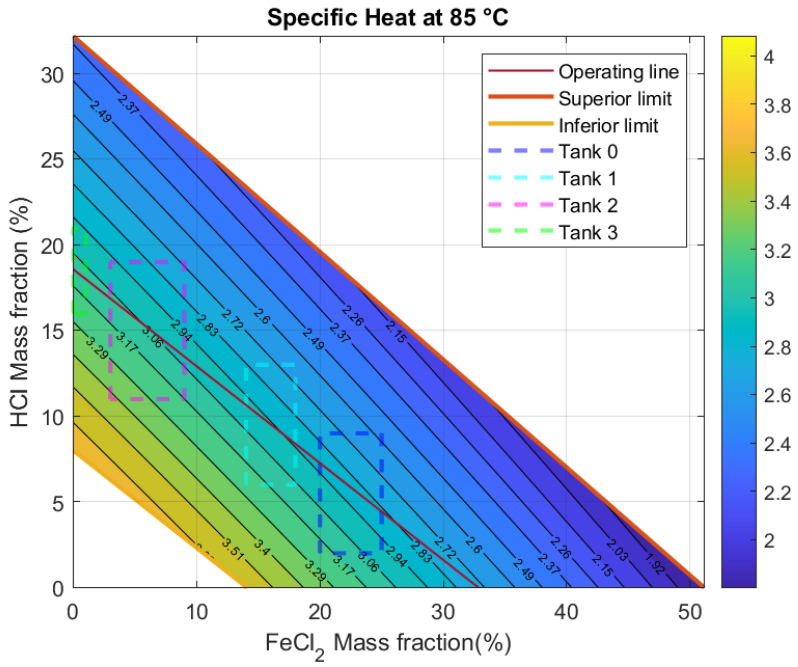

Figure 6 – Specific heat capacity surface plot in feasible operational region for HCl pickling solution at 85°C. The operating line is based on a regenerated pickling solution with 18% of HCl and 1% of $FeCl_2$. Each pickling tank region is represented by rectangles delimited by the concentration ranges. The values range from 2.5 to 3.5 kJ·(kg·K)$^{-1}$.

for each tank at each analyzed temperature. A CV ranging from 0.3% to 1.9% is found. This shows that the heat of vaporization barely vary within a pickling tank. The maximum and minimum average values were 1793 and 2286 kJ·kg^{-1}, respectively. Regarding the temperature influence on the property value, two distinct behaviors are observed: one for high $FeCl_2$ concentrations and the other for low concentrations. In the first case, an increase in temperature is associated with a decrease in property value (TK00 and TK01 region). For the region of low $FeCl_2$ concentration (TK02 and TK03), the opposite occur. An average value of 0.47 kJ·(kg·°C)$^{-1}$ was found for the ratio between property and temperature variation, showing a low temperature influence on the heat of vaporization.

2.4.4 Specific heat capacity

Specific heat is a key phycochemical parameter for mass and energy balance calculations and other engineering applications. This information's precision contributes to more reliable process engineering development, particularly in the early phases of plant design. The surface plot of specific heat capacity for HCl pickling solutions at 85°C is displayed in Figure 6. The values range from 2.5 to 3.5 kJ·(kg·K)$^{-1}$. Similar to heat of vaporization, the specific heat capacity decreases as the $FeCl_2$ concentration increases.

Table 9 displays the average specific heat capacity values and coefficient of variation for each tank and temperature. The coefficient of variation (CV) is a measure of the property dispersion at each temperature and tank region. The temperature influence is measured

Table 9 – Average specific heat capacity and coefficient of variation in each pickling tank at different temperatures. Specific heat is in kJ·(kg·K)$^{-1}$ and temperature in °C. CV refers to coefficient of variation. TK 00 through TK03 consist of each tank.

Temperature	TK00		TK01		TK02		TK03	
	Average	CV	Average	CV	Average	CV	Average	CV
65	2.88	4.9%	2.93	4.5%	3.03	5.1%	3.06	2.8%
70	2.88	4.8%	2.93	4.5%	3.04	5.1%	3.07	2.7%
75	2.88	4.8%	2.94	4.4%	3.05	5.0%	3.08	2.7%
80	2.89	4.8%	2.95	4.4%	3.06	5.0%	3.09	2.7%
85	2.90	4.8%	2.95	4.4%	3.07	5.0%	3.10	2.7%

Table 10 – Average viscosity and coefficient of variation for each pickling tank and temperature. The viscosity is in mPa·s^{-1} and temperature in °C. CV refers to coefficient of variation. TK 00 through TK03 consist of each tank.

Temperature	TK00		TK01		TK02		TK03	
	Average	CV	Average	CV	Average	CV	Average	CV
65	0.95	6.2%	0.87	5.9%	0.73	7.7%	0.67	3.6%
70	0.89	6.3%	0.81	6.0%	0.69	7.8%	0.63	3.6%
75	0.83	6.4%	0.76	6.0%	0.65	7.8%	0.60	3.7%
80	0.78	6.5%	0.72	6.1%	0.61	7.9%	0.57	3.8%
85	0.74	6.5%	0.68	6.2%	0.58	8.0%	0.54	3.9%

by the ratio between the property variation and temperature variation, a average of 0.001 kJ·(kg·K^2)$^{-1}$, showing a minimal temperature effect within the working range.

2.4.5 Viscosity

Viscosity has a significant impact on pipe calculations, particularly in head loss analyses. Figures 7a and 7b depict viscosity surface plots at 65°C and 85°C. A significant impact of temperature on viscosity is observed. At 65°C, a range of 0.5 to 1.5 mPa·s^{-1} is observed, whereas at 85°C the values range from 0.4 to 1.3. The viscosity of a substance shows a reduction in response to an elevation in temperature. The opposite effect is observed regarding $FeCl_2$ concentration.

The average viscosity values and coefficient of variation (CV) for each tank and temperature are presented in Table 10. CV ranges from 3.6% to 6.5%, indicating high dispersion around the average. The average values range from 0.54 to 0.95 mPa·s^{-1}. The global average for this property is 0.72 mPa·s^{-1}. Regarding the temperature influence, the average value for the ratio between property variation and temperature variation is 0.01 mPa·s·K^{-1}. While viscosity decreases as the temperature increases, $FeCl_2$ concentration has the opposite effect on viscosity values.

2.4.6 Thermal conductivity

Thermal conductivity is a crucial parameter for calculating heat transfer coefficients, having a significant effect on heat exchanger calculations. Neglecting the effects of composition and temperature on design specifications could result in problems. Figure 8 depicts

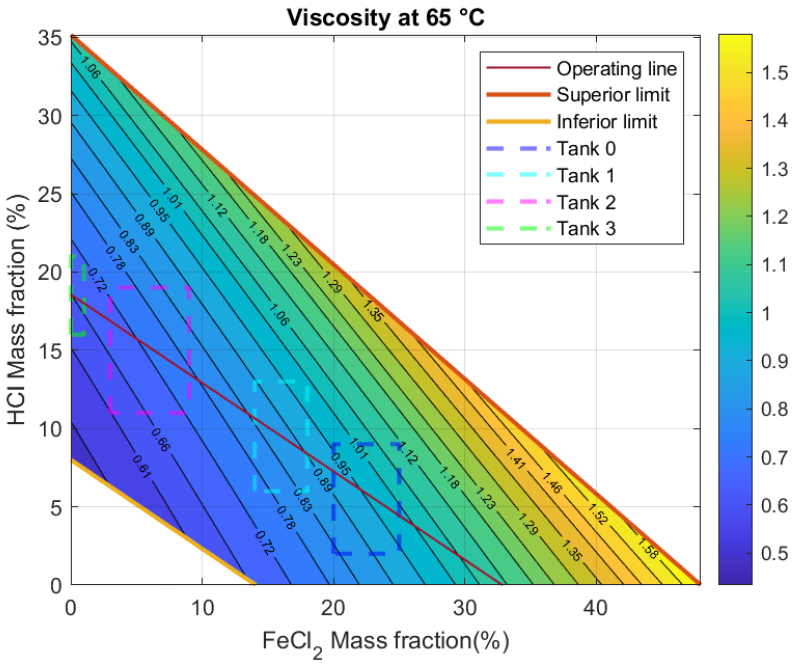

(a)

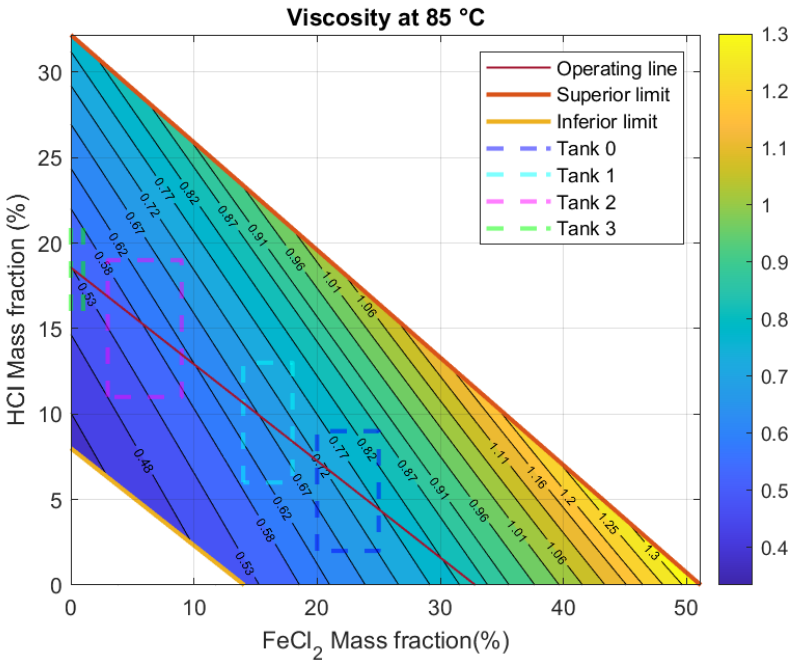

(b)

Figure 7 – Viscosity surface plots for HCl pickling solutions at 65°C (Figure 7a) and 85°C (Figure 7b). The operating line is based on a regenerated pickling solution with 18% of HCl and 1% of $FeCl_2$. Each pickling tank region is represented by rectangles delimited by the concentration ranges. The viscosity values range from 0.4 to 1.2 $mPa{\cdot}s^{-1}$.

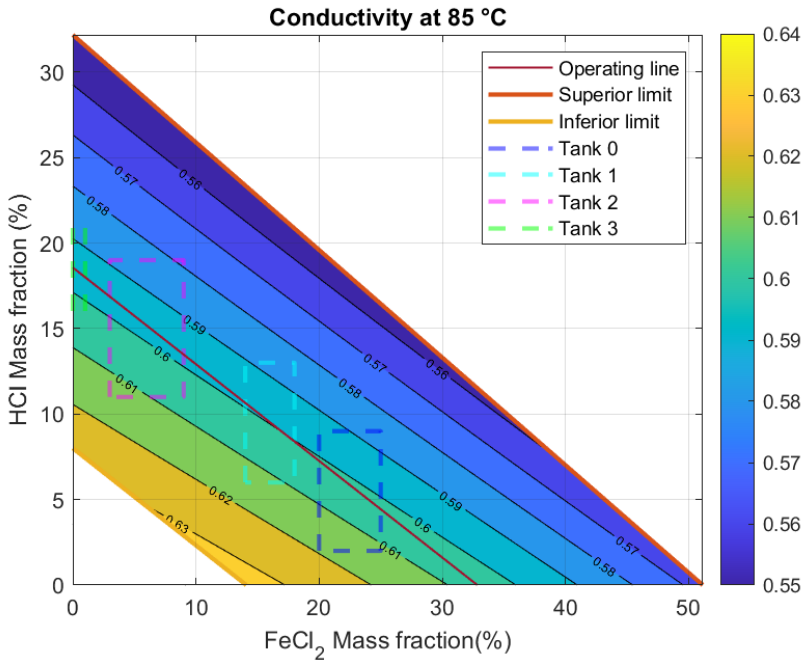

Figure 8 – Thermal conductivity surface plot of in feasible operational region for HCl pickling solution at 85°C. The operating line is based on a regenerated pickling solution with 18% of HCl and 1% of $FeCl_2$. Each pickling tank region is represented by rectangles delimited by the concentration ranges. The values range from 0.55 to 0.64 $W{\cdot}(m{\cdot}K)^{-1}$ in the operating region.

Table 11 – Average thermal conductivity and coefficient of variation according each pickling tank as a function of temperature. The thermal conductivity unit it is at $W{\cdot}(m{\cdot}K)^{-1}$ and temperature in °C. CV refers to coefficient of variation. TK 00 through TK03 consist of each operational tank.

Temperature	TK00		TK01		TK02		TK03	
	Average	CV	Average	CV	Average	CV	Average	CV
65	0.59	1.3%	0.59	1.2%	0.58	1.4%	0.58	0.8%
70	0.59	1.3%	0.59	1.2%	0.59	1.4%	0.58	0.8%
75	0.60	1.3%	0.59	1.2%	0.59	1.4%	0.59	0.8%
80	0.60	1.3%	0.60	1.2%	0.59	1.4%	0.59	0.8%
85	0.60	1.3%	0.60	1.2%	0.60	1.4%	0.59	0.8%

a surface plot of the pickling solution bath at 85°C as a function of HCl and $FeCl_2$ mass fractions. Higher concentrations of $FeCl_2$ and HCl results in a lower conductivity, showing a negative effect of the solutes in the property value.

Table 11 displays the average thermal conductivity and coefficient of variation for each tank and temperature. It shows that temperature has a favorable effect on thermal conductivity. The average value for the ration between property variation and temperature variation is 0.001 $W{\cdot}(m{\cdot}K^2)^{-1}$. The average values range from 0.60 to 0.58 $W{\cdot}(m{\cdot}K)^{-1}$. The coefficient of variation (CV) ranged from 0.8% to 1.3%, showing low deviation around the average.

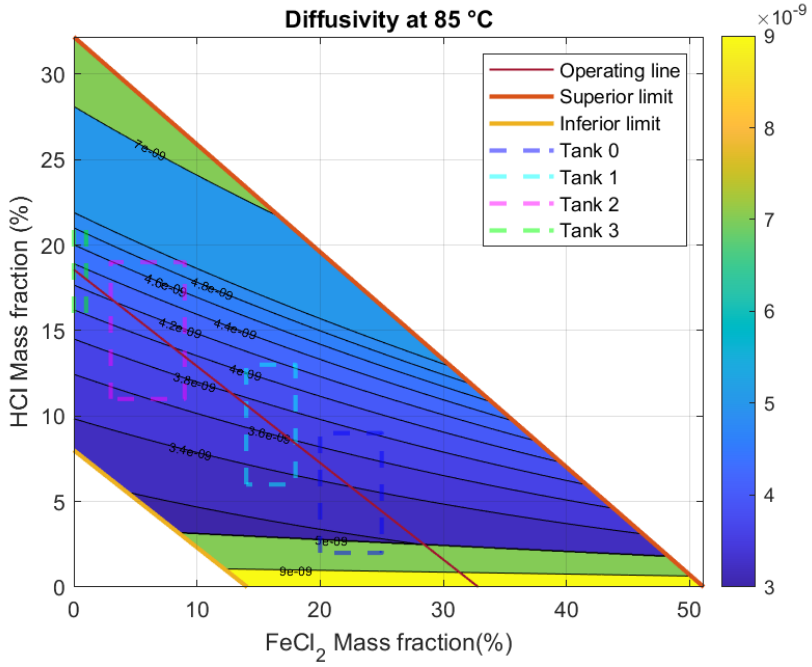

Figure 9 – Diffusion coefficient surface plot in feasible operational region for HCl pickling solution at 85°C. The operating line is based on a regenerated pickling solution with 18% of HCl and 1% of $FeCl_2$. Each pickling tank region is represented by rectangles delimited by the concentration ranges. The values range from $3{\cdot}10^{-9}$ to $9{\cdot}10^{-9}$ $m^2{\cdot}s^{-2}$.

Table 12 – Average HCl diffusion coefficient and coefficient of variation for each pickling tank and temperature. The diffusion is in $10^{-9}m^2{\cdot}s^{-1}$ and temperature in °C. CV refers to coefficient of variation. TK 00 through TK03 consist of each operational tank.

Temperature	TK00		TK01		TK02		TK03	
	Average	CV	Average	CV	Average	CV	Average	CV
65	3.65	31.1%	3.56	6.9%	4.01	9.0%	4.30	5.8%
70	3.68	30.7%	3.59	6.7%	4.03	8.8%	4.32	5.8%
75	3.73	30.9%	3.62	6.6%	4.06	8.7%	4.33	5.7%
80	3.77	31.2%	3.66	6.5%	4.08	8.6%	4.35	5.6%
85	3.81	31.0%	3.69	6.4%	4.11	8.5%	4.38	5.6%

2.4.7 HCl diffusion coefficient

The diffusion coefficient value in the pickling bath solution is important to examine dispersion. Pickling can be defined as a reactive heterogeneous process, thus it is vital to determine the mass transfer rate at the liquid-solid interface. In Figure 9, HCl diffusion coefficient surface plot at 85°C is displayed. The values range from 3 to 9 $\cdot 10^{-9}$ $m^2{\cdot}s^{-2}$, showing the large influence of solutes concentration on the diffusion coefficient, expected from the molarity concentration-dependent calculation criterion. At the operating region, the diffusivity ranges from 3 to 5 $\cdot 10^{-9}$ $m^2{\cdot}s^{-2}$.

Table 12 displays the average values for each tank and temperature in order to analyze the effect of thermal variation on the diffusion coefficient. An increase in temperature has a

positive effect on the property value, whereas $FeCl_2$ concentration has the opposite effect, to be expected from the decrease in HCl molarity. The ratio between property variation and temperature variation averaged $5.7 \cdot 10^{-12}$ $m^2 \cdot (s^2 \cdot K)^{-1}$. Regarding the coefficient of variation, it is observed a high dispersion in the Tank 0 region, explained by the molarity transition point, in which the calculation mode changes from concentrated system to diluted system. The average values ranged from 3.56 to 4.38, a overall average of 3.94.

2.4.8 Semi-quantitative physicochemical property classification

It is proposed three key factor for categorizing each physicochemical property: 1) Material Variation (MV), 2) Temperature Variation (TV) and 3) Coefficient of Variation (CV). MV and TV are intended to evaluate the influence of temperature and iron chloride concentration through the working tanks. CV relates to both temperature and concentration influence in a working tank.

1. **Material Variation (MV)**: Measures the influence of ferrous chloride concentration on the properties. A 5x3 matrix is built from the ratio between the property and $FeCl_2$ variation across tanks for each temperature. The MV is defined as the ratio between the matrix average value and the property average value, multiplied by the tank $FeCl_2$ concentration range.
2. **Temperature Variation (TV)**: Measures the influence of temperature on the properties. A 4x4 matrix is built from the ratio between the property and temperature variation in each tank. The TV is defined as the ratio between the matrix average value and the property average value, multiplied by the temperature range.
3. **Coefficient of Variation (CV)**: It measures the dispersion of the property values within a tank. Assuming that the process follows a normal distribution, the minimum and maximum CVs are multiplied by six. The objective is to cover 99.72% of the values around the average.

Supplementary material presents a detailed calculation for MV and TV for the density property. Each property is categorized with an index between 1 and 4. Table 13 displays the criteria.

In Table 13, MV indexes from 1 to 4 are considered, 1 representing the lowest influence level (up to 5%) and 4 representing values greater than 20%. For the Coefficient of Variation (CV), only two indexes are proposed (1 and 2). CV 1 represents a low dispersion (up to 5 percent), indicating low variation in a working tank. Temperature variation (TV) has three indexes. The first refers to values up to 5%, and the third represents values greater than 11%.

A matrix for classification of acid pickling bath physicochemical properties based on variance and temperature and $FeCl_2$ influence is proposed, based on IEC 61511 and 61508 standards and inspired by SIL (Safety Integrity Level) loop classification (OMEIRI; INNAL; HAMAIDI, 2015). Figure 10 presents the proposed matrix.

Table 13 – Classification criteria for semi-quantitative analysis of physicochemical properties of acid pickling baths. MV refers to the Material Variation, that measures the influence of iron chloride concentration across working tanks. TV is the temperature variation, that measures the influence of temperature in working tanks. CV refers the coefficient of variation multiplied by six. This covers 99.72% of the values in a working tank.

Index	MV		CV		TV	
	Min.	Max.	Min.	Max.	Min.	Max.
1	0%	5%	0%	5%	0%	5%
2	6%	10%	>6%		6%	10%
3	11%	20%	-		>11%	
4	>20%		-		-	

		TV3	TV2	TV1
MV1	CV1	CLASS I	CLASS I	CLASS I
	CV2	CLASS II	CLASS II	CLASS I
MV2	CV1	CLASS II	CLASS II	CLASS I
	CV2	CLASS III	CLASS II	CLASS II
MV3	CV1	CLASS III	CLASS II	CLASS II
	CV2	CLASS III	CLASS III	CLASS III
MV4	CV1	CLASS IV	CLASS III	CLASS III
	CV2	CLASS IV	CLASS III	CLASS III

Figure 10 – A semi-quantitative matrix is utilized for the classification of physicochemical properties of acid pickling solutions. There are four potential classes available, with a range from one to four. Higher the class, more complex the approach to computing the property value. CV consists of six times the value of the coefficient of variation; MV refers to the iron chloride concentration influence regarding the property and TV evaluates the thermal variation of the property.

Table 14 – Ranking of the in the physicochemical properties evaluated. The seven physical properties were classified from I to IV according each parameter evaluated.

Property	MV		TV		CV		Class
	Value	Index	Value	Index	Value	Index	
Density	16%	3	1%	1	12%	2	III
Vapor pressure	17%	4	83%	3	20%	2	IV
Heat of vaporization	27%	4	0%	1	12%	2	III
Viscosity	38%	4	24%	3	48%	2	IV
Specific heat	7%	2	1%	1	31%	2	II
Thermal conductivity	2%	1	2%	1	8%	2	I
HCl diffusion coefficient	1%	1	3%	1	187%	2	I

In Figure 10, four property classes are defined based on matrix region. Class I indicates a low rigorous calculation. In the other hand, properties classified as class IV have more requirements to calculate the physical property.

Based on the property class, the following assumptions could be assumed:

- **Class I**: The property can be assumed to be constant within and between tanks;
- **Class II**: The property can be assumed to be constant within a tank, but not between tanks;
- **Class III**: The property can be assumed constant with temperature or concentration;
- **Class IV**: It is not recommended to assume that the property is constant in and between tanks.

Assuming, for instance, that the MV, CV and TV indexes are, respectively, 2, 1 and 3, the property is classified as class II. This means that the estimated property for a tank can be assumed to be constant within it, but not between tanks. Thus once a property has been estimated within the operating ranges of a tank, it does not require temperature or composition corrections.

Based on this classification methodology, Table 14 presents the classification of each analyzed property. All properties were classified with CV2. This means that the simultaneous effect of concentration and temperature in a working tank is significant. As for the temperature influence (TV), the only properties that are significantly temperature-dependent are vapor pressure and viscosity, rated as TV3. This is explained by the temperature exponential nature of these equations. Regarding the influence of concentration, it was observed that diffusivity and thermal conductivity exhibited a little dependence on concentration, in contrast to vapor pressure, heat of vaporization, density, and viscosity, which displayed substantial variations. The specific heat showed a moderate influence from concentration.

In summary, thermal conductivity and diffusivity are Class I, so it is acceptable to consider the property constant over the different working tanks. Vapor pressure and viscosity were classified as class IV, meaning that for these properties it is recommended to adjust the property as a function of temperature and concentration. Properties classified as Class II (specific heat) can be assumed to be constant in the reference tank, but not between them. For Class III properties (density and heat of vaporization), it is suggested that the property is assumed to be constant inside a tank, but at least one correction (temperature or concentration) must be made, choosing the higher index between MV and TV.

2.5 Conclusions

The research effort was centered around evaluating the physicochemical properties of acid pickling within composition and temperature ranges. The semi-quantitative analysis method allowed the classification of acid pickling properties into four distinct classes (I to IV), with increasing composition and temperature dependence. Density, vapor pressure, heat of vaporization of evaporation, viscosity, specific heat, and HCl diffusion coefficient were evaluated. Thermal conductivity and mass diffusivity, class I, have low variation over the investigated concentration and temperature range. Parameters such as viscosity and vapor pressure, class IV, have a strong relationship with temperature and iron concentration. Specific heat is class II, indicating intermediate interference from composition and temperature, so it can be assumed constant inside a tank. Density and heat of vaporization are class III, requiring at least one correction from temperature or concentration, choosing the one with higher variation.

The equations provided for physicochemical properties calculations are based on published scientific literature. Assumptions were employed in order to provide a consistent approach to perform computations. Experimental studies are necessary to evaluate the reliability of the presented equations. Even so, the plots serve as a reference for professionals and scientists in this industry to estimate the value of physicochemical properties related to acid pickling with HCl.

This study establishes a foundational framework for making simplifications in mathematical models utilized in process simulators, as well as for determining the appropriate dimensions of lines and industrial equipment. Additionally, it covers the operational calculations that will be performed by the supervisory system, known as the Distributed Control System (DCS), within a production plant. Subsequent research efforts pertaining to mathematical models will enhance the capacity to evaluate the influence of physicochemical parameters on the operational parameter of a plant.

3 Kinetic and phenomenological modelling to estimate maximum speeds of pickling lines using dimensionless numbers: a typical chemical reactor engineering approach

General note

This chapter will serve as the basis for the paper entitled "Kinetic and phenomenological modelling to estimate maximum speeds of pickling lines using dimensionless numbers: a typical chemical reactor engineering approach", which will be submitted to specialized journals in the field of chemical engineering, by José Octávio Sierra Fernandez, Diogo Guebert, Luismar M. Porto and Agenor De Noni Jr. Abstract, keywords, acknowledgements and references were omitted. It should be noticed that some minor amendments were performed in the text presented herein, but the methodology, results and conclusions reported in the original paper submitted were not essentially affected.

3.1 Introduction

During the carbon steel hot rolling process, the material is formed at high temperatures and exposed to ambient air. As a result, an oxidation layer forms on the steel surface. The intense thermal conditions, 450 to 800 °C, allow the formation of various oxides, including FeO, Fe_2O_3 and Fe_3O_4 (FENG-I, 1988) (CAO et al., 2014). Scale is the industrial term for this surface layer, which is typically composed by FeO around 85% (w/w), with thicknesses ranging from 5 to 12 μm (ROBSON, 1993). Scale removal is required in industrial units for quality and finishing purposes. Acid pickling is the most common industrial process for scale removal, especially using hydrochloric acid as the pickling agent (LI et al., 2005) (HUDSON, R M; BROWN; WARNING, C J, 1967).

Hydrogen chloride pickling is the prevalent technology in industrial plants, although there are alternative options as presented by Bornmyr (1995), Turkdogan (1971) and Guan *et al.* (2014). According Kladnig (2008), the main advantage of HCl as a pickling agent is its pickling velocity, which is approximately 10 times faster than H_2SO_4 . The main disadvantage of hydrochloric acid, according to Hudson (1994), is the production of acid fumes. Continuous lines are commonly constituted by series-arranged systems of HCl tanks, organized in a countercurrent form. As demonstrated by Gines *et al.* (2002), chemical reactions occur when concentrated acid comes into contact with the steel surface:

$$2\,HCl + FeO \longrightarrow H_2O + FeCl_2 \tag{34}$$

$$6\,HCl + Fe_2O_3 \longrightarrow 3\,H_2O + FeCl_3 \tag{35}$$

$$8\,HCl + Fe_3O_4 \longrightarrow 4\,H_2O + FeCl_2 + 2\,FeCl_3 \tag{36}$$

$$2\,HCl + Fe \longrightarrow FeCl_2 + H_2 \tag{37}$$

Due to FeO being the primary component in the scale, the Equation (34) is predominant among others. The undesirable Reaction, Equation (37) is the result of excessive acid contact with the material (overpickling) (GUAN et al., 2014). This demonstrates that the residence time required for the pickling is a highly sensitive parameter to be controlled to avoid over- or under-pickling. For the design and operation of pickling lines, it is necessary to understand the acid attack velocities as a function of concentration and temperature. Numerous authors have conducted research concerning the chemical kinetics of HCl pickling (HEMMELMANN; XU; KRUMM, 2013) (YAMAGUCHI; YOSHIDA; SAITO, 1994) (GINES et al., 2002) (JATUPHAKSAMPHAN et al., 2010).

Some authors propose empirical equations adjusted to well-defined experimental ranges in order to describe the kinetics of the pickling process (HUDSON, R. M.; WARNING, C. J., 1982) (YAMAGUCHI; YOSHIDA; SAITO, 1994). In these two papers, logarithmic mathematical equations were developed to determine the pickling time as a function of temperature and concentration, Equation (38) and (39). These equations cannot be extrapolated to other operational scenarios, despite being useful for estimations. According to Wen (1968) the acid FeO dissolution is a typical non-catalytic heterogeneous reaction and factors such as scale composition and external resistance can affect the phenomenon. Furthermore, the lack of a rate law in the conventional Arrhenius equation format presents certain challenges in the phenomenological approach to constructing mathematical models, particularly those involving partial differential equation (PDE) systems.

$$\log t = A + B \cdot \log C_{HCl} + D \cdot (T + 459)^{-1} \tag{38}$$

$$t = a \cdot \exp\left[-\theta \cdot \ln\left(\frac{5}{30}\right)\right] \cdot D^{-log\ 6} \tag{39}$$

In Equation (38), A, B and D are model constants. C_{HCl} is the concentration of HCl in $g\cdot(100\cdot\ cm^3)^{-1}$; T is the temperature, in °F; and t is the pickling time, in seconds, required for the material to be descaled. Regarding the Equation (39), θ is the acid temperature, in °C, D is the acid mass fraction, in %. t is the time in seconds and a is a constant.

Despite the prevalence of uncertainties about 10%, it is common practice in an industrial environment to estimate pickling times using empirical equations. Typically, laboratories are equipped with experimental devices for conducting tests on production materials. However, factors such as line speed impact the measurement. This was demonstrated by Hudson (1994), who indicated different empirical parameters for situations in which the velocity exceeds 1.5 $m\cdot s^{-1}$. This demonstrates that mass transfer effects and kinetic resistance must be taken into account. Therefore, the rate law must be known in an independent format, where

kinetics is not associated with mass and heat transfer factors. Thus, the rate law becomes free from transport phenomena. In other words, it is only a function of temperature and HCl concentration.

Gines *et al.* (2002), also suggests an empirical expression, carried out a kinetic study presenting a rate law in an elementary format of exponent 0.86, typical of chemical reaction engineering. The frequency factor and activation energy are presented. Jatuphaksamphan *et al.* (2010) conducted research on the rate law governing the reaction of HCl under steel strips. The ideas are intriguing, but two are questionable: 1) Gines *et al.* (2002) conducted a study whereby the kinetics of pickling were examined. The author determined the pickled fraction, also known as conversion, by employing a sigmoidal function known as the Johnson-Mehl-Avrami (JMA) function. The function illustrates that the pickled fraction exhibits a variation proportional to the power of t raised to the exponent n. and 2) None of the expressions developed took into account the effect of the oxide layer, only parameters related to the fluid phase.

Despite being a common approach for this type of system (leaching) (FOGLER, 2016) (LEVENSPIEL, 1998), the application of Shrinking Core Model (SCM) was not used to solve the problem in the literature reviewed. To evaluate the behavior of acid pickling through HCl, this study aims to develop a phenomenological kinetic model using experimental data from literature. The main idea is to use the Shrinking Core Model (SCM) to evaluate the maximum speed of continuous stripping lines.

3.2 Material and methods

3.2.1 Kinetic modelling

The proposed kinetic model will be based on the following assumptions:

1. Regarding the samples used in the experiment described in (GINES et al., 2002), it is assumed that both sides of the sample have the same dimensional characteristics. The explanation is that during the hot rolling process, both surfaces of the material were exposed to the identical process conditions and duration;
2. The chemical kinetics are assumed to be the rate-limiting step in the process. According to Deng *et al.* (2019), the porosity of scale is approximately 4.8%, indicating a solid with a low void fraction. This allows us to conclude that the solid's diffusion could be neglected. Regarding resistance to external mass transfer, according to Hudson (1994), once the velocity exceeds 1.5 $m \cdot s^{-1}$, it has no effect on the pickling rate. It is assumed that the pickling line is turbulent;
3. It is proposed that the solid phase will consist of a singular component, FeO. According to numerous authors, approximately 85 percent of scale is composed by FeO (FENG-I, 1988);
4. As shown by Equation (34), only one irreversible chemical reaction occurs. Regarding the above assumption, there are no other pathway that can form other

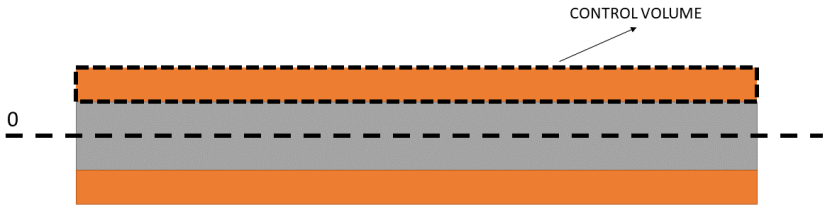

Figure 11 – Control volume for a metallic strip sample. Symmetry is assumed based on the underlying premises. The ratio of thickness between scale and base metal is enhanced. The dimension ratio between scale and base metal is typically three orders of magnitude greater.

oxides;

5. The concentration of ferrous chloride has no effect on the rate of the reaction. According to Hudson (1994), Fe^{+2} concentrations have an effect if they exceed 34 g·(100· mL)$^{-1}$. In this case, an assumption is made that experimental systems do not exceed this limit;
6. It is assumed that the thermodynamic conditions in the fluid phase, namely temperature and concentration of HCl and $FeCl_2$, remain constant. In Gines's work, the author considered a 3 x 3 cm^2 sample with a thickness of 1.8 mm. This demonstrates that a sample's volume does not exceed 2% of the volume of a 100 ml flask. This difference in volume has a negligible effect on thermodynamic variables;
7. The kinetic law is proposed to be based on $r_{HCl} = kC_{HCl}^{m}$. Authors such as Jatuphaksamphan *et al.* (2010) and Gines *et al.* (2002) demonstrated that kinetics are accurately represented by a rate law with this format. In the case of Jatuphaksamphan *et al.* (2010), the authors defined m as 1, while Gines *et al.* (2002) found in their experiments a value of 0.86.

According the assumptions, it is initially proposed a balance to the solid's control volume, as depicted in Figure 11.

The molar balance for the scale was established based on the hypotheses and the proposed scheme.

$$\frac{d}{dt}\left(\rho_{FeO}^{*} \cdot V\right) = -r_{FeO} \cdot V \tag{40}$$

Keep in mind that V refers to the control volume, to which the balance applies, and t refers to time; note that the scale thickness decreases as the pickling rate increase (r_{FeO}). As a result, $V = S \cdot e$ can be defined, where S is the surface area of a flat plate and e is its reduced thickness as a result of acid attack.

Importantly, the rate at which the solid's thickness decreases must be related to the

acid concentration in the liquid phase. Specially, the stoichiometric proportionality between the reaction rates:

$$-\frac{r_{\mathrm{FeO}}}{1} = -\frac{r_{\mathrm{HCl}}}{2} \tag{41}$$

Rewriting Equation (40) in terms of thickness and substituting the solid reaction rate term with respect to HCl pickling rate (r_{HCl}), results in the following:

$$\frac{1}{e}\frac{de}{dt} = -\frac{1}{2}\frac{1}{\rho^*_{\mathrm{FeO}}} r_{\mathrm{HCl}} \tag{42}$$

To examine the behavior of the pickled fraction over time, an expression for the reaction rate is introduced, as stated in the premises. In terms of temperature and concentration dependence, the expression is:

$$\frac{1}{e}\frac{de}{dt} = -\left(\frac{1}{2}\right)\frac{k_0}{\rho^*_{\mathrm{FeO}}} \cdot \exp\left(-\frac{Ea}{RT}\right) C^m_{\mathrm{HCl}} \tag{43}$$

$$e = e_0 \cdot \exp\left[-\left(\frac{1}{2}\right)\frac{k_0}{\rho^*_{\mathrm{FeO}}} \cdot \exp\left(-\frac{Ea}{RT}\right) C^m_{\mathrm{HCl}} \cdot t\right] \tag{44}$$

In Equation (43), k_0 is pickling rate frequency factor; Ea is the activation energy; R is the ideal gas constant; T is the temperature and C_{HCl} refers to HCl molar concentration in liquid phase. Note that m represents the exponent of the pickling rate.

In order to present the kinetic expression in its final form, the Pickled fraction (X) is defined as.

$$X = \frac{e_0 - e}{e_0} \tag{45}$$

In Equation (45), e_0 refers to the initial scale thickness. By substituting the pickled fraction in Equation (44), the final form of the kinetic expression is obtained:

$$X = 1 - \exp\left[-\left(\frac{1}{2}\right)\frac{k_0}{\rho^*_{\mathrm{FeO}}} \cdot \exp\left(-\frac{Ea}{RT}\right) C^m_{\mathrm{HCl}} \cdot t\right] \tag{46}$$

To complete the analysis of the chemical descaling rate, it is advantageous to present the expression in a final surface area-based format as recommended by Fogler (FOGLER, 2016).

$$N_{\mathrm{HCl}} = r_{\mathrm{HCl}} \cdot e \tag{47}$$

Based on the Equation (47), N_{HCl} is the acid molar flux and the r_{HCl} is the volumetric pickling rate. Considering the product of r_{HCl} and e, a new variable it is proposed: HCl pickling rate per surface area (r'_{HCl}).

$$r'_{HCl} = \left[(k_0 \cdot e) \cdot \exp\left(-\frac{Ea}{RT}\right)\right] C^m_{HCl} \tag{48}$$

Equation (48) establishes a relationship between the concentration of hydrochloric acid (HCl) in the liquid phase and the thickness of scale formed on the surface of the material. This particular approach exhibits an advancement above previous propositions in the academic literature due to its inclusion of both phases.

3.2.2 Reactor modelling

The mathematical model applied to the pickling system is based on the solid phase's material and thermal energy balance. The main idea of the solid phase modelling is to use the Plug Flow Reactor (PFR) approach to develop the balances equations. Figure 12 presents a relationship between the classic PFR approach and scale balance used in this paper. For the material balance scenario, the scale defines the control volume. In the context of energy balancing, it is necessary to account for the dimensional difference between the scale and the metal strip, which therefore affects the thermal inertia. As a result, the base metal is regarded as the control volume.

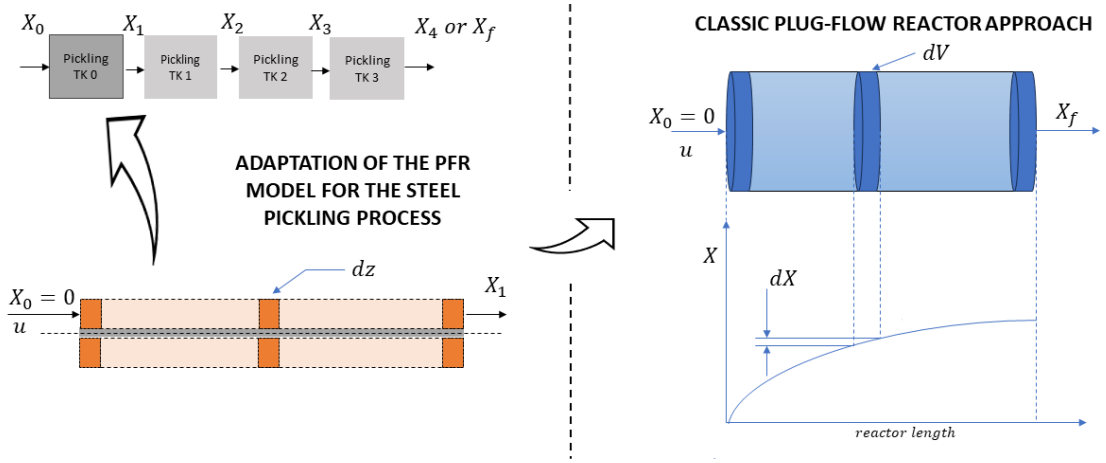

Figure 12 – Phenomenological approach applied to the solid phase of the pickling process. The main idea is to applying PFR (plug-flow reactor) classic model to evaluate the behavior of scale removal from the metallic surface. On the right-hand side, the classic PFR approach is shown, following a typical conversion behavior along the reactor. On the left-hand side, the approach for the solid phase model is presented. Note that for each pickling tank, equipment in series, one reactor, or adapted PFR, was considered.

The material balance in scale is presented by the Equation (49). There are three terms in the equation: 1) a transient term, 2) an advective term, and 3) a material consumption term. Note that the consumption term and the Equation (48) are related.

$$\frac{\partial}{\partial t}(\rho^*_{FeO} S \cdot e) + u \cdot \frac{\partial}{\partial z}(\rho^*_{FeO} S \cdot e) = -r'_{HCl} \Theta_{\frac{FeO}{HCl}} S \tag{49}$$

In the above equation, u represents the flow velocity of the metal strip and z represents the dimension parallel to the surface flow velocity vector. In addition, $\Theta_{\frac{FeO}{HCl}}$ represents the stoichiometric ratio of iron oxide to hydrochloric acid. Mathematically, it is possible to simplify the material balance equation in order to facilitate the approach; thus, the Equation (50) is presented.

$$\frac{\partial e}{\partial t} + u \cdot \frac{\partial e}{\partial z} = -\frac{r'_{HCl}\Theta_{\frac{FeO}{HCl}}}{\rho^*_{FeO}} \tag{50}$$

Equation (50) is a Partial Differential Equation (PDE). It requires an initial condition (IC) and a boundary condition (BC) to be solved. They were defined as described by Eq. (51) and Eq. (52).

$$\text{I.C.:} \quad e(0,\forall z) = e_0 \tag{51}$$

$$\text{B.C.:} \quad e(\forall t, 0) = e_{in} \tag{52}$$

It is essential to remember that e_0 represents the scale thickness at initial time, while e_{in} represents the scale thickness that enters the first pickling tank. Note that, for tanks in series, the initial thickness of a tank equals the final thickness of the previous one.

The energy balance is analogous to the mass balance. However, there is an unique distinction. In addition to the energy generation/consumption term, there is a liquid phase heat transfer term: the heat transfer from the solid to the pickling bath. The Equation (53) illustrates this difference.

$$\frac{\partial}{\partial t}(\rho_s c_{p,s} \cdot S \cdot e_s T_s) + u \cdot \frac{\partial}{\partial z}(\rho_s c_{p,s} S \cdot e_s \cdot T_s) = r'_{HCl}\Delta H_{rx}.S - \lambda S(T_s - T_b) \tag{53}$$

In Equation (53), note that the thermal balance was applied to the entire metallic surface, denoted by the subscript "s". Equation (54) has been mathematically simplified:

$$\frac{\partial T_s}{\partial t} + u \cdot \frac{\partial T_s}{\partial z} = -\frac{r'_{HCl}\Delta H_{rx}}{\rho_s c_{p,s} e_s} + \frac{\lambda}{\rho_s c_{p,s} e_s}(T_s - T_b). \tag{54}$$

In Equation (54), T_s and T_b refer, respectively, to the steel and pickling bath temperatures. ρ_s and $c_{p,s}$ represent the density and specific heat of the steel, respectively. Lastly, λ, ΔH_{rx}. and e_s pertain to the convective coefficient of solid-liquid heat transfer, heat of reaction, and scale-free metal strip thickness, respectively.

Equations (51) and (52) represent, respectively, the initial and boundary conditions.

$$\text{I.C.:} \quad T_s(0,\forall z) = T_{s,0} \tag{55}$$

$$\text{B.C.:} \quad T_s(\forall t, 0) = T_{s,in} \tag{56}$$

In above equations, it is essential to note that $T_{s,0}$ and $T_{s,in}$ represent the temperature of the metallic strip at time zero and the temperature at the tank's inlet, respectively, similarly to the approach adopted for the material balance.

3.2.2.1 Dimensionless form

To simplify the use of the reactor model, dimensionless equations will be presented. According to Ruzicka (2008) (RUZICKA, 2008), the purpose of converting the equations into dimensionless form is to minimize the quantity of process parameters needed and facilitate a more comprehensive comprehension of the prevailing phenomena.

To illustrate variations in scale thickness, various dimensionless quantities are employed, including the pickled fraction X, time τ, length ζ, acid concentration ψ, and temperature θ.

$$\tau = \frac{u}{L} \cdot t \tag{57}$$

$$\zeta = \frac{z}{L} \tag{58}$$

$$\psi = \frac{C_{\text{HCl}}}{C_{\text{HCl},tk}} \tag{59}$$

$$\theta = \frac{T_s}{T_b} \tag{60}$$

In the preceding equations, authors define L as the linear length of a pickling tank and $C_{\text{HCl},tk}$ as the acid concentration in a given pickling tank. Using the above definitions, we can manipulate the Equations (50) and (54) to make them dimensionless:

$$\frac{\partial X}{\partial \tau} + \frac{\partial X}{\partial \zeta} = Da \cdot \exp\left(-\frac{Arr}{\theta}\right) \cdot \psi^m \cdot (1 - X) \tag{61}$$

$$\text{I.C.:} \quad X(0, \forall \zeta) = X_0 \tag{62}$$

$$\text{B.C.:} \quad X(\forall \tau, 0) = X_{in} \tag{63}$$

$$\frac{\partial \theta}{\partial \tau} + \frac{\partial \theta}{\partial \zeta} = Da \cdot Da_T \cdot \gamma \cdot s \cdot \exp\left(-\frac{Arr}{\theta}\right) \cdot \psi^m \cdot (1 - X) + St \cdot \gamma \cdot \Phi \cdot (\theta - 1) \tag{64}$$

$$\text{I.C.:} \quad \theta(0, \forall \zeta) = \frac{T_{s,0}}{T_{b,0}} \tag{65}$$

$$\text{B.C.:} \quad \theta(\forall t, 0) = \frac{T_{s,in}}{T_{b,in}} \tag{66}$$

Two dimensionless groups are introduced in Equation (61): Modified Damkohler number (*Da*) and Arrhenius number (*Arr*). The *Da* in this context is a relationship between the system's advective velocity and the reaction velocity. The *Arr* number relates the molar activation energy of the reaction to the fluid's potential energy. Each group is mathematically presented below by Equations (67) and (68).

$$Arr = \frac{Ea}{R \cdot T_b} \tag{67}$$

$$Da = k_0 \cdot \Theta_{\frac{\text{FeO}}{\text{HCl}}} \cdot \frac{L}{u} \cdot \frac{C^m_{\text{HCl},tk}}{\rho^*_{\text{FeO}}} \tag{68}$$

It is important to note that the Damkohler number is modified in this work in relation to the standards found in petrochemical processes.The authors proposed the term "Pickling number" to refer to *Da*.

Regarding Equation (64) the following dimensionless groups is shown: γ, s, Φ, Da_T and St. Note that γ refers to the volumetric specific heat of the pickling bath ($\rho_{tk} \cdot c_{p,tk}$) to the steel. The ratio of scale to steel strip thickness is defined as s. Φ is the ratio between reactor length (L) and the strip thickness (e_s). The thermal Damkohler number is Da_T (ratio between the heat of reaction and the thermal capacity of the fluid). Finally, Thermal Stanton number (St) is defined as the ratio of the convective heat transfer between the liquid-solid phase and the fluid's advective heat capacity.

$$\gamma = \frac{\rho_{tk} \cdot c_{p,tk}}{\rho_s \cdot c_{p,s}} \tag{69}$$

$$s = \frac{e_0}{e_s} \tag{70}$$

$$\Phi = \frac{L}{e_s} \tag{71}$$

$$Da_T = \frac{\Delta H_{rx.} \cdot \rho^*_{\text{FeO}}}{\rho_{tk} \cdot c_{p,tk} \cdot T_b \cdot \Theta_{\frac{\text{FeO}}{\text{HCl}}}} \tag{72}$$

$$St = \frac{\lambda}{\rho_{tk} \cdot c_{p,tk} \cdot u} \tag{73}$$

Finally, the initial and boundary conditions of the PDE's used are described in Equations (62), (63), (65) and (66).

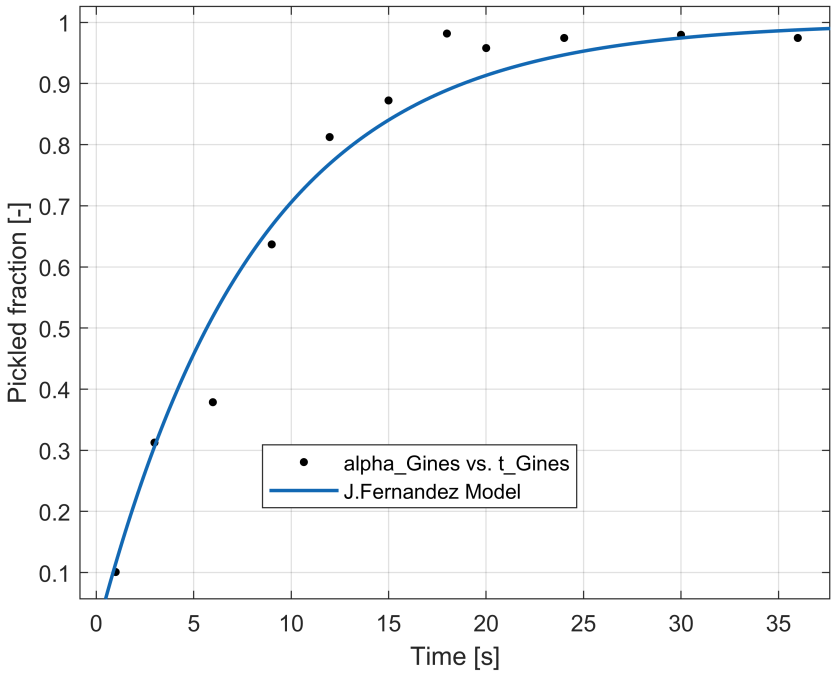

Figure 13 – A non-linear regression curve was constructed using experimental data obtained from the study conducted by Gines *et al.* (2002). The pickling solution under consideration has a temperature of 78 degrees Celsius. It contains 9.6 grams of hydrochloric acid (HCl) per 100 milliliters and 6.9 grams of ferrous chloride ($FeCl_2$) per 100 milliliters. The model is represented by the continuous line, while the experimental data is shown by the dots.

3.2.3 Kinetics data

To estimate the kinetic parameter k_0, the authors did not conduct any experiments. Instead, it was used information from Figure 9 available in Gines *et al.* (2002). In this figure, experimental points of the pickled fraction X *versus* time t are presented. GRABIT a graphical tool box available in MATLAB, were used to extracted the experimental points. To perform the curve fitting another Matlab tool box was used. `Curve Fitter Toolbox` was used to plot the non-linear regression model considering as reference the Equation (46).

3.2.4 Computational tools

The hyperbolic PDE system was solved using the software MATLAB, utilizing a backward finite difference discretization for the time and space partial derivatives. Being an explicit method, the solution was found iterating over the independent variables domains using a fixed step size of 0.004 for the dimensionless time domain and 0.02 for the dimensionless space domain.

3.3 Results and discussions

3.3.1 Kinetics parameters

Figure 13 presents the curve proposed from the kinetic model (Equation (46)) developed in this work, fitted to data from literature (GINES et al., 2002).

Table 15 presents the curve fit parameters obtained using MATLAB. From R^2, it is observed that the model shows a reasonable agreement with the experimental data in comparison with the sigmoidal adjustment proposed by Gines *et al.* (2002), which is 0.977.

Table 15 – Nonlinear regression parameters based on the proposed model using experimental points extracted from Gines *et al.* (2002).

Parameters	**Values**
SSE	0.03827
R - square	0.9632
Adjusted R - square	0.9632
RMSE	0.06186
Kinetic constant (s^{-1})	0.122

Based on the mathematical model, appropriate kinetic parameters for HCl acid pickling process are necessary. Table 16 presents a summary of the kinetic parameters used in this work, including their reference.

Table 16 – Kinetic parameters used in the mathematical model proposed in this work.

Parameters	**Values**	**Reference**
k_0 ($mol^{0.14}\cdot(m^{0.42}\cdot s)^{-1}$)	$1.45\cdot10^7$	From this paper
$\Delta H_{rx.}$ ($kJ\cdot mol^{-1}$)	-63.5	Beck *et al.* (2007)
m	0.86	Gines *et al.* (2002)
$\Theta_{\frac{FeO}{HCl}}$	0.5	Equation (34)
Ea ($J\cdot mol^{-1}$)	38990	Gines *et al.* (2002)
R ($J\cdot(mol\cdot K)^{-1}$)	8.314	Green (2007)

3.3.2 Descaling time

Well established empirical equations from literature were compared to the model developed in this work in order to assess the proposed kinetic model. The typical equation for calculating pickling time is:

$$\log t = A + B \cdot \log C_{HCl} + D \cdot T^{-1} \tag{74}$$

In Equation (74), A, B, and D are empirical constants; C_{HCl} is the concentration of HCl, in $g\cdot(100\cdot cm^3)^{-1}$; T is the temperature, in K; and t is the pickling time, in seconds, required for the material to be descaled.

The proposed kinetic model were compared to those developed by Hudson (1994) and Gines *et al.* (2002), in order to assess the model's accuracy. In Table 17, the parameters utilized in these works are shown.

The parameters in Table 17 were analyzed under the following assumptions:

Table 17 – This summary describes the parameters that were taken into consideration by Hudson (1994) and Gines *et al.* (2002) in their respective studies. The values assigned to the material utilized in the studies are derived from the average of the samples employed. The parameters of the empirical models, namely A, B, and D, contain identical units and are associated with a common reference equation.

Parameter	Hudson (1991)	Gines et al. (2002)
Steel type	ingot-cast low-carbon	commercial hot-rolled steel
Scale amount ($kg \cdot m^{-2}$)	0.036	0.041
Scale thickness (μm)	6.6	7.9
HCl concentration range ($g \cdot (100 \cdot cm^3)^{-1}$)	1 - 14	3 - 11
Temperature range (°C)	66 - 93	80 - 90
Iron II concentration ($g \cdot (100 \cdot cm^3)^{-1}$)	up to about 30	4 - 12
A	-2.220	-6.183
B	-0.870	-0.776
D	1569	2967

1. The HCl concentration range analyzed was between 3 and 11 $g \cdot (100 \cdot cm^3)^{-1}$;
2. The studied temperature range was between 80 and 90 °C. The models were compared at three different temperatures: 80, 85, and 90 °C;
3. Despite the empirical model developed by Gines *et al.* (2002) taking the Iron II effect into account, the effect is ignored in this work. According to Hudson (1994), the influence of Fe content in solution (as $FeCl_2$) is negligible unless it exceeds the limit of 34 $g \cdot (100 \cdot cm^3)^{-1}$;
4. The ratio between the scale amount and scale thickness was employed in order to determine the molar density of the scales. The only constituent being considered is FeO;
5. As noted by Gines *et al.* (2002), the analytical procedures employed to evaluate pickling times rely on visual examinations, specifically, unaided eye observations. Consequently, the analysis may have been conducted under the assumption that the pickling process was not fully completed. The utilization of microscopy would be necessary in order to conduct a meticulous visual examination. Many kinetic expressions are formulated using sigmoidal equations, which have an asymptotic behavior approaching 1. In this study, a reference value of 0.973 is assigned to the pickled fraction in order to compare it with the visually determined pickling completion seen during the studies. The reference value utilized in this study was determined based on the minimal value as reported by Gines et al. (2002).

Figure 14 presents the results obtained comparing the kinetic model proposed in this work with the empirical model of Hudson (1994). There was good agreement with the model in all scenarios studied. The average error between the models for the temperatures of 80, 85 and 90 °C, respectively, were: 6%, 1% and 3%, demonstrating an error of less than 10%

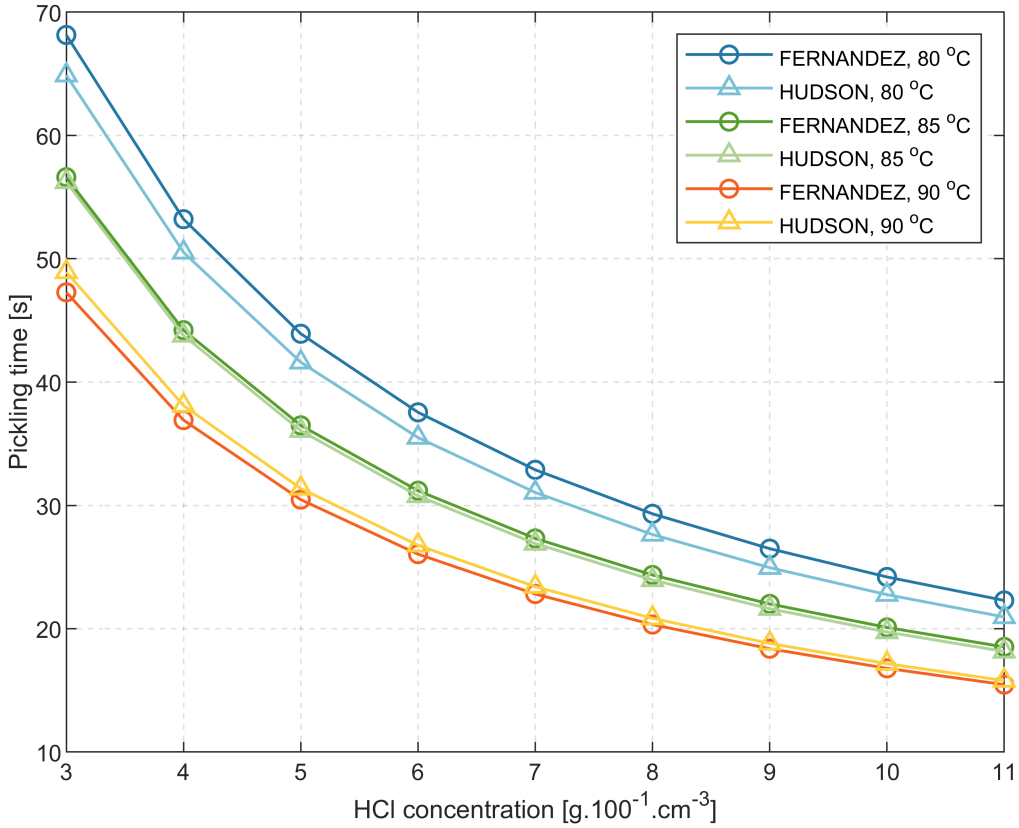

Figure 14 – Comparisons between the empirical model provided out by Hudson (1994) and the phenomenological kinetic model created in this work. The analysis was conducted using three distinct working temperatures, specifically 80, 85, and 90 degrees Celsius. Additionally, a range of hydrochloric acid concentrations between 3 and 11 grams per 100 cubic centimeters was considered. The study conducted by Fernandez *et al.* demonstrated a high level of agreement between their model and the Hudson model when considering temperatures of 85 and 90 degrees Celsius. The average errors observed were consistently below 3%. At the temperature of 80 degrees Celsius, the average error exhibited the highest value, reaching a magnitude of 6%. The kinetic model employed a conversion rate of 97.2% as a benchmark for pickling completion, based on the asymptotic behavior approaching 1 of the pickled percentage.

in the thermal and concentration range studied.

Figure 15 presents the results obtained comparing the kinetic model proposed in this work with the empirical model of Gines *et al.* (2002). In this case, there were more discrepancy in comparison to the data from Hudson (1991). The average error between the models for the temperatures of 80, 85 and 90 °C, respectively, were: 14%, 6% and 3%, demonstrating an error exceeding 10% in the studied thermal and concentration range.

The comparison between the proposed kinetic model and the models from literature shows that the developed expression can be used to compute the pickling time required for industrial operation. The main reason for the errors found, while negligible in most scenarios,

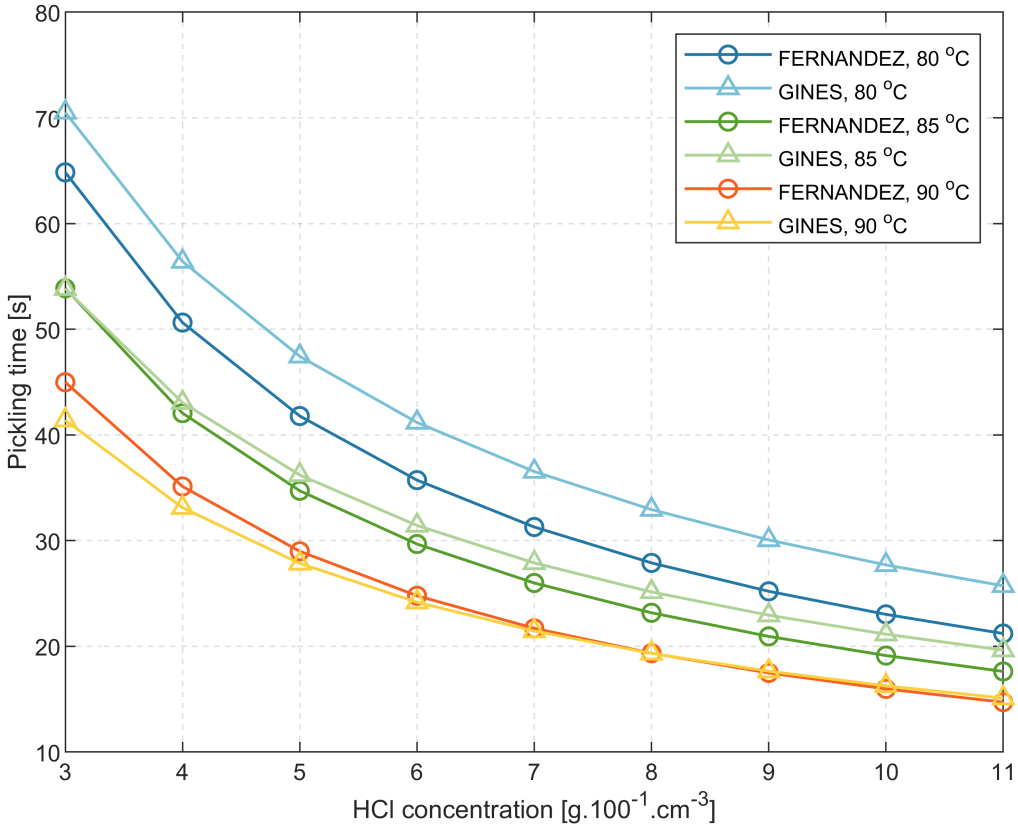

Figure 15 – Comparative result between the empirical model presented out by Gines et al. (2002) and the phenomenological kinetic model created in this work. The investigation was conducted using three distinct working temperatures, specifically 80, 85, and 90 degrees Celsius. Additionally, a range of hydrochloric acid concentrations between 3 and 11 grams per 100 cubic centimeters was employed. The model proposed by Fernandez et al. demonstrated a high level of agreement with the Gines model when considering temperatures of 85 and 90 degrees Celsius. The average errors observed were consistently below 6%. Under the condition of 80 degrees Celsius, the average error exhibited the highest value, reaching a magnitude of 15 percent. The kinetic model employed a conversion rate of 97.2% to represent pickling descaling based on eye inspection, owing to the asymptotic trend of the pickled percentage approaching 1.

Table 18 – Carbon steel parameters used as a reference to compare the reactor model with the results from Gines *et al.* (2002).

Parameter	Value	Reference
W (kg·m^{-2})	0.043	Gines *et al.* (2002)
e_{in} (m)	$8{\cdot}10^{-6}$	Gines *et al.* (2002)
ρ^{*}_{FeO} (mol·m^{-3})	74815	$\rho^{*}_{\mathrm{FeO}} = \frac{W}{e_{in}\cdot 0.071}$
e_s (m)	$1.8{\cdot}10^{-3}$	Gines *et al.* (2002)
$c_{p,s}$ (kJ·(kg·K)$^{-1}$	0.434	Bergman *et al.* (2011)
ρ_s (kg·m^{-3})	7870	Bergman *et al.* (2011)

is the fact that the kinetic constant was extracted based on a single experimental curve where the concentration of HCl, Fe $^{+2}$ and temperature were well defined. It is believed that if the study is extrapolated to more experimental curves, the tendency is to obtain more reliable parameters.

Another critical point in the study is the pickling descaling being qualitative, and not quantitative. In future studies, it would be interesting to use a quantitative reference to define the relationship between the visual inspection of the pickled sample and the value measured using a more robust analytical tool. This would allow for a greater precision regarding the actual and apparent (naked eye) pickled fraction.

3.3.3 Maximum line speed

The partial differential equation system described in Section 3.2.2 can be applied to compute the maximum speed of a pickling line and compare the results to those found in the literature, specifically in the work of Gines *et al.* (2002).

To test the consistency of the suggested model, the same technical information supplied in the reference literature is employed for analysis purposes. In Gines *et al.* (2002), the authors computed the maximum pickling speed using two methods: 1) an empirical equation derived from experimental tests, and 2) a JMA-type equation derived from a constructed kinetic model. It is recommended in the technical literature Hudson (1994) to use the following expression to calculate maximum pickling speed:

$$u_{\mathrm{max.}} = \Sigma_{j=1}^{n} \frac{L_j}{t_{dj}} \tag{75}$$

In Equation (75), $u_{\mathrm{max.}}$ is the maximum line speed; N is the number of pickling tanks in series; L_j is the length of each tank, in meters; and t_{dj} is the pickling time, in seconds, required to complete descaling a sample of material, typically an expression in the form of Eq. (74).

Tables 18 and 19 present a summary of the parameters adopted in the developed reactor model, including their references.

Table 19 – Parameters for the four pickling tanks considered to evaluate the reactor model, at the same conditions from the work of Gines *et al.* (2002).

Parameter	**TK00**	**TK01**	**TK02**	**TK03**	**Reference**
x_{HCl}	3%	6%	7%	8%	Gines *et al.* (2002). Reference value in g·(100 mL^{-1}).
x_{FeCl_2}	13%	9%	11%	9%	Gines *et al.* (2002). Reference value in g·(100 mL^{-1}).
T	362	363	360	368	Gines *et al.* (2002)
L	20.5	20.5	20.5	20.5	Gines *et al.* (2002)
ρ_{tk}	1097	1078	1101	1087	Authors previous work (SIERRA FERNANDEZ et al., 2023b). Density modelling based in Laliberte (2004)
$c_{p,tk}$	3.47	3.48	3.33	3.33	Authors previous work (SIERRA FERNANDEZ et al., 2023b). Specific heat modelling based in Laliberté (2009)
μ_{tk}	0.51	0.48	0.53	0.48	Authors previous work (SIERRA FERNANDEZ et al., 2023b). Viscosity modelling based in Laliberté (2007)
k_{tk}	0.63	0.63	0.62	0.62	Authors previous work (SIERRA FERNANDEZ et al., 2023b)
$C_{HCl,tk}$	1028	1667	2222	2500	From Gines *et al.* (2002). Reference value in g·(100 mL^{-1}).

A series of four pickling tanks were considered, as described in Table 19, to compare the reactor model with the traditional technical approach. A HCl concentration and temperature condition was considered for each tank. The dimensionless numbers required by the model for each tank physical conditions (TK00 to TK03) are presented in the Table 20.

Table 20 – Dimensionless parameters required by the pickling reactor model developed in this work. The dimensionless groups calculation are based on physical properties tables from the reference material and pickling tanks operational conditions, according to Gines *et al.* (2002).

Parameter	TK00	TK01	TK02	TK03	Reference
Da	$2.2{\cdot}10^{5}$	$3.4{\cdot}10^{5}$	$4.3{\cdot}10^{5}$	$4.8{\cdot}10^{5}$	Equation (68)
Da_T	$3.6{\cdot}10^{-5}$	$3.7{\cdot}10^{-5}$	$3.8{\cdot}10^{-5}$	$3.8{\cdot}10^{-5}$	Equation (72)
Arr	12.9	12.9	13.0	12.7	Equation (67)
γ	1.1	1.1	1.1	1.1	Equation (69)
s	$8.9{\cdot}10^{-3}$	-	-	-	Equation (70).
Φ	$2.3{\cdot}10^{4}$	$2.3{\cdot}10^{4}$	$2.3{\cdot}10^{4}$	$2.3{\cdot}10^{4}$	Equation (71)
Re	$1.5{\cdot}10^{8}$	$1.6{\cdot}10^{8}$	$1.5{\cdot}10^{8}$	$1.6{\cdot}10^{8}$	-
Pr	2.8	2.7	2.9	2.6	-
Nu	$1.5{\cdot}10^{5}$	$1.6{\cdot}10^{5}$	$1.5{\cdot}10^{5}$	$1.6{\cdot}10^{5}$	$Nu = 0.0308 \cdot Re^{4/5} \cdot Pr^{1/3}$
St	$3.6{\cdot}10^{-4}$	$3.7{\cdot}10^{-4}$	$3.5{\cdot}10^{-4}$	$3.7{\cdot}10^{-4}$	$St = \frac{Nu}{Re \cdot Pr}$

The parameters defined in Table 20 were used to simulate the pickling tanks behavior. The idea is to use the reactor model as a phenomenological alternative to estimate the maximum speed of pickling lines given certain operational and design conditions. The dynamic behavior of the system was evaluated for an interval of 4 residence times, and the velocities resulting in final conversions of 97.3 and 99.2% were calculated. These conditions are considered to be equivalent to a qualitatively finished strip.

Table 21 – Comparison of maximum pickling speeds evaluated between empirical and reactor model. The empirical models are based on logarithmic expressions defined from three coefficients and a function of hydrochloric acid concentration and temperature. The presented sigmoidal model was an evolution in relation to the existing one in the literature and takes into account the kinetic effects. The reactor model is based on a partial differential equation that takes into account kinetic and transport parameters. The results indicate that the empirical coefficients of Gines *et al. (2002)* and the assumption of a 99.2% conversion significantly deviate from the speed values as noted in the error.

Parameter	Empirical model		Sigmoidal model	Reactor model	
	Hudson (1991)	Gines et al. (2002)	Gines et al. (2002)	X=97.3%	X=99.2%
Max. velocity ($m{\cdot}min^{-1}$)	204	240	202	193	144
Error (compared with X= 97.2%)	5.7%	24.3%	4.6%	-	-

Table 21 compares the proposed reactor model with empirical and sigmoidal models from other works. For the defined operational and design configurations, the results demon-

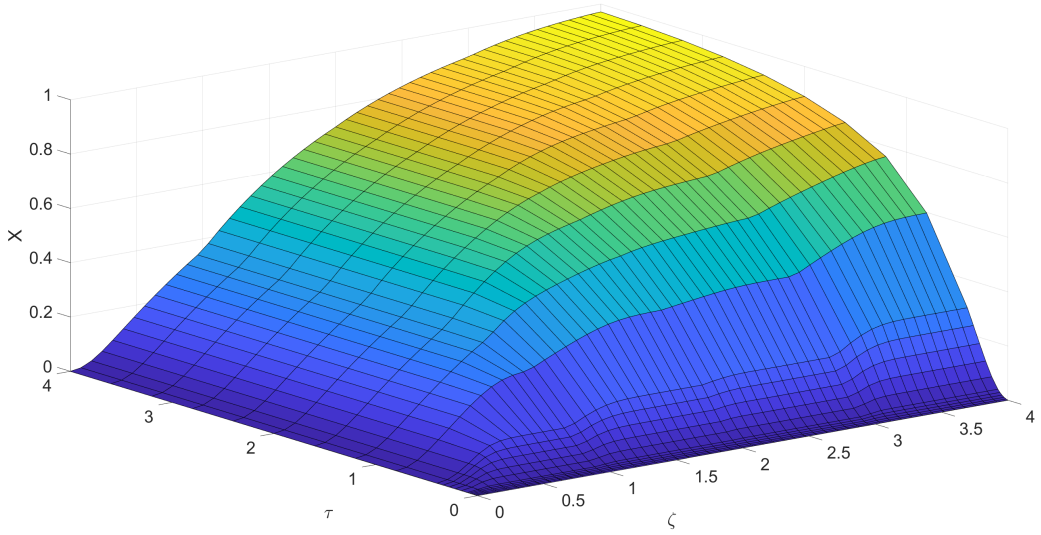

Figure 16 – Pickled fraction transient behavior over four tanks in series. ζ refers to the dimensionless length axis, τ refers to dimensionless time and X refers to the scale stripped fraction. The surface plot was created considering a speed of 193 m·min^{-1} and a final pickled fraction of 97.3%. In approximately four dimensionless times, or 24 seconds, the system enters a steady state.

strate that the maximum pickling speed ranges from 144 to 240 m·min^{-1} considering 99.2% conversion in the proposed model and by the empirical model presented by Gines *et al.* (2002). The reactor model maximum velocity for a final conversion of 97.2% showed good consistency with the velocities predicted by the empirical model byHudson (1994) and for the sigmoidal model by Hudson (1994), with errors of less than 10%

The proposed model maximum speed amplitude shows a variation of 25% in relation to the average value of 197 m·min^{-1}. In addition, it is observed that assuming a conversion of 99.2% is somewhat exaggerated, indicating that the conversion value corresponding to the qualitative inspection carried out in industry is closer to 97%.

3.3.4 Transient analysis

Figure 16 shows the pickled fraction transient behavior over the four pickling tanks. The simulation was carried out considering a speed of 193 m·min^{-1} for the metallic surface, and the pickled fraction at the exit of the system to be 97.2%. From the surface graph, it is seen that the system enters steady state in an interval of four residence times.

Figures 17a and 17b show, respectively, the pickled fraction profile at the first residence time and at the interval between third and fourth time. The interval was segmented in intervals consisting of 10% of the total time interval. From Figure 17b it is shown that the tanks are roughly stabilized, only the last one still showing some variation. Thus after around 24 seconds the system can be considered to be in steady state.

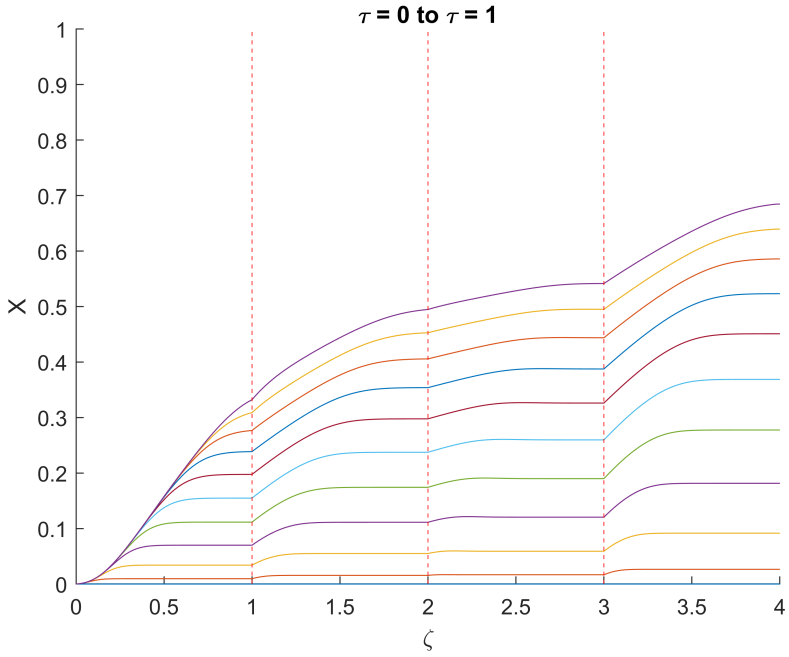

(a)

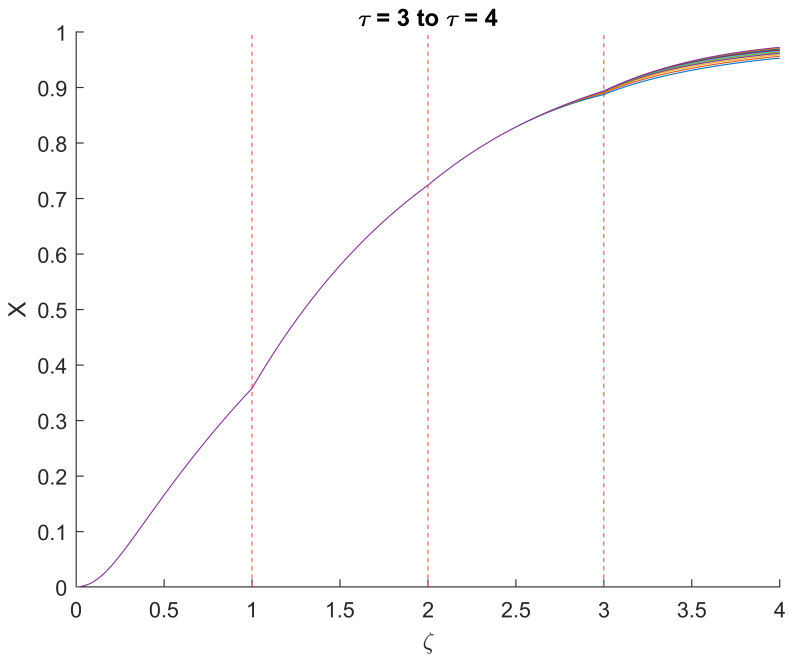

(b)

Figure 17 – Pickled fraction evolution over four tanks in series. Figure 17a refers to the time period between 0 and 1 residence times (τ). The colored curves represent the behavior of a fraction of 10% of the evaluated interval, that is, 2.3 seconds. The dotted vertical lines delimit the interface between tanks. It shows that the entire system is roughly in steady state at the interval between 3 to 4 residence times, only the last tank showing a minimal variation on the pickled fraction over time.

3.3.5 Material balance

Based on the results for the pickled fraction in the tanks, a mass balance was performed to estimate the mass flow rate between pickling tanks, as well as to estimate the amount of acid solution required for the system. Table 22 presents the summary of the calculated material balance.

Table 22 – Mass balance along the pickling line. ΔX refers to the pickling variation between two adjacent tanks. For this calculation purposes, it was considered a steel strip width of 1.8 m and that the concentrated acid bath enters the system with 17% acid in weight and at a temperature of 60 °C. Ferrous chloride and water are considered to be generated stoichiometrically by the reactions.

Phase	**Parameters**	**Strip inlet**		**TK00 outlet**		**TK01 outlet**		TK02 outlet		TK3 outlet		Acid inlet	
Solid	X		0%		35.6%		72.3%		89.5%		97.2%		-
	ΔX		0%		35.6%		36.8%		52.7%		44.5%		-
	FeO ($kg \cdot h^{-1}$)		1793		1155		496		189		50		-
Interface	FeO ($kg \cdot h^{-1}$)		0		638		659		307		139		-
Liquid	**Composition**	Mass flow	**mass frac.**	Mass flow	Mass frac.	Mass flow	Mass frac.	Mass flow	Mass frac.	Mass flow	Mass frac.	Mass flow	Mass frac.
	$FeCl_2$	-	-	3149	21%	2024	14%	861	6%	320	2%	75	1%
	HCl	-	-	531	4%	1178	8%	1847	13%	2158	16%	2299	17%
	H_2O	-	-	11384	76%	11224	78%	11059	80%	10982	82%	10947	82%
	Total ($kg \cdot h^{-1}$)	-	-	15063	100%	14426	100%	13767	100%	13460	100%	13321	100%

In Table 22 six different regions of the pickling system are considered, that is, the four different tanks, a metallic strip inlet region and a concentrated acid inlet. The surface enters the system at a temperature of 25 °C. The acid bath at the inlet has an acid mass fraction of 17% and is at 60 °C. The required acid demand was calculated based on the amount of scale entering the system. The $FeCl_2$ and H_2O were calculated from FeO mass flow rate and the reaction stoichiometric. The acid mass flow rate is defined as the amount of acid entering the previous stage plus the amount of iron chloride and water generated in the chemical reaction. It is important to keep in mind, that the process of elaborating the material balance using the reactor model is iterative. Ideally, one should return to the model with the update of the concentrations calculated by the balance and, thus, obtain a new pickled fraction profile. The process should run until a minimal (tolerable) error is found. For the example developed here, this practice was not used because the intention was only to demonstrate the potential of the tool.

3.3.6 Heat loss analysis

The proposed mathematical approach does not take into account the effect of evaporation, that is expected to be the main source of thermal losses in the system, although a thermal balance was modeled in order to assess the thermal behavior. As a significant thermal gradient is only observed in the first tank, Figure 18 shows the TK00 surface graph.

In Figure 18, it is observed that the metallic surface reaches thermal equilibrium with the bath at approximately 20% of the first tank length (4 m). The system reaches the steady state in less than 1 residence time. The heat consumption required for the first pickling tank was estimated to be approximately 2278 kW, or equivalent to 3.7 ton·h^{-1} of saturated steam at low pressure. For future work, it would be interesting to take into account the effect of evaporation in the required thermal consumption analysis for the pickling system.

3.4 Conclusions

This paper presents a typical chemical engineering approach for evaluating scale consumption throughout a pickling system. A reactor model applied to an acid pickling system was developed with the aim of being an alternative to the typical empirical or sigmoidal models available in literature. Data from literature was used to estimate kinetic parameters required for the proposed phenomenological model, based on the Shrinking Core Model (SCM). Comparing the results with empirical equations data showed good consistency for well-defined ranges of concentration and temperature, even though the kinetic data was extracted from a single kinetic curve.

In order to examine the phenomenon of scale removal from material surfaces, a mathematical model based on partial differential equations was employed. This model facilitated the derivation of a series of dimensionless quantities, with particular emphasis on the modified Damkoehler number or Pickling number. This number is determined by the relationship between the flow velocity of the metallic surface and the kinetic velocity associated with the

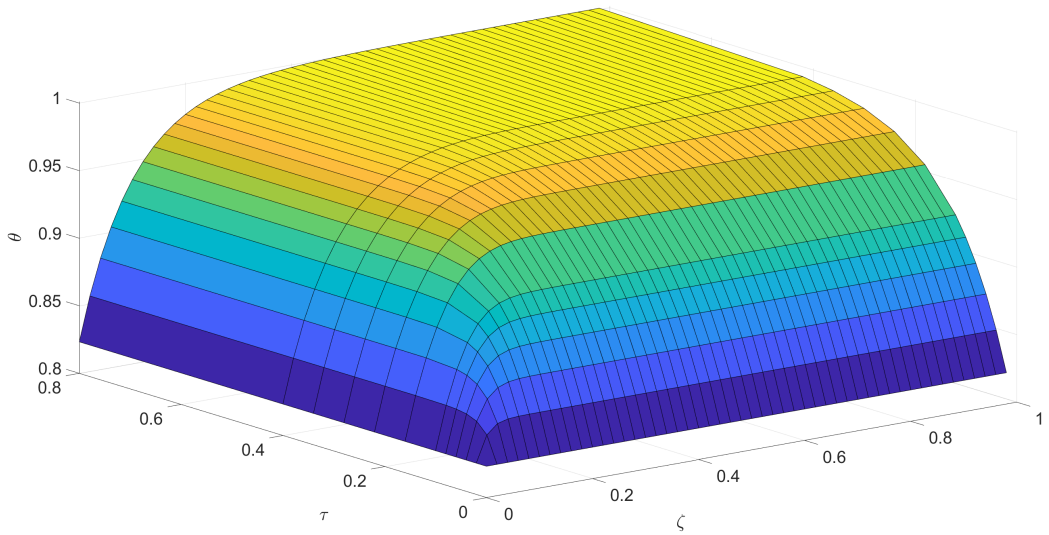

Figure 18 – Transient thermal profile in the first pickling tank. The generated surface is based on the strip metal thermal balance, considering a constant pickling bath temperature. ζ refers to the dimensionless axis and τ to the residence time. On the first tank the temperature needs to be raised from ambient temperature to the bath temperature. The temperature reaches thermal equilibrium in approximately 0.4 residence times. As other sources of thermal losses along the system are not considered, it was not observed significant thermal variations on the other tanks. At around 20% (approximately 4 m) of the first tank length the metallic strip is already in thermal equilibrium.

pickling process. A magnitude order of 10^5 was determined for the Pickling number value. The researchers created an approach based on the model to determine the residence time required to achieve steady state. Additionally, they conducted liquid phase mass balance calculations for the purpose of design.

A thermal balance on the metallic surface showed that significant thermal loss only occurs in the first tank, although the balance did not take into account evaporation and other losses to the environment, resulting in a negligible thermal gradient in the other tanks.

The aforementioned methodology has the potential to enhance the formulation of design equations for comparable systems, hence enabling the evaluation of energy and productivity improvement to enhance the sustainability of the process. Furthermore, potential areas for enhancing the models pertaining to evaporation and the transfer ratio of solutes at the interface between a solid and a liquid were highlighted.

4 MODELLING AND SIMULATION OF THE INDUSTRIAL ACID PICKLING PROCESS WITH HCl: A CHEMICAL REACTOR PHENOMENOLOGICAL APPROACH

General note

This chapter will serve as the basis for the paper entitled "Modelling and simulation of the industrial acid pickling process with HCl: a chemical reactor phenomenological approach", which will be submitted to specialized journals in the field of chemical engineering, by José Octávio Sierra Fernandez, Diogo Guebert, Luismar M. Porto and Agenor De Noni Jr. Abstract, keywords, acknowledgements and references were omitted. It should be noticed that some minor amendments were performed in the text presented herein, but the methodology, results and conclusions reported in the original paper submitted were not essentially affected.

4.1 Introduction

The industrial process of acid pickling is a physicochemical operation responsible for removing iron oxide (scale) from the surface of metal strips. The operation is carried out making use of a chemical agent, for example hydrochloric acid. According to Kladnig (2008) the main advantage of applying HCl is due to higher reaction speeds, as well as resulting in better finishing conditions. Due to advantages like those, industrial application using HCl is the most common. On the other hand, Hudson (1994) mentioned that the main disadvantage of applying hydrochloric acid is the fact that it generates excessive acid fumes.

Typically, according to Isopescu *et al.* (2015), the acid pickling process using hydrochloric acid, regardless of the characteristics of the equipment, consists of applying an acid solution of HCl; a surface chemical reaction occurs resulting in the formation of $FeCl_2$. As the reaction takes place on the surface, the pickling bath loses its effectiveness due to the increase in the concentration of iron II ions in the solution. Industrially, the operation takes place in countercurrent, that is, pickling tanks arranged in series (normally three or four tanks) are exposed to different concentrations of HCl. As it is countercurrent, the baths with the highest acid concentration come into contact with the surface leaving the system, *i.e.*, the last tank. The solution with low contents of acid comes into contact with the new material, which is inserted into the first tank of the system. A series of tanks is arranged in a cascades arrangement to facilitate the flow of fluids between the different stages. Always from the most concentrated in terms of HCl to the lowest. On regards to the thermal configurations of the different tanks, industrially, temperatures ranging from 65 to 85 °C are used. Depending on the composition of the solution in terms of HCl and ferrous salts, the operating temperatures make an environment favorable to evaporation.

Regarding the thermal conditions of the different pickling baths, typically in industrial practice, the process is operated at identical temperatures, or with a variation of less than 5%, in all Hudson (1982) tanks. However, the composition of the baths undergoes significant

variation. In terms of HCl, as it is a countercurrent operation, the first bath usually presents concentrations of 3% to 5%; the last has a concentration ranging from 16% to 18%. When analyzed in terms of $FeCl_2$ composition, the behavior is reversed: in the last bath the concentrations of this salt are at a minimum, and in the first bath the concentrations are at a maximum. Therefore it is expected that, regardless of the operating temperatures at which the process operates, an evaporation gradient will occur. This gradient is gradually increased as you advance from the first to the last tank. The present scenario results in a discussion of the potential impact of evaporation on operational efficacy and the potential advantages of operating the tanks at varying temperatures. Hudson *et al.* (1967) investigated the influence of evaporation as a relevant factor in the pickling operation using HCl.

In the context of chemical processes, particularly those involving chemical reactions, it is observed that reaction temperatures have a significant impact on the rate law, as discussed by Fogler (2016). This phenomenon can be attributed to the Arrhenius law. Therefore, it is postulated that the fluctuation of thermal conditions during the operation of the reaction medium has the potential to exert a substantial influence on the conversion efficiency of a specific chemical reactor. This is an incentive to evaluate the impact of potential evaporation losses on the efficacy of the pickling procedure.

In the field of industrial operations, pickling lines, particularly those characterized by turbulent flow, are meticulously engineered and appropriately set up to facilitate controlled evaporation. This involves the implementation of a gas collection system for each process tank, which efficiently collects the generated gases and manages them through gas scrubbing systems, as described in Hudson's work on pickling (HUDSON, R., 1994). The reason for industrial operations employing this safety precaution comes from the subsequent motives:

1. According to the National Fire Protection Agency (NFPA), HCl is classified as a hazardous substance, classified in level 3 of 4 levels (CROWL; LOUVAR, 2001);
2. Organization Safety and Health Administration (OSHA) recommends that in an environment where workers are exposed, the maximum concentration in the environment in terms of HCl should be 5 ppm (BENINTENDI, 2021).

In general, the objective of this work is to present a phenomenological approach in order to evaluate the influence of evaporation on the maximum speed of turbulent acid pickling lines. Furthermore, it is of interest to the authors to conduct a preliminary validation of the model using operational data from an industrial facility in order to verify its consistency by comparison with the maximum design velocities against simulated velocities.

4.2 Material and methods

4.2.1 Phenomenological approach

The methodology employed to represent the physical problem in this instance originates in commercial frameworks seen in process simulators; that is, the pickling system is segmented into a series of unit operations. Each of the blocks depicted in Figure 19 represents

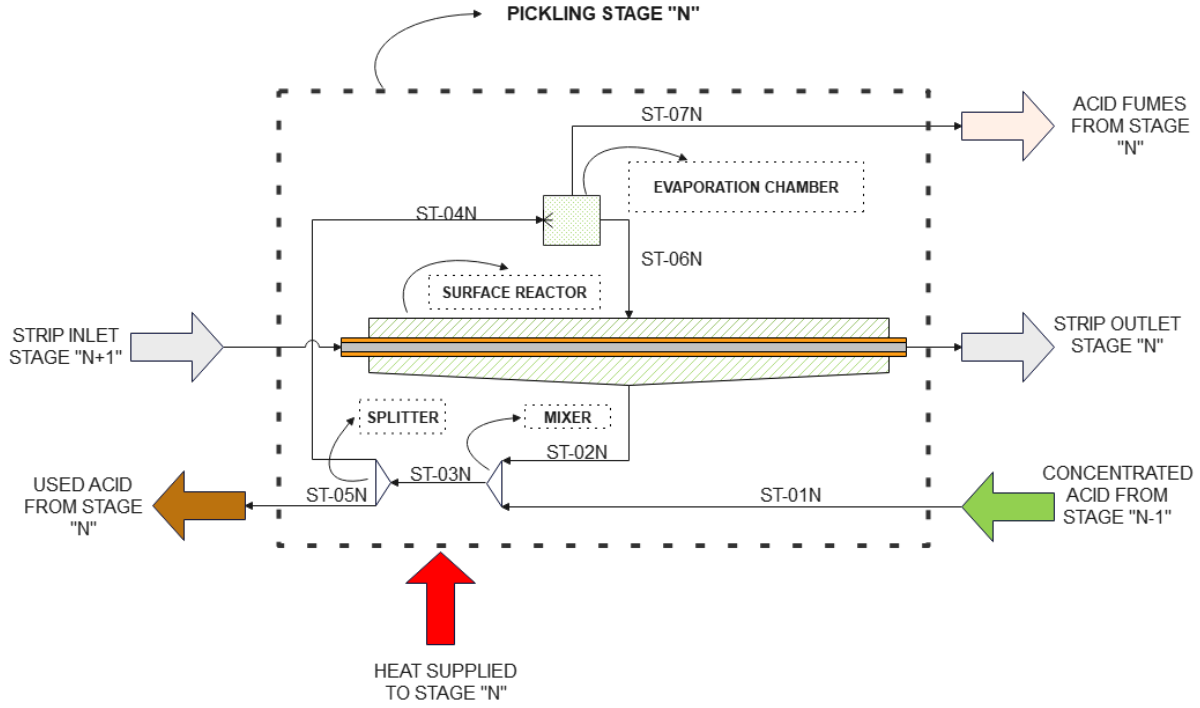

Figure 19 – Conceptual block diagram for a generic pickling stage "N".

a characteristic equation.

The graphic depicted above illustrates the battery constraints of the procedure, which will now be described. The aforementioned statement refers to the envelope that encompasses all the unit operations involved in the process. It should be noted that inside this block, there exists a total of six process streams, with four of them facilitating communication between pickling steps, while the remaining two do not serve this purpose.

Regarding the process streams that communicate between the stages, there are:

1. Concentrated acid from stage "N-1";
2. Used acid from stage "N";
3. Strip inlet from stage "N+1";
4. Strip outlet from stage "N".

In other hand, process streams that do not communicate between stages, is called as utility streams:

1. Heat supplied to stage "N";
2. Acid fumes from stage "N".

Based on the description of each process and utility streams, is important describe the unit operations present inside the envelope (pickling stage "N"):

- Pickling bath concentrated in acid comes from stage "N-1" (ST-01N) and is mixed in the MIXER-N with stream ST-02N (bath collection stream from SURFACE REACTOR-N). A perfect mix is performed and then the ST-03N STREAM leaves the system and feeds the SPLITTER-N.
- In the SPLITTER-N, the ST-05N stream leaves the system with the same volumetric flow as the ST-01N. The objective is to ensure that the system level remains constant in the model. The difference between the stream ST-03N and ST-05N consists of the load that goes to the EVAPORATION CHAMBER-N. Is important to point out that in this stream, heat is supplied in order to guarantee that the operational temperatures remain in compliance with the specifications of the industrial process.
- When entering the EVAPORATION CHAMBER-N, two streams are calculated and therefore defined: ST-06N is the amount of liquid remaining after the evaporation process in the *sprinklers*, and ST-07N is the stream of acid fumes and evaporated water. The ST-07N stream goes to a non-modeled exhaust and gas washing system. The ST-06N stream, on the other hand, refers to the effective charge that will go to the pickling tank and that will have contact with the metallic surface.
- As mentioned, the reaction operation occurs with a total of four material streams, namely: ST-06N, effective pickling bath stream that loses mass and thermal energy after the evaporation phenomenon; ST-02N, liquid stream leaving the SURFACE REACTOR-N with an increase in the amount of iron ions and, consequently, a reduction in the amount of free acid. In addition, there is the *steel strip input stream from stage "N+1"*, enriched with scale film and *steel strip output from stage "N"*. Which consists of metallic strip with reduced oxide content.

4.2.2 Mathematical modelling

4.2.2.1 Initial considerations and assumptions

According to the phenomenological approach, some initial considerations and assumptions were adopted to develop the mathematical model of the pickling system:

I. Regarding the fluid and solid phases:

a) The liquid phase is composed only of three components: H_2O, $FeCl_2$ and HCl. In industrial practice, it is known that the phase includes $FeCl_3$, Fe_2O_3 and other metals. However, given that their amount is less than 4% in weight, the authors chose to not consider those components;

b) The solid phase (scale) is formed by three different layers of iron oxide: FeO, Fe_3O_4 and Fe_2O_3 (FENG-I, 1988), (CHEN; YUEN, 2005). However, the most representative component is precisely FeO with a mass percentage that varies from 85 to 95% (YAMAGUCHI; YOSHIDA; SAITO, 1994). Due to this, it is assumed that the solid phase is formed by a single component FeO;

c) Regarding evaporation along the tanks, it is considered that only HCl and H_2O evaporate.

II. Both in the liquid and solid phases, Fe^{+3} is inevitably found among the components not considered by the model. Thus, not accounting for this quantity would result in significant deviations in the results. To get around this problem, it will be assumed that Iron III found in both mentioned phases will be considered as Iron II. That is, when receiving a composition input in liquid phase, the molar amount of total iron (II and III) in solution will be computed. In this way, all this quantity will be converted to $FeCl_2$. For the solid phase, the same will apply, with the distinction that the existing moles of iron will be converted to FeO.

III. Regarding the chemical reactions:

a) As mentioned in the previous assumptions, the solid phase is composed exclusively of FeO, as a result the only chemical reaction that occurs in this system will be:

$$FeO + 2HCl \longrightarrow FeCl_2 + H_2O \tag{76}$$

b) The reaction consists of a heterogeneous system and, therefore, occurs at the solid-liquid interface;

c) The chemical reaction will be treated as irreversible;

d) The kinetic modelling will be based in the authors previous work (SIERRA FERNANDEZ et al., 2023a).

IV. Considering that scale thickness has an order of magnitude of 10^{-6} m, in the mathematical approach of the interface, it will be assumed that the variation in solid thickness of the scale does not interfere in the solid-liquid interface;

V. The phenomenon of evaporation will be studied considering the surface area of the *sprinklers* plus the upper liquid surface;

VI. The heat losses from the pickling stage, *i.e.* exchanges due to the contact of the surfaces of the equipment with the environment (pipes, among others) will be neglected;

VII. Regarding the physical properties of the fluid in the different unit operations, they will be treated as constants in each operation. As a calculation approach, the

properties will always be recalculated under the output conditions (composition and temperature) that will be fed in the next operation.

VIII. The physical-chemical equations required to model the problem, such as specific mass, vapor pressure, among others, will be calculated according to the authors' previous work (SIERRA FERNANDEZ et al., 2023b).

4.2.2.2 Evaporation modelling

The aim of analyzing the evaporation system in the pickling tanks is:

1. Compute the HCl concentration profile in liquid phase during the chemical reaction on the scale surface;
2. Evaluate the temperature profile due the evaporation phenomena;
3. Analyze the impacts of evaporation losses in the performance of the pickling plant (evaporation rate *vs.* chemical reaction).

The same approach as proposed in literature by Crowl (2001) was used to model the evaporation effect through the pickling system. The evaporation mass flow can be considered as a function of vapor pressure:

$$\dot{m}_{ev.,i} \propto (P_{\text{vap.,i}} - P_i) \tag{77}$$

According to Eq. (77) the evaporation rate ($\dot{m}_{ev.,i}$) is proportional to the difference between the vapor pressure of solute ($P_{\text{vap.,i}}$) and the partial pressure of the solute in gas phase (P_i). In molar terms, this mass transfer rate could be represented as:

$$\dot{n}_{ev.,i} = \frac{k_{ev.,i} \cdot A_{sprk.}}{R \cdot T}(x_i \cdot P_{sat.,i} - y_i \cdot P) \tag{78}$$

In Equation (78), $\dot{n}_{ev.,i}$ is the molar flow of generic compound "i" ; $k_{ev.,i}$ is the convective mass transfer coefficient between the liquid and gas phase; $A_{sprk.}$ is the surface area available to evaporate; R is the ideal gas constant; T is the operational temperature; x_i is the molar fraction of generic compound "i" in liquid phase; y_i is the molar fraction of generic compound "i" in gas phase and P is the absolute pressure in the pickling tank.

The mathematical relationship used to calculate the convective mass transfer coefficient is based in Crowl (2001):

$$k_{ev.,i} = k_{ev.,\text{H}_2\text{O}} \cdot \left(\frac{M_i}{M_{\text{H}_2\text{O}}}\right)^{1/3} \tag{79}$$

According to the literature (CROWL; LOUVAR, 2001), the reference evaporative mass transfer coefficient for water ($k_{ev.,\text{H}_2\text{O}}$) is 0.83 cm·s^{-1} at a temperature of 25 °C. No temperature dependency of the mass transfer coefficient was assumed in this paper. Therefore,

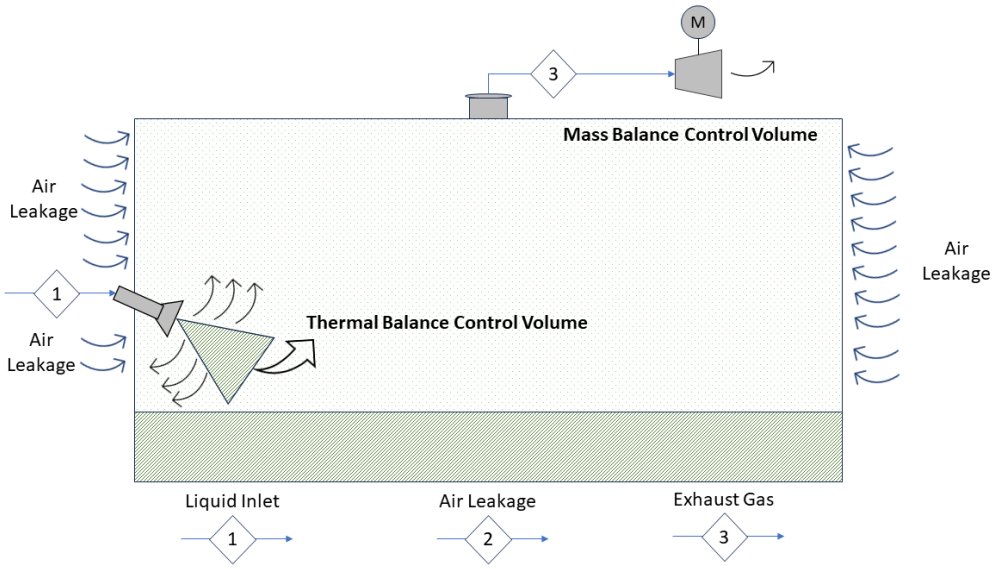

Figure 20 – Scheme of the control volume adopted for the evaluation of evaporation in the pickling system.

note that $k_{ev.,i}$ is only a function of Generic solute "i" molar mass (M_i) and Water molar mass (M_{H_2O}).

The evaporation mathematical modelling is developed with some assumptions:

I. The system will be evaluated in a transient state;

II. The physicochemical properties used are not a function of temperature or concentration;

III. Bernoulli's equation will be considered to calculate the evaporated flow in the pickling tank;

I.V. A constitutive relationship is used to represent the volumetric flow-rate through the tank's gaskets.

V. The pickling tank was considered as an adiabatic system. An energy balance is used to compute the heat loss in liquid phase due the sprinklers.

VI. A linear relation was used to distribute the liquid through each sprinklers;

VII. Only HCl and H_2O are able to evaporate to gas phase.

The phenomenological approach used to develop the differential equations considers the head space or gas phase present above the liquid level as control volume. The only exception is in the energy balance, which considers the liquid volume discharged by the sprinklers set as control volume. To be clear, Figure 20 present a block diagram of the relationship between each stream considered in the model.

In Figure 20 the stream "1" refers to the acid flow feed in the pickling tank. In an industrial pickling tank, typically sprinklers distribute the flow along the metallic surface. The

set of sprinklers is called "Header". The stream "2" is the total air leakage by the pickling tank gaskets. The stream "3" consists in the exhausted gas aspirated by the exhaust system, composed of industrial fans and scrubbers.

Based on Figure 20, eight equations were developed to model the evaporation system in a pickling tank:

1. HCl molar balance in gas phase;
2. H_2O molar balance in gas phase;
3. O_2 molar balance in gas phase;
4. N_2 molar balance in gas phase;
5. Energy balance in sprinklers' liquid discharge;
6. Constitutive equation of gaskets' air leakage;
7. Exhaust gas flow through the exhaust system;
8. Liquid surface area available to evaporate.

- **HCl molar balance in gas phase**

Equation (80) represents the transient material balance for HCl in the head space of a generic pickling tank. The material balance was developed taking into account the HCl molar flow. Note that only two terms are written in the right-hand side of the equation: 1) the evaporated HCl from liquid to gas phase ($\dot{n}_{ev.,\mathrm{HCl}}$) and 2) Exhaust term resulted from the shaft work of the fans. Is important to keep in mind that this equation was written considering algebraic simplifications.

$$\frac{dy_{\mathrm{HCl},3}}{dt} = \frac{k_{ev.,\mathrm{HCl}} \cdot A_{sprk.}}{V_{chamber}} \cdot \left(\frac{P_{vap.,\mathrm{HCl},1}}{P_3} \cdot x_{\mathrm{HCl},1} - y_{\mathrm{HCl},3} \right) - \frac{\dot{q}_3}{V_{chamber}} \cdot y_{\mathrm{HCl},3} \tag{80}$$

$$y_{\mathrm{HCl},3}(0) = y_{\mathrm{HCl},3,0} \tag{81}$$

In Equation (80), $y_{\mathrm{HCl},3}$ is the HCl molar fraction in gas phase ; $V_{chamber}$ is the Pickling tank chamber volume ; $P_{\mathrm{vap.,HCl},1}$ is the HCl vapor pressure in liquid phase ; $k_{ev.,\mathrm{HCl}}$ is the Convective mass transfer coefficient of HCl between the liquid and gas phase ; $x_{\mathrm{HCl},1}$ is the HCl molar fraction in liquid phase ; P_3 is the Chamber suction pressure and $\dot{q}_3$ is the Outlet gas volumetric flow . Regarding Eq. (81), the subscript "0" indicates the initial condition.

- **H_2O molar balance in gas phase**

Equation (82) represents the transient material balance for H_2O in the head space of a generic pickling tank. The material balance was developed taking into account the H_2O molar flow. The balance equation developed for water is similar to the approach considered for HCl. The only difference is the inclusion of the air leak term, second term in the right-hand

side of the equation. This term takes into account the amount of water entering the chamber through the atmospheric air leakage.

$$\frac{dy_{H_2O,3}}{dt} = \frac{k_{ev.,H_2O} \cdot A_{sprk.}}{V_{chamber}} \cdot \left(\frac{P_{vap,H_2O,1}}{P_3} \cdot x_{H_2O,\,1} - y_{H_2O,3} \right) + \\ + \frac{\dot{q}_2 \cdot P_2 \cdot T_3}{V_{domo} \cdot T_2 \cdot P_3} y_{H_2O,\,2} - \frac{\dot{q}_3}{V_{chamber}} \cdot y_{H_2O,3} \tag{82}$$

$$y_{H_2O,3}(0) = y_{H_2O,3,0} \tag{83}$$

In Equation (82), $y_{H_2O,3}$ is the H_2O molar fraction in gas phase ; $P_{vap.,H_2O,1}$ is the H_2O vapor pressure in liquid phase ; $k_{ev.,H_2O}$ is the Convective mass transfer coefficient of H_2O between the liquid and gas phase ; $x_{H_2O,1}$ is the H_2O molar fraction in liquid phase ; $y_{H_2O,2}$ is the H_2O molar fraction in atmospheric condition ; P_3 is the Chamber suction pressure ; P_2 is the Atmospheric pressure ; T_3 is the Chamber temperature ; T_2 is the Ambient temperature and $\dot{q}_3$ is the Outlet gas volumetric flow . Regarding Eq. (83), the subscript "0" indicates the initial condition.

- **O_2 molar balance in gas phase**

The Equation (84) represents the O_2 molar balance in the pickling chamber. Inlet and outlet terms are present in the right-hand side of the equation. The term "inlet" refers to the quantity of oxygen that enters the chamber as a result of air leakage. The outlet term consists of the amount of oxygen removed from the system by the fans shaft work.

$$\frac{dy_{O_2,3}}{dt} = \frac{\dot{q}_2 \cdot P_2 \cdot T_3}{V_{domo} \cdot T_2 \cdot P_3} y_{O_2,\,2} - \frac{\dot{q}_3}{V_{domo}} \cdot y_{O_2,3} \tag{84}$$

$$y_{O_2,3}(0) = y_{O_2,3,0} \tag{85}$$

In Equation (84), $y_{O_2,3}$ is the O_2 molar fraction in gas phase and $y_{O_2,2}$ is the O_2 molar fraction in atmospheric condition . Regarding Eq. (85), the subscript "0" indicates the initial condition.

- **N_2 molar balance in gas phase**

The Equation (86) presents the N_2 molar balance in the pickling chamber. Inlet and outlet terms are present in the right-hand side of the equation. The term "inlet" denotes the quantity of nitrogen that enters the chamber as a result of air leakage. The outlet term consists of the amount of nitrogen removed from the system by the fans shaft work.

$$\frac{dy_{N_2,3}}{dt} = \frac{\dot{q}_2 \cdot P_2 \cdot T_3}{V_{domo} \cdot T_2 \cdot P_3} y_{N_2,\,2} - \frac{\dot{q}_3}{V_{domo}} \cdot y_{N_2,3} \tag{86}$$

$$y_{N_2,3}(0) = y_{N_2,3,0} \tag{87}$$

In Equation (86), $y_{N_2,3}$ is the N_2 molar fraction in gas phase and $y_{N_2,2}$ is the N_2 molar fraction in atmospheric condition . Regarding Eq. (87), the subscript "0" indicates the initial condition.

- **Energy balance in sprinklers' liquid discharge**

The thermal energy balance will be developed considering some assumptions:

I. The liquid molar density (ρ_l^*), the liquid volume discharged by the sprinkler (V_L) and the liquid specific heat ($c_{p,l}$) are constants;
II. The liquid and vapor in the gas phase are in thermodynamic equilibrium;
III. The enthalpy of vaporization $\Delta H_{v,i}$ is calculated considering the gas phase temperature (T_3).

Based in these three assumptions, the energy thermal balance is shown in Eq. (88).

$$\frac{dT_3}{dt} = \frac{\dot{n}_1}{\rho_l^* V_l}(T_1 - T_3) - \frac{\dot{n}_1 \varphi_{ev.}}{\rho_l^* V_l c_{p,l}} \Delta H_v(T_3) \tag{88}$$

Regarding the Equation (88), $\dot{n}_1$ is the total liquid molar flow discharged in a sprinkler and $\varphi_{ev.}$ is the fraction of evaporated liquid. Equation (89) presents the initial condition.

$$T_3(0) = T_{3,0} \tag{89}$$

The mathematical definition of $\varphi_{ev.}$ is given by Eq. (90).

$$\begin{aligned} \varphi_{ev.} = \Bigg[& \frac{k_{ev.,HCl} \cdot A_{sprk.}}{R \cdot T_3}(x_{HCl,1} \cdot P_{sat.,HCl,1} - y_{HCl,3} \cdot P_3) + \\ & + \frac{k_{ev.,H_2O} \cdot A_{sprk.}}{R \cdot T_3}(x_{H_2O,1} \cdot P_{sat.,H_2O,1} - y_{H_2O,3} \cdot P_3) \Bigg] \frac{1}{\dot{n}_1} \end{aligned} \tag{90}$$

- **Constitutive equation to gaskets' air leakage**

Typically in industrial process operating under vacuum or depression conditions, it is common to occur air leakage from equipment sealing gaskets. Turton *et al.* (2008) presents an equation to compute the air leakage mass flow as a function of equipment volume:

$$\dot{q}_2 = \gamma_2 \cdot V_t^{2/3} \cdot \rho_2^{-1} \tag{91}$$

In Equation (91), there are two important parameters that describe the extension of the leakage: 1) γ_2 represents the air permeability through the pickling tank gasket, and 2) V_t consists in the pickling tank volume. It is important to observe in Equation (91) that the

flowrate of leakage remains constant and does not vary with respect to time. This paper proposes that the volumetric flow rate of leakage can be enhanced through the utilization of a form of analysis that considers the square root of the pressure difference between the inlet and outlet pressure. The given equation, denoted as Equation (91), can be reformulated as follows:

$$\dot{q}_2 = \gamma_2^* \cdot V_t^{2/3} \cdot \rho_2^{-1} \cdot \sqrt{P_2 - P_3} \tag{92}$$

The improved Equation (92) uses the value proposed by Turton *et al.* (2008) for the gasket constant γ_2^*. The only difference is regarding the unit of this new parameter: $2.64{\times}10^{-4}$ $\text{kg}\cdot(\text{m}^2\cdot\text{s}\cdot\text{Pa}^{0.5})^{-1}$.

- **Exhaust gas flow through fans system**

To calculate the gas outlet volumetric flow-rate the Equation (93) is defined.

$$\dot{q}_3 = C_V \cdot \sqrt{P_3 - P_{vent}} \tag{93}$$

In the equation above C_V is the hydraulic constant of the exhaust system and P_{vent} is the suction pressure of the vent system. This equation is commonly used in gas line systems (SEBORG et al., 2010). The hydraulic constant can be calculated using the Equation (94).

$$C_V = \frac{\pi \cdot d_{3,int.}^2}{4} \cdot \sqrt{\frac{2}{(1+K)\rho_3}} \tag{94}$$

In the equation above, d_3 is the outlet gas duct internal diameter and K is the head loss fitting constant.

- **Liquid surface area available to evaporate**

In this work the available liquid surface area is composed by the liquid triangular surface area of each sprinkler ($A_{sprk.}^*$). Figure 21 shows a sketch of the typical arrangement of one sprinkler used in pickling lines. A lateral and superior view can be visualized indicating the main parameters of the triangular surface geometry.

The relationship developed to calculate the liquid surface area of one sprinkler ($A_{sprk.}^*$) is given below as a function of each geometry parameter:

$$A_{sprk.}^* = 2 \cdot \tan\left(\frac{\hat{C}}{2}\right) \cdot \frac{a}{\sin(\hat{B})} \cdot \frac{b}{\cos(\hat{B})} \tag{95}$$

The mathematical function above is for a single sprinkler. Typically, in industrial plants a set of sprinklers ($N_{sprk.}$) exists in a pickling tank. Usually 48 to 96 sprinklers are used in an industrial line. The final expression to estimate the total surface area is:

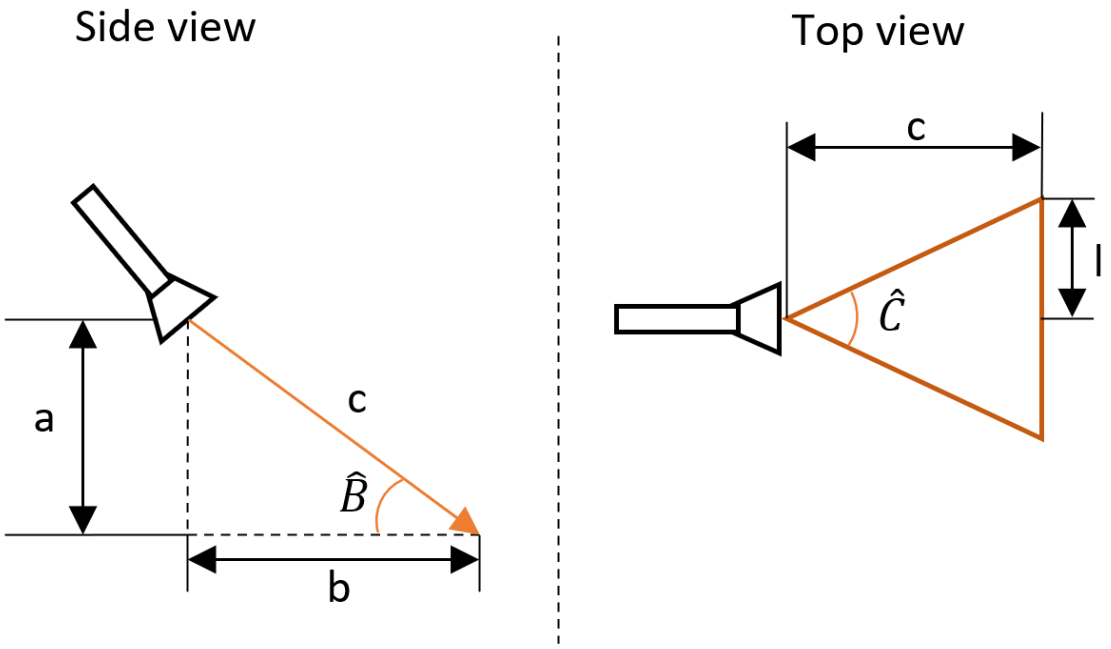

Figure 21 – The diagram illustrates the configuration of a single sprinkler within a turbulent acid pickling system. The side view indicates the following geometric parameters *a*, *b* and *c*. These three parameters are a function of the jet injection angle ($\hat{B}$). A top view presents the angle $\hat{C}$, resulting from the considered geometry, triangular. "*l*" consists of the base dimension of the right triangle.

$$A_{sprk.} = A^{*}_{sprk.} \cdot N_{sprk.} \tag{96}$$

It is interesting to note that the liquid surface area formed by a set of sprinklers has the same order of magnitude as the rectangular area of a pickling tank.

4.2.2.3 Reactor modelling

The mathematical model used to simulate the internal parts of the pickling tanks is based on material and energy balances in solid and fluid phases. A system of partial differential equations was developed. Figure 22 presents a sketch of the control volumes applied in the model.

In Figure 22 the color profile concerns each of the phases under analysis. Regarding the solid phase, the gray color represents the metallic strip. The orange color illustrates the oxide layer (scale). In relation to the liquid phase, the hatched region in shades of green illustrates a film of liquid representing the pickling bath. In terms of dimensions, for a well-defined tank, L corresponds to the length of the reactor. The variables e_s, e_0 and e_L refer to the thicknesses, respectively, of the metal strip, scale (initial) and liquid film. The front view of the figure allows identifying the width of the metal strip. It is important to note that u_z corresponds to the linear velocity of the pickling line and C_{HCl} is the molar concentration of HCl.

For the development of the mathematical model, the following assumptions were

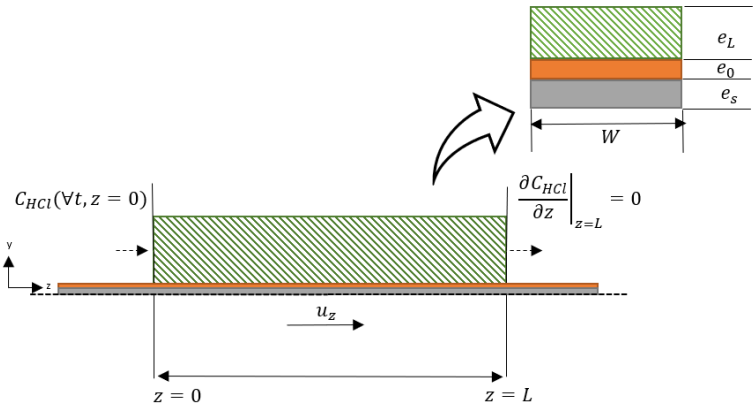

Figure 22 – Scheme of the phenomenological approach of the surface reactor.

adopted:

1. It is assumed that a film of thickness e_L is formed on the strip surface. The film thickness is calculated based on the recirculating volumetric flow rate in the pickling tank Q_r, the line speed u_Z and the metallic strip width W. To calculate the thickness of the liquid film, scale thickness is neglected, as well as a system symmetry condition is assumed. Thus, the Equation (97) can be used to calculate the liquid film thickness:
$$e_L = \frac{Q_r}{W \cdot u_Z} \cdot \frac{1}{2} \tag{97}$$
2. With the film formed, it is considered that a continuous concentration of acid enters the end $z = 0$ of the reactor. This concentration refers to the concentration of acid present in the liquid phase after evaporation.
3. All the material load that entered the boundary $z = 0$ leaves the system at the boundary $z = L$. The volumetric flow rate of the system is maintained, a necessary condition to ensure that there is no variation in the liquid film, however the mass flow rate is modified due to the variation in the composition of the liquid.
4. From a temporal perspective, the phenomenon is observed to occur concurrently, requiring a solution of material and energy balances as a system of equations. In this context, a kinematic behavior is proposed for the volumetric scale of the solid phase. The descaling operation advances at a clearly defined rate along the z-axis (acsz), and as the acid attack occurs place, the thickness of the descaling layer is uniformly reduced. For this purpose, the equations applied to the solid phase balance will be developed proposing scale thickness as the dependent variable.
5. As it is a heterogeneous model (solid-liquid), solid and liquid phase balances will be developed. For analysis purposes, the reagent consumption term - HCl, will be the same regardless of the balances. Thus, there will be no mass transfer term between phases. The hypothesis for such a choice is motivated by the fact that the kinetic term takes into account the influence of the thickness of the solid (scale)

and the acid concentration of the liquid phase.

- **Material balance in solid phase**

The balance in the solid phase is shown in Equation (98).

$$\frac{\partial e}{\partial t} + u_z \cdot \frac{\partial e}{\partial z} = -\frac{r'_{\mathrm{HCl}} \Theta_{\frac{\mathrm{FeO}}{\mathrm{HCl}}}}{\rho^*_{\mathrm{FeO}}} \tag{98}$$

The Equation (98) consists of a Partial Differential Equation (PDE) where the independent variables are time t and the axis parallel to the movement of the metal strip, z; with respect to the dependent variable, e is the scale thickness in the solid phase. A total of three terms in the equation represent different physical phenomena of mass transfer. The first term on the left side of the equation refers to the transient term, in the sequence there is an advection term, represented by a first derivative with respect to z. As for the right side of the expression, there is a kinetic term, which indicates the consumption of FeO and HCl.

In terms of initial and boundary conditions applied to Equation (98), they are defined by the Equations (99) and (100):

$$\text{I.C.:} \quad e(0, \forall z) = e_i \tag{99}$$

$$\text{B.C.:} \quad e(\forall t, 0) = e_0 \tag{100}$$

The details of the mathematical development of the Equation (98) are presented in the previous work of the authors (SIERRA FERNANDEZ et al., 2023a). Regarding the aforementioned equation, the following assumptions were adopted for development:

1. As mentioned earlier, the advective term is assumed to move with the same speed as the metallic surface u_z;
2. Pickling rate law r'_{HCl} is defined as:

$$r'_{\mathrm{HCl}} = \left[(k_0 \cdot e) \cdot \exp\left(-\frac{Ea}{RT_s} \right) \right] C^m_{\mathrm{HCl}} \tag{101}$$

3. The kinetic properties: k_0 - frequency factor, Ea - activation energy, and m - kinetic coefficient of pickling velocity were defined in the work of (SIERRA FERNANDEZ et al., 2023a). Furthermore, the same reference presents the definitions of $\Theta_{\frac{\mathrm{FeO}}{\mathrm{HCl}}}$ - stoichiometric coefficient, and ρ^*_{FeO} - molar specific mass of FeO.

Based on the assumptions discussed above, the Equation (98) is adapted into a dimensionless format. As a result two independent variables τ - dimensionless time, ζ - dimensionless length, and the dependent variable X - conversion. The Equation (102) presents the mathematical definition of X:

$$X = \frac{e_0 - e}{e_0} \tag{102}$$

Equation (103) is the final format of the dimensionless differential mass conservation equation in the solid phase.

$$\frac{\partial X}{\partial \tau} + \frac{\partial X}{\partial \zeta} = Da \cdot \exp\left(-\frac{Arr}{\theta_s}\right) \cdot \psi^m \cdot (1 - X) \tag{103}$$

In Equation (103) two dimensionless groups are defined: the Damköhler number *Da* and the Arrhenius number *Arr*. The equations (104) and (105) are the mathematical definition those parameters.

$$Da = k_0 \cdot \Theta_{\frac{FeO}{HCl}} \cdot \frac{L}{u_z} \cdot \frac{C^m_{HCl,0}}{\rho^*_{FeO}} \tag{104}$$

$$Arr = \frac{Ea}{R \cdot T_{s0}} \tag{105}$$

For Equation (103) the initial and boundary conditions are defined by Equations (106) and (107).

$$\text{I.C.:} \quad X(0, \forall \zeta) = X_i \tag{106}$$

$$\text{B.C.:} \quad X(\forall \tau, 0) = X_0 \tag{107}$$

The initial condition X_i consists of the initial conversion at time zero. X_0 is the pickled fraction at the pickling tank inlet.

- **Thermal balance in solid phase**

The thermal balance in the solid phase is represented by the Equation (108), as follows:

$$\frac{\partial T_s}{\partial t} + u \cdot \frac{\partial T_s}{\partial z} = \frac{r'_{HCl} \Delta H_{rx.}}{\rho_s \cdot c_{p,s} \cdot e_s} - \frac{\lambda}{\rho_s \cdot c_{p,s} \cdot e_s}(T_s - T) \tag{108}$$

The Equation (108) consists of a Partial Differential Equation (PDE) where the independent variables are time t and the axis parallel to the movement of the metal strip, z; with respect to the dependent variable, there is T_s, temperature of the solid (considering only the metallic structure as a reference). A total of four terms in the equation represent different physical phenomena of heat transfer. The first term on the left side of the equation refers to the transient term, in the sequence there is an advection term, represented by a first derivative with respect to z. As for the right side of the expression, there is a kinetic term, which refers

to the heat generated through the chemical reaction and another term indicating the convective thermal flow between the fluid and solid phases. This term is responsible for adding or removing heat from the system.

In terms of initial and boundary conditions applied to Equation (108), they are defined by the Equations (109) and (110):

$$\text{I.C.:} \quad T_s(0,\forall z) = T_{si} \tag{109}$$

$$\text{B.C.:} \quad T_s(\forall t, 0) = T_{s0} \tag{110}$$

Details of the mathematical development of Equation (108) are presented in the previous work of the authors (SIERRA FERNANDEZ et al., 2023a). Still with respect to the aforementioned equation, the following assumptions were adopted for development:

1. As mentioned earlier, the advective term is assumed to move with the same speed as the metallic surface u_z;
2. The thermal balance takes the metal strip as a reference and disregards the scale layer on the surface of the material. This approach is reasonable given that there is an order of magnitude difference between the volumes, *i.e.*, the scale layer is 1000 times smaller than the thickness of the metallic strip;

Based on the assumptions discussed above, the Equation (108) is adapted into a dimensionless format. To do so is defined the two independent variables τ - dimensionless time, ζ - dimensionless length, and the dependent variable θ_s - dimensionless temperature of the solid.

Equation (111) is the final format of the dimensionless differential thermal conservation equation in the solid phase.

$$\frac{\partial \theta_s}{\partial \tau} + \frac{\partial \theta_s}{\partial \zeta} = Da \cdot Da_T \cdot \gamma \cdot s \cdot \exp\left(-\frac{Arr}{\theta_s}\right) \cdot \psi^m \cdot (1-X) - St \cdot \gamma \cdot \Phi \cdot (\theta_s - \Gamma\theta) \tag{111}$$

In Equation (111) new dimensionless groups are defined: the thermal Damköhler number Da_T, the ratio of volumetric thermal capacity between the fluid and the metallic strip γ, the ratio of scale thickness and the thickness of the metallic strip s and, finally, the ratio between the thickness of the liquid film and the metallic strip Φ. The Equations (112), (113), (114) and (115) are the mathematical definitions of each of the parameters.

$$Da_T = \frac{\Delta H_{rx.} \cdot \rho^*_{\text{FeO}}}{\rho \cdot c_p \cdot T_{s0} \cdot \Theta_{\frac{\text{FeO}}{\text{HCl}}}} \tag{112}$$

$$\gamma = \frac{\rho \cdot c_p}{\rho_s \cdot c_{p,s}} \tag{113}$$

$$s = \frac{e_0}{e_s} \tag{114}$$

$$\Phi = \frac{e_L}{e_0} \tag{115}$$

For Equation (111) the initial and boundary conditions are defined by Equations (116) and (117).

$$\text{I.C.:} \quad \theta(0,\forall\zeta) = \frac{T_{si}}{T_{s0}} \tag{116}$$

$$\text{B.C.:} \quad \theta(\forall\tau, 0) = 1 \tag{117}$$

- **HCl molar balance in fluid phase**

As shown in Figure 22, the study will be carried out assuming that there is a concentration gradient in the *bulk* phase at z, that is, an axis parallel to the movement of the metallic strip. Due to the thickness of the liquid film being of millimeter order, any concentration gradient on the y-axis is neglected. Thus, the elementary molar balance equation in the fluid phase becomes:

$$\frac{\partial C_{\text{HCl}}}{\partial t} + u_z \frac{\partial C_{\text{HCl}}}{\partial z} - \mathcal{D}_{eff.} \frac{\partial^2 C_{\text{HCl}}}{\partial z^2} = -r'_{\text{HCl}} \cdot e_L^{-1} \tag{118}$$

The Equation (118) consists of a Partial Differential Equation (PDE) where the independent variables are time t and the axis parallel to the movement of the metal strip, z; with respect to the dependent variable there is the term C_{HCl}, molar concentration of HCl in the fluid phase. A total of four terms in the equation represent different physical phenomena of mass transfer. The first term on the left side of the equation refers to the transient term, then there is an advection term, represented by a first derivative with respect to z and, finally, a dispersion term represented by a second derivative with respect to z. As for the right side of the expression, there is a convective mass transfer term, which indicates the transfer of solute from the fluid phase to the solid surface (solid-liquid interface).

Regarding the initial and boundary conditions applied to Equation (118), there are the Equations (119), (120) and (121), respectively:

$$\text{I.C.:} \quad C_{\text{HCl}}(0,\forall z) = C_{\text{HCl},i} \tag{119}$$

$$\text{B.C.I:} \quad C_{\text{HCl}}(\forall t, 0) = C_{\text{HCl},0} \tag{120}$$

$$\text{B.C.II:} \quad \left.\frac{\partial C_{\text{HCl}}}{\partial z}\right|_{z=L} = 0 \tag{121}$$

The Equation (118) assumes the following assumptions:

1. Regarding the advection term, it is assumed that the fluid moves with the same velocity as the metallic surface u_z;
2. The dispersion term $\mathcal{D}_{eff.}$ is constant and already takes into account the diffusion effect. It was defined using a simplified approach adapted from Cussler (2009) (CUSSLER, 2009). The idea is to calculate the dispersion coefficient as a laminar dispersion: Taylor dispersion. That is, considering it as a function of the mass diffusion coefficient of HCl in the liquid solution D_{HCl}. Adapting the equation using the hydraulic diameter as a reference, there is:

$$\mathcal{D}_{eff.} = \frac{1}{4 \cdot 48 \cdot \pi^2} \cdot \frac{(W \cdot u_z)^2}{D_{\text{HCl}}} \tag{122}$$

Based on the assumptions discussed above, the Equation (118) is adapted into a dimensionless format. For that, define, respectively, the two independent variables τ - dimensionless time, ζ - dimensionless length, and the dependent variable ψ - dimensionless concentration of HCl in the bulk phase.

$$\tau = \frac{u_z}{L} \cdot t \tag{123}$$

$$\zeta = \frac{z}{L} \tag{124}$$

$$\psi = \frac{C_{\text{HCl}}}{C_{\text{HCl},0}} \tag{125}$$

Equation (126) presents the final format of the expression for molar balance of HCl in the fluid phase.

$$\frac{\partial \psi}{\partial \tau} + \frac{\partial \psi}{\partial \zeta} - \frac{1}{Pe}\frac{\partial^2 \psi}{\partial \zeta^2} = -Da \cdot \kappa \cdot \Phi^{-1}(1 - X) \cdot \exp\left(\frac{-Arr}{\theta_s}\right) \cdot \psi^m \tag{126}$$

In the Equation (126) some new additional groups appeared: the mass transfer Peclet (Pe) and the molar ratio between the scale and the molar concentration of HCl (κ). Below are the mathematical definitions:

$$Pe = \frac{u_z \cdot L}{\mathcal{D}_{eff.}} \tag{127}$$

$$\kappa = \frac{\rho^*_{\text{FeO}}}{\Theta_{\frac{\text{FeO}}{\text{HCl}}} \cdot C_{\text{HCl},0}} \tag{128}$$

For the Equation (126), the initial and boundary conditions are defined by the Equations (129), (130) and (131).

$$\text{I.C.:} \quad \psi(0,\forall\zeta) = \frac{C_{\text{HCl},i}}{C_{\text{HCl},0}} \tag{129}$$

$$\text{B.C.I:} \quad \psi(\forall\tau, 0) = 1 \tag{130}$$

$$\text{B.C.II:} \quad \left.\frac{\partial\psi}{\partial\zeta}\right|_{\zeta=1} = 0 \tag{131}$$

Where $C_{\text{HCl},0}$ is the concentration of HCl entering the pickling tank and $C_{\text{HCl},i}$ is the initial concentration inside the control volume.

- **Thermal balance in fluid phase**

The mathematical approach for computing fluid phase behavior is similar to that developed for the fluid phase solute. Below is the Equation (132):

$$\frac{\partial T}{\partial t} + u_z\frac{\partial T}{\partial z} - \alpha\frac{\partial^2 T}{\partial z^2} = -\frac{\lambda}{\rho\cdot c_p\cdot e_L}(T - T_s) \tag{132}$$

The Equation (132) consists of a Partial Differential Equation (PDE) where the independent variables are time t and the axis parallel to the motion of the metal strip, z; with respect to the dependent variable there is T, temperature of the fluid in the liquid phase. A total of four terms in the equation represent different physical phenomena of heat transfer. The first term on the left side of the equation refers to the transient term, then there is an advection term, represented by a first derivative with respect to z and, finally, a thermal diffusion term represented by a second derivative with respect to z. As for the right side of the expression, there is a convective heat transfer term, which indicates the heat transfer of solute from the fluid phase to the solid surface (solid-liquid interface).

In terms of initial and boundary conditions applied to Equation (132), they are defined by the Equations (133), (134) and (135):

$$\text{I.C.:} \quad T(0,\forall z) = T_i \tag{133}$$

$$\text{B.C.I:} \quad T(\forall t, 0) = T_0 \tag{134}$$

$$\text{B.C.II:} \quad \left.\frac{\partial T}{\partial z}\right|_{z=L} = 0 \tag{135}$$

The Equation (132) assumes the following assumptions:

1. Regarding the advection term, it is assumed that the fluid moves with the same velocity as the metallic surface u_z;

2. It is considered that the convective heat transfer term at the solid-liquid interface is proportional to the thermal gradient between the liquid temperature T and the solid surface temperature T_s. Note that λ refers to the convective heat transfer coefficient;
3. The physicochemical properties of the fluid: ρ - specific mass of the fluid phase, c_p - specific heat, and α - thermal diffusivity, are functions of temperature and composition as defined in the authors' previous work (SIERRA FERNANDEZ et al., 2023b).

Based on the assumptions described above, the Equation (132) is rewritten into a dimensionless form. For this, define the two independent variables τ - dimensionless time, ζ - dimensionless length, and the dependent variable θ - dimensionless temperature. Considering that the thermal gradient is a function of the temperatures between the liquid and solid phases, the dimensionless variable θ_s is also defined, which consists of the

$$\theta = \frac{T}{T_0} \tag{136}$$

$$\theta_s = \frac{T_s}{T_{s0}} \tag{137}$$

Substituting the dependent and independent variables in Equation (132), the dimensionless thermal balance takes the following form:

$$\frac{\partial\theta}{\partial\tau} + \frac{\partial\theta}{\partial\zeta} - \frac{1}{Pe_T}\frac{\partial^2\theta}{\partial\zeta^2} = -St \cdot (\theta - \frac{1}{\Gamma}\theta_s) \tag{138}$$

In the Equation (132) two dimensionless groups are defined: the heat transfer Peclet number Pe_T and the Stanton number St. The Equations (139) and (140) represent the mathematical definition of those parameters.

$$Pe_T = \frac{u_z \cdot L}{\alpha} \tag{139}$$

$$St = \frac{\lambda \cdot L}{\rho \cdot c_p \cdot e_L \cdot u_z} \tag{140}$$

The correlation for computing the Liquid-solid convective heat transfer coefficient (λ) was extracted from Bergman *et al.* (2011). The correlation applied to a flat-plate was adopted, considering as characteristic dimension the Pickling tank length (L).

$$
\begin{aligned}
Nu &= 0.0308 \cdot Re^{\frac{4}{5}} \cdot Pr^{\frac{1}{3}}; \\
Re &= \frac{\rho \cdot u_z \cdot L}{\mu}; \\
Pr &= \frac{c_p \cdot \mu}{\alpha}; \\
Nu &= \frac{\lambda \cdot L}{k}.
\end{aligned}
\tag{141}
$$

In Eq. (141) Nu is the Nusselt number, Re is defined as the Reynolds number, and Pr is the Prandtl number. Furthermore, μ is the viscosity of the fluid and k is its coefficient of thermal conductivity of the fluid phase.

It is also important to mention another dimensionless parameter Γ:

$$
\Gamma = \frac{T_0}{T_{s0}} \tag{142}
$$

For the Equation (132), the initial and boundary conditions are defined by the Equations (143), (144) and (145).

$$
\text{I.C.:} \quad \theta(0,\forall\zeta) = \frac{T_i}{T_0} \tag{143}
$$

$$
\text{B.C.I:} \quad \theta(\forall\tau, 0) = 1 \tag{144}
$$

$$
\text{B.C.II:} \quad \left.\frac{\partial\theta}{\partial\zeta}\right|_{\zeta=1} = 0 \tag{145}
$$

Where T_0 is the temperature of the fluid phase at the reactor inlet and T_i is the initial temperature inside the control volume at time zero.

4.2.2.4 Mixer and splitter

The mixing and separating unit operations represents, as far as the industrial process is concerned, the working tank. Where the product is obtained from the previous stage, is collected by gravity from the pickling reactor and then an output stream flows to the separation operation. From this stream leaving the mixer, part of the material is recirculated and another part is transported to the subsequent stage.

For the mathematical development of this set of operations, some assumptions are listed:

1. The analysis regime is stationary and does not present any kind of spatial gradient;
2. The amount of material entering the pickling stage - ST-01N, is conserved and, therefore, leaves the system by the ST-05N stream. The idea is to ensure that there is no accumulation in the system through a possible level increase. In industrial

practice, volume control is performed using a level control loop. In this way, the amount supplied in the control volume must compensate the amount evaporated (ST-07N);

3. In the mixer operation, the outlet temperature of the ST-03N stream is calculated assuming that the specific heat of the liquid is constant;
4. For the separator, the system is assumed to be isothermal;
5. In terms of thermal supply, it is considered that the ST-04N stream obtains a thermal load required to guarantee the pre-defined operating temperature;
6. The recirculated volumetric flow will be based on the regenerated bath flow supplied to the entire pickling system.

- **Mixers equations**

In terms of mass balance the following equation is defined:

$$\dot{q}_{03N} \cdot C_{j,03N} = \dot{q}_{01N} \cdot C_{j,01N} + \dot{q}_{02N} \cdot C_{j,02N} \tag{146}$$

Considering that the ST-02N stream consists of the material leaving the reactor, the following expression is defined to calculate the average value of the outlet concentration in a given residence time (τ):

$$\dot{q}_{02N} \cdot C_{j,02N} = 2 \cdot u_z \cdot W \cdot e_L \cdot \frac{C_{j,06N}}{\tau} \int_{\tau}^{\tau+\Delta\tau} \psi(\forall\tau,1) d\tau \tag{147}$$

For the application of the thermal energy balance, the following equation is used:

$$T_{03N} = \frac{1}{\dot{q}_{03N}} \left(\dot{q}_{02N} T_{02N} + \dot{q}_{01N} T_{01N} \right) \tag{148}$$

- **Splitter equations**

As already mentioned, the splitter operation is stationary and has no phenomena of mass or heat transfer, only a hydraulic separation of the flow coming from the mixer. Thus, some equations are required to evaluate the separation operation.

The generic recycle flow in each stage $\dot{q}_{04N}$ is defined based on the volumetric flow fed into the global process $\dot{q}_{ARP}$. That is, the flow rate that the entire pickling system needs to guarantee the stoichiometric removal of the FeO present on the surface. The R recycle parameter is varied in order to improve the unit's operating conditions. The Equation (149) provides the mathematical definition:

$$\dot{q}_{04N} = R \cdot \dot{q}_{ARP} \tag{149}$$

With respect to the mass flow required by the pickling process, $\dot{m}_{ARP}$ is calculated based on a reference material, the design speed of the pickling line $u_{z,design}$, and the mass fraction of HCl: x_{HCl}:

$$\dot{m}_{ARP} = 2 \cdot W \cdot e_0 \cdot u_{z,design} \cdot \frac{\rho^*_{\mathrm{FeO}}}{\Theta_{\frac{\mathrm{FeO}}{\mathrm{HCl}}}} \cdot M_{\mathrm{HCl}} \cdot \frac{1}{x_{\mathrm{HCl}}} \tag{150}$$

It is known that the operational process has losses by evaporation, in addition, the used bath that leaves the last stage remains with an amount between 3 to 5% in HCl. Thus, this quantity must be compensated in the volume to be supplied by the system. Therefore, a design efficiency parameter η_{design} and the specific mass under the conditions of composition and temperature of the regenerated bath ρ_{ARP} are defined. Equation (151) presents the definition for calculating the volumetric flow of regenerated bath in the pickling line.

$$\dot{q}_{ARP} = \frac{\dot{m}_{ARP}}{\eta_{design} \cdot \rho_{ARP}} \tag{151}$$

Regarding the calculation for the amount of bath that is transferred to the next stage (ST-05N), the Equation (152) is defined.

$$\dot{m}_{05N} = \dot{m}_{01N} - \dot{m}_{07N,st}. \tag{152}$$

In Equation (152), $\dot{m}_{07N}$ is defined as the mass flow evaporated in the reference stage "N" in steady state.

4.2.3 Problem statement: solution algorithm strategy

The intention of this work is to develop a mathematical model applied to turbulent acid pickling lines that allow: 1) The Design of new industrial units and 2) The evaluation of different operational scenarios, in particular having the possibility of analyzing the behavior of the system given a new type of material (steel strips).

Based on those two demands, the mathematical models were implemented in MATLAB using the following solution algorithm present in Figure 23.

The implementation of the model was based on the following assumptions:

1. As developed in Sierra Fernandez *et al.* (2023), it is assumed that for a conversion of 99.2%, to the naked eye, it is assumed that the material has been completely pickled;
2. The physicochemical properties functions used to solve the mathematical model were extracted from Sierra Fernandez *et al.* (2023);
3. The solution of the material and energy balance streams were extracted after 4 residence times of the system. In other words, the solution is considered to be in steady-state.

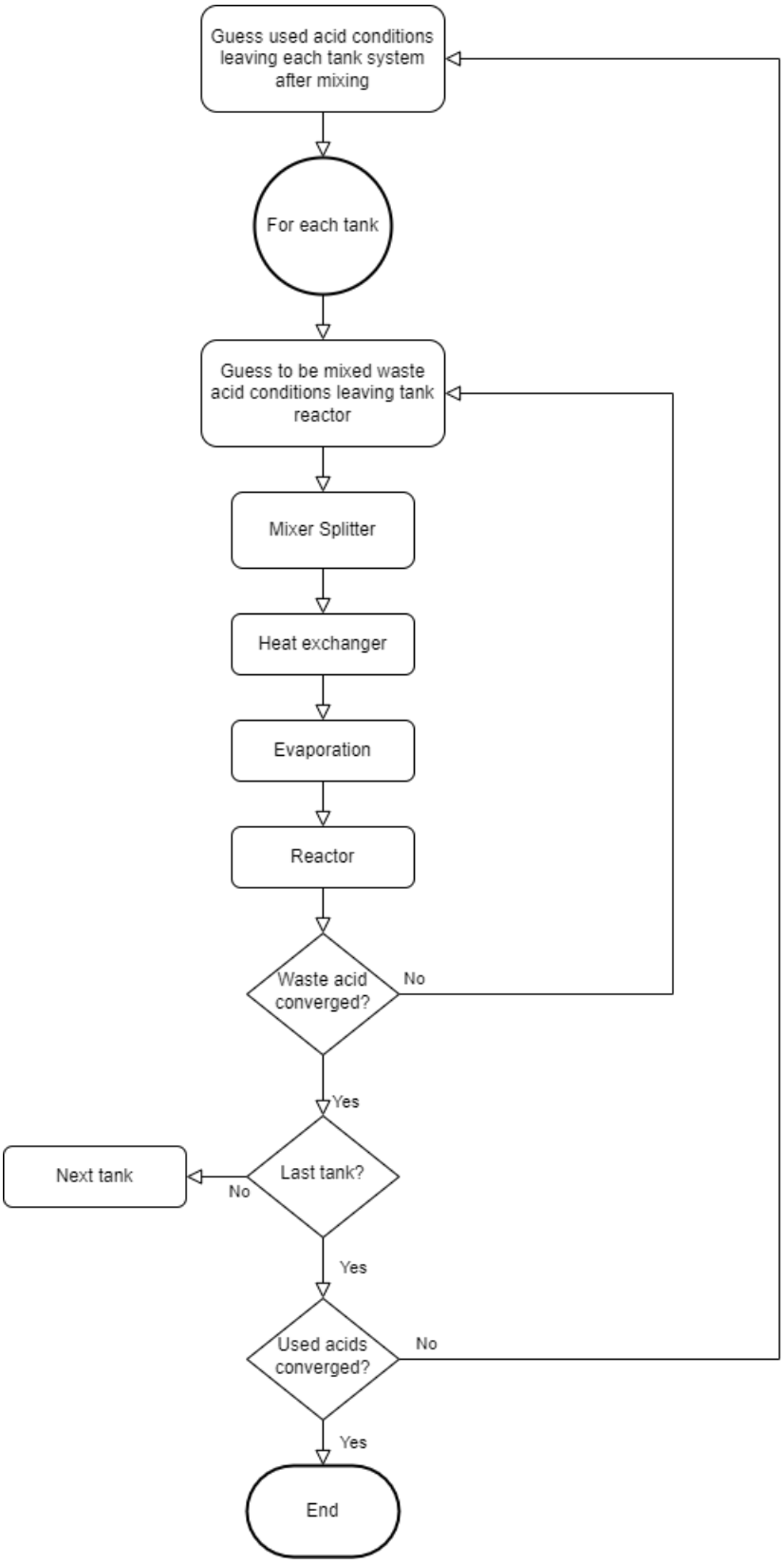

Figure 23 – PDE solution algorithm applied to an industrial turbulent acid pickling line.

In addition to applying the solution of the turbulent pickling model, the authors evaluated the impacts of evaporation on the reaction speed, independently of the liquid phase balances. For this purpose, the solid phase balance was coupled to the evaporation system. Based on the different thermal conditions solutions, it was previously identified which thermal conditions most affect the performance of the equipment.

4.2.4 Computational tools and numerical method

The code was implemented in Matlab programming language using an object-oriented approach to allow for the creation of reusable modular models representing streams, phases and systems, each entity having their behavior described by properties and methods, and an interface to interact with other objects.

Regarding the partial differential equations system models that describe the evaporation chamber and tank reactor behavior, it was solved through finite difference discretization using the Forward Time-Centered Space (FTCS) scheme. Appendix C present the equations in a numerical form.

The tolerance criteria used for the mass balance and convergence of guesses was 1% relative error, and to find the maximum line velocity that satisfies the conversion criteria of 99.2%, an custom root-finding algorithm were used.

4.3 Results and discussions

4.3.1 Field data extraction

The data used for the simulation setup were based on an industrial unit located in the south of Brazil that operates with a line of four pickling tanks, using HCl as a pickling agent and that processes carbon steel.

In terms of operation, the unit currently runs under the following conditions:

- *Current operating temperature of the tanks*: in terms of design, the unit is capable of operating the process with a range in each tank of 65 to 85 °C. However, currently the plant has been operating with a narrower range, 75 to 85 °C. This condition is dependent on the type of steel to be processed.
- *Coil characteristics*: this parameter is a function of a series of indicators, *e.g.*, the hot rolling temperature. However, the following conditions apply:
    a) Thickness: 1.85 to 5.00 mm;
    b) Width: 920 to 1870 mm.
- *Characteristics of the regenerated bath*: the acid regeneration unit (ARP) is capable of delivering the pickling bath with the following operating range:
    a) Temperature: 50 to 70 °C;
    b) Concentration of HCl by weight: 16% to 21%;
    c) Concentration of $FeCl_2$ by weight: 0% to 1%;

Table 23 – Model parameters required for numerical simulation - Base Case. The parameters come from an industrial unit located in the south of Brazil. The specific surface area of a sprinkler was calculated considering: a, b, $\hat{B}$ and $\hat{C}$, respectively, 0.153 and 0.471 m; 18 and 60 °.

Parameter	Unit	Material Inlet	TK-00	TK-01	TK-02	TK-03	Regenerated acid
Material type	-	LCT	-	-	-	-	-
Scale surface density	$kg{\cdot}m^{-2}$	$4.3{\cdot}10^{-2}$	-	-	-	-	-
Strip width	mm	1238	-	-	-	-	-
Steel thickness	mm	4.77	-	-	-	-	-
Steel density	$kg{\cdot}m^{-3}$	7834	-	-	-	-	-
Steel specific heat	$kJ{\cdot}(kg{\cdot}K)^{-1}$	0.43	-	-	-	-	-
Temperature	°C	25.0	80.0	80.0	80.0	80.0	60.0
$FeCl_2$ mass fraction in reg. acid	%	-	-	-	-	-	0.5%
HCl mass fraction in reg. acid	%	-	-	-	-	-	18.0%
Number of sprinklers	-	-	96	96	96	96	-
Sprinkler surface area	m^2	-	27.2	27.2	27.2	27.2	-
Sprinkler liquid thickness	mm	-	1.0	1.0	1.0	1.0	-
Pickling tank volume	m^3	-	187.0	187.0	187.0	187.0	-
Chamber volume	m^3	-	63.0	63.0	63.0	63.0	-
Reactor length	m	-	20.5	20.5	20.5	20.5	-
Acid fumes outlet duct diameter	mm	-	150	150	150	150	-
Tank pressure	kPa	-	99.3	99.3	99.3	99.3	-
Vent pressure	kPa	-	97.3	97.3	97.3	97.3	-
Recycle flow-rate	$m^3{\cdot}h^{-1}$	-	42	42	42	42	-

- *Recycle rate*: the recycle rate is a variable parameter. Typically, regardless of the tank, the system is capable of operating in a range of 35 to 55 $m^3{\cdot}h^{-1}$.

As far as material-specific details are concerned, another important parameter is scale thickness. This parameter is mainly influenced by the rolling temperature, cooling time and chemical composition of the steel (CAO et al., 2014). For the purposes of this study, two types of material will be considered:

- Low Coil Temperature (LCT): consists of coils with temperatures lower than 540 °C;
- High Coil Temperature (HCT): consists of coils with temperatures up to 720 °C.

With regard to scale thickness, due to lack of information, it is considered that coils of the LCT type have a scale thickness equal to 5 μm. As for the HCT type, thicknesses equal to 10 μm. It is important to point out that regardless of the material, in this study, the physicochemical properties of the base steel will be considered indifferent, that is, specific mass and specific heat, regardless of their classification, will be considered equal.

Table 23 presents the set-up configurations for the base case.

In addition to the baseline scenario, two extreme operating scenarios will also be evaluated, as shown in Table 24.

It is important to keep in mind that in relation to the base case, all parameters related to the project, *i.e.*, dimensions, layout, among others, were maintained and kept as shown on Table 23. Only the operating conditions of the system were modified.

Table 24 – Other scenarios evaluated. Worst case condition is an operational case more difficult to the system. This scenario should result in more required residence time in the pickling system. The best case is the opposite. This scenario should result in the minimum residence time required along pickling line.

Parameter	Unit	Worst case	Best case
Material type	-	HCT	LCT
Strip width	mm	1870	920
Strip thickness	mm	5.00	1.85
Tanks operational temperature	°C	75	85
Regenerated acid temperature	°C	50	70
Regenerated acid HCl conc.	%	16%	21%
Regenerated acid $FeCl_2$ conc.	%	1%	0%
Recycle flow-rate	$m^3 \cdot h^{-1}$	35	55

4.3.2 Assumptions for the study

To study the industrial process of acid pickling, some assumptions were adopted:

1. The reference conversion considered for the last tank was 99.2%, regardless of the studied scenario. The reason for not considering 100% conversion is justified in the literature by Gines *et al.* (2002). The authors mention that with the naked eye it was identified that the material can be considered pickled in a conversion range of 97.3% to 99.2%. Therefore, the highest value is adopted to avoid under sizing the system.

   the pickling process, heat losses exist. In addition to losses to the environment, two others are of major relevance: 1) loss through evaporation and 2) heat loss for the metallic strip. As a result, in the industrial process heat exchangers supply this load. For mathematical modeling purposes, the exchanger consists of a simple algebraic operation that raises the temperature to the desired operating condition - *set-point*. For example, imagine the temperature operating point in a given tank is 80 °C and that in the working loop it loses 10 °C. Then the thermal exchange procedure delivers this loss and computes the heat required by use of an enthalpy balance. Thermal losses to the environment were not considered in this study.
2. For the study, as shown in Eq. (151), an efficiency factor η_{design} must be assumed to compensate for acid losses in the process, as well as to guarantee a concentration of hydrochloric acid in the last tank. For this purpose, in all studied scenarios this arbitrary factor was assumed as 80%. That is, 20% more HCl is added in comparison to the stoichiometric amount to remove 100% of scale.
3. For the studies in the liquid phase, especially in the recirculation process of the baths, no momentum balance was carried out to evaluate the head losses in the line. Thus, it is only reported that the line pressure was not taken into account in the model.
4. Regarding to the evaporation circuit, no momentum study was carried out in order

to evaluate head losses in the acid fume aspiration circuit. Only a pressure gradient was assumed between the tanks and the main fume collection duct.

5. In industrial practice it is added a volume of regenerated acid to the TK-03 tank, based on empirical knowledge by type of material processed. For each pickling reactor, a buffer tank with a capacity of 25 m^3 receives the transferred volume. The excess volume, by means of a control loop, from the last tank is transferred to the next, which is called cascading. For simulation purposes, it is assumed that between the tanks the same volumetric flow is transferred.
6. Typically in acid pickling lines, especially the turbulent type - as is the case, an Stretch Bending Unit (SBU) system is used. The idea of this equipment is to fracture the structure of the scale in order to facilitate the action of the acid (YAMAGUCHI; YOSHIDA; SAITO, 1994). In this work, this type of influence was not considered in the kinetics. Also, in the SBU operation, it is expected that some of the scale, typically the outermost layers, will be removed. Actions of this type were not modeled, thus, it was considered that the fraction of scale fed is the nominal one.

Based on those assumptions, the pickling process was studied taking as reference three base scenarios: Base Case, Best Case, and Worst Case. The specifications for each case are detailed in Tables 23 and 24.

4.3.3 Base case study

4.3.3.1 Steady state analysis

To evaluate the performance of the pickling system, initially, the mass and energy balance results extracted from the stationary condition were evaluated. To facilitate the interpretation of the process streams, Figure 24 presents a Block Flow Diagram (BFD) of the process contemplating a total of four tanks in series.

In Figure 24, a total of 19 process streams are named. For each stream of interest, a diamond indicates its respective number. Note that some process streams, especially five, have a blue arrow. Typically, these streams are considered to be the battery limits of the process. In addition to the four tanks (TK-00 to TK-03), an individual heat exchanger for each system is also illustrated, as well as a block representing the splitter and mixer set. The mass and energy balance solutions are shown in Table 25. As mentioned in the methodology section, the error criterion adopted for closing the mass balance was 1%.

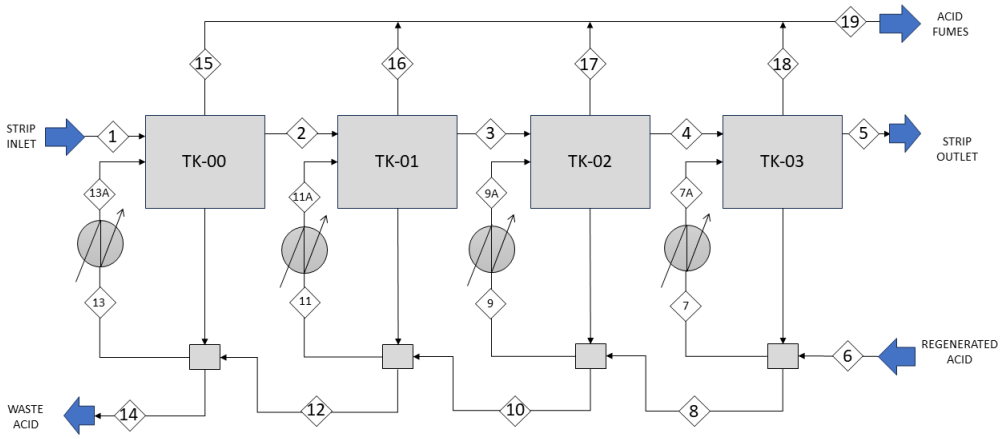

Figure 24 – Industrial acid pickling process Block Flow Diagram - BFD. Each diamond indicates a process stream solved by the steady state simulation.

Table 25 – Mass and energy balance results of the base case in stationary condition. In terms of numerical solution, closing errors of less than 1% are expected. For the case of this application, the global balance closure error was 0.89%.

Stream	1	2	3	4	5	6	7A	8	9A	10
Description	Strip inlet	Strip to TK-00	Strip to TK-01	Strip to TK-02	Strip to TK-03	Regenerated acid	Recycle TK-03	Acid to TK-02	Recycle TK-03	Acid to TK-01
Phase	Solid	Solid	Solid	Solid	Solid	Liquid	Liquid	Liquid	Liquid	Liquid
Compound										
Steel	99.71%	99.80%	99.92%	99.98%	100.00%	0.00%	0.00%	0.00%	0.00%	0.00%
FeO "scale"	0.29%	0.20%	0.08%	0.02%	0.00%	0.00%	0.00%	0.00%	0.00%	0.00%
H_2O	0.00%	0.00%	0.00%	0.00%	0.00%	81.50%	80.66%	80.66%	78.11%	78.13%
HCl	0.00%	0.00%	0.00%	0.00%	0.00%	18.00%	17.96%	17.97%	14.07%	14.09%
$FeCl_2$	0.00%	0.00%	0.00%	0.00%	0.00%	0.50%	1.38%	1.37%	7.82%	7.77%
O_2	0.00%	0.00%	0.00%	0.00%	0.00%	0.00%	0.00%	0.00%	0.00%	0.00%
N_2	0.00%	0.00%	0.00%	0.00%	0.00%	0.00%	0.00%	0.00%	0.00%	0.00%
Total [kg·h^{-1}]	592927	592386	591702	591341	591239	6001	45189	6016	47149	6276
Temperature [°C]	25.0	32.5	40.7	46.8	53.2	60.0	80.0	70.4	80.0	69.1
Vol. flow [m^3·h^{-1}]	75.7	75.6	75.5	75.5	75.5	5.6	42.0	5.6	42.0	5.6
Normal vol. flow [Nm^3·h^{-1}]										

Stream	11A	12	13A	14	15	16	17	18	19
Description	Recycle TK-03	Acid to TK-00	Recycle TK-03	Waste acid	Fumes from TK-00	Fumes from TK-01	Fumes from TK-02	Fumes from TK-03	Acid fumes
Phase	Liquid	Liquid	Liquid	Liquid	Vapor	Vapor	Vapor	Vapor	Vapor
Compound									
Steel	0.00%	0.00%	0.00%	0.00%	0.00%	0.00%	0.00%	0.00%	0.00%
FeO "scale"	0.00%	0.00%	0.00%	0.00%	0.00%	0.00%	0.00%	0.00%	0.00%
H_2O	74.85%	74.92%	72.35%	72.35%	9.64%	9.49%	9.28%	9.17%	9.40%
HCl	7.77%	7.79%	3.12%	3.12%	0.00%	0.02%	0.10%	0.25%	0.09%
$FeCl_2$	17.38%	17.29%	24.53%	24.53%	0.00%	0.00%	0.00%	0.00%	0.00%
O_2	0.00%	0.00%	0.00%	0.00%	21.05%	21.09%	21.11%	21.10%	21.09%
N_2	0.00%	0.00%	0.00%	0.00%	69.30%	69.41%	69.50%	69.47%	69.42%
Total [kg·h^{-1}]	50011	6654	52302	6963	1522	1521	1520	1521	6084
Temperature [°C]	80.0	68.2	80.0	70.4	78.0	78.0	77.8	77.7	77.9
Vol. flow [m^3·h^{-1}]	42.0	5.6	42.0	5.6	1614.0	1611.3	1608.2	1607.1	6440.6
Normal vol. flow [Nm^3·h^{-1}]					1230.5	1228.7	1226.8	1226.3	4912.3

For the Base Case, the results of Table 25 indicate a requirement for regenerated bath load in the order of 5.6 $m^3 \cdot h^{-1}$, with a concentration of 18% by weight of HCl. Based on this flow-rate, the system calculates the concentrations along the baths that satisfy the pickling profile in the solid. In terms of acid concentration, respectively, the following values were found: 17.97%, 14.09%, 7.79%, and finally 3.12%. It should be noted that this behavior makes it clear that the TK-01 is the tank that presents the best performance in terms of solids conversion. Approximately 40% of the solid amount is converted at this stage. In contrast, in the case studied, the TK-03 - the last tank practically does not contribute to scale removal. The main reason for the TK-01 to present the best performance in terms of conversion is due to the fact that the strip has a higher temperature compared to the first stage (TK-00), which results in a faster reaction rate.

The use of the conversion is evidenced by Figure 25. In it, the upper graph demonstrates two curves: the first, in blue and continuous, indicates the scale removal profile in the solid phase (X); the discontinuous curve between the different stages, in orange, indicates the reagent consumption HCl in the bath. From the profile, it is clear that the highest scale consumption, respectively, is TK-01 (ζ from 1 to 2) and TK-00 (ζ from 0 to 1). The profile in the last stage corroborates what is observed in the mass balance table, that is, TK-03 practically does not contribute to the process. It should be noted that for each stage presented, the concentration base for the dimensionless solution of the liquid phase (ψ) is different between the stages, *i.e.*, the adopted reference concentrations correspond to the acid concentration entering the tanks at steady state. Unlike the conversion curve where the dimensionless base, regardless of the tank, is the same. Note that although the TK-01 output ψ indicates 0.9 and the TK-00 indicates 0.82, the highest concentration variation is that of the second tank (TK-01), given that the reference concentration is almost two and a half times greater.

Regarding to the thermal behavior of the solid phase, it is observed that, despite the thickness of the material being thin (4.7 mm), it does not reach thermal equilibrium with the liquid phase in any of the working tanks. This is evidenced by the exit condition of the metallic strip around 53 °C. The key point to note from this is that the proposed heat transfer term is co-current. Thus, as the interaction between phases progresses, the thermal gradient is reduced. By this logic, for the system to reach equilibrium, an infinite area would be needed to reach this condition. Another interesting point to note is that the tank that gained the most temperature with respect to the solid phase was the second, TK-01. This is related to the fact that the pickling chemical reaction is exothermic and, in turn, this equipment is what results in a higher conversion. A critical point in relation to the observed thermal condition is that in industrial practice heat transfer tends to be cross-current. Thus, for future work, it might be interesting to reassess this arrangement.

Figure 25, the bottom graph illustrates dimensionless heat transfer in the reactors. The issue of discontinuity is analogous to that considered in the concentration profile. Despite observing the thermal currents of solid and liquid crossing each other, something that would

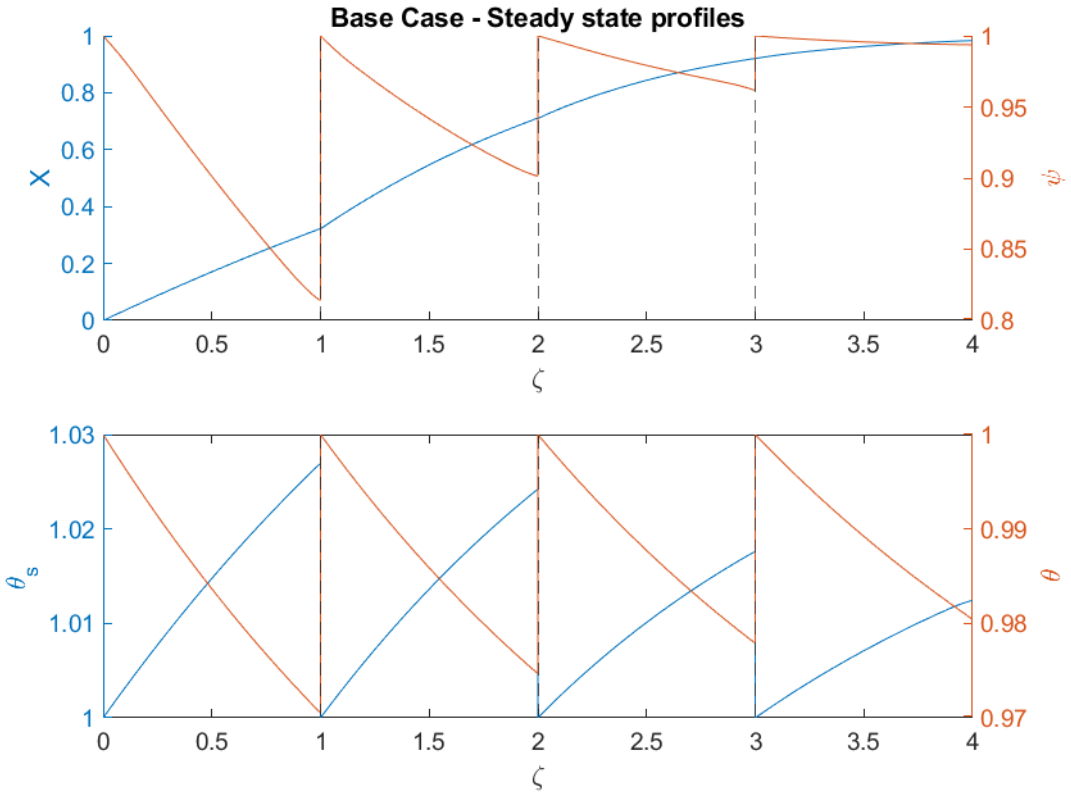

Figure 25 – Mass and thermal profile of the Base Case in steady state. The upper graph details information relevant to the conversion of reagents in the system under analysis. The conversion (X) indicates the intensity of the stripping along the four reactors in series (ζ). Analogously, the consumption of HCl in liquid phase is defined as ψ. Similar to the mass behavior, the bottom graph shows the thermal profile of the system in the solid and liquid phases. θ_s consists of the dimensionless variable that demonstrates the thermal gain of the metallic strip; θ indicates the dimensionless thermal variable related to the liquid phase along the reactors. The presented results were obtained by defining a final conversion in the last reactor (ζ from 3 to 4) of 99.2%. For this condition, the drag speed of the metallic strip was 3.55 m·s^{-1}. In terms of the dimensionless variables presented in the two graphs, it should be noted that they were defined using as a reference the entry conditions of the system in steady state. Therefore, especially in the mass profile, there are discontinuities in relation to the reference value at the entrance.

seem inconsistent with the laws of thermodynamics, the heat transfer conditions are consistent and proven by the mass and energy balance table. The main reason for the streams to cross is due the distinct definition of reference temperature for dimensionless solution. Another important point is that to interpret the results, the reference must be used in absolute thermal units. Observing the thermal behavior of the reactors, it is noted that as the tanks advance, from the direction of the solid inlet to the outlet, the gradient in the liquid phase decreases. Keep in mind that from one stage to another the temperature of the plate rises. Regarding the temperature of the solid phase, the gains are more significant in the first two tanks. Finally, due to the physical layout of the plant, the temperatures entering the reactor are always compensated by a heat exchanger. Thus, regardless of the stage, the temperature of the liquid phase, despite the evaporative effect, tends to be the same. However, as the solid advances, the thermal gradient tends to decrease, as the strip has already gained heat in the previous stage. Thus, in the last stage the thermal gains in the solid have the smallest gradient.

Regarding the effect of evaporation on the behavior of the mass and energy balance, it was observed that water has a greater tendency to evaporate compared to HCl. This is evidenced in previous work by the authors (SIERRA FERNANDEZ et al., 2023b). The key point is that, in practice, the mass flow rate evaporated along the stages is practically the same, around 1520 $kg \cdot h^{-1}$. This corresponds to approximately 3% of the recirculated volume. Keep in mind that the acid fumes is composed approximately 90% in atmospheric air. In terms of thermal loss, it was noted that it varies from 2.0 to 2.4 °C. The greater the acid concentration, the greater the level of loss. The same trend was observed in relation to the concentration of the vapor phase in terms of HCl. It was evident that the higher the acid concentration in the baths, the higher the hydrochloric acid concentration in the head space of the tanks. The variation reached up to 100 times difference between the first and last bath (25 ppm to 2536 ppm). The effect of evaporation can influence the reaction phenomenon in two ways: 1) it reduces negatively as it results in a thermal reduction of the bath following the reaction operation and 2) Due to the effect of water loss, the bath is concentrated in HCl, possibly increasing the acid attack. These two effects influence the reaction in opposite ways, so a more detailed assessment should be made to assess this behavior.

4.3.3.2 Evaporation impacts in pickling velocity

As noted, the effect of evaporation has two opposite impacts on the reaction condition. One points towards a temperature decrease due to the need for heat supply for the liquid to evaporate; consequently lowering the temperature of the bath and therefore lowering the reaction rate. On the other hand, because the vapor pressure of H_2O is higher than that of HCl, it tends to evaporate in greater quantities; as a result, the bath is more concentrated in terms of acid, which results in an increase in reaction speed. Due to this complex behavior, the Base Case condition was evaluated for five different system temperatures: 65, 70, 75, 80 and 85 °C. Based on these different scenarios, the speed that satisfies a conversion of

Table 26 – Influence of evaporation on the productivity of a pickling line. The results indicate the speeds of the metallic strip that result in final conversions of 99.2% for simulations without and with evaporation, respectively ideal and real case. The Base Case was used as a reference to generate the results; only the tank temperatures were varied. Evaporation influence ranges vary from 2.8 to 4.8% in terms of productivity reduction. The thermal condition of 80 °C had the greatest influence on productivity, 4.8%. The conditions of 70 and 85 °C indicate the values of lesser influence 2.8 %.

Temperature [°C]	**Velocity [m·s^{-1}]**		**Evaporation Effect [%]**
	Ideal	**Real**	
65	2.07	2.00	3.5%
70	2.55	2.48	2.8%
75	3.18	3.05	4.3%
80	3.72	3.55	4.8%
85	4.35	4.23	2.8%

99.2% was evaluated considering the effect with and without evaporation.

The results of the evaporation influence analysis are presented in Table 26. Notably, regardless of the chosen temperature, it is noted that, as expected, evaporation negatively interferes with system performance. This is observed because the Ideal case, without evaporation, always shows higher velocities than the Real case. In order to better interpret it, a parameter called the Evaporation Effect was defined, which consists of the ratio between the ideal and the real speed. These percentage results demonstrate that the range of influence of evaporation varies from 2.8% to 4.8% on the productive performance of the plant. The compensatory effect of concentration and thermal loss are evidenced by the fact that the most influent evaporation condition was at 80 °C; and the smaller ones are both at 85 and 70 °C. This is an indicator that there is a non-linear trend in evaporative heat loss.

4.3.3.3 Transient analysis

In terms of transient analysis, it was observed that the system reaches a stationary condition in an interval of 4 residence times. For the Base Case, this corresponds to approximately 23 seconds. Because it is a model implemented in a dimensionless form, the interpretation of the surface graphs depend on the considered initial condition. For the solid phase, it is considered that at time zero the metallic surface is inside all the tanks under the inlet conditions. That is, at room temperature and with the maximum scale thickness. With respect to the liquid phase, in the initial condition it is assumed that the entire system is flooded with pickling bath at the concentration conditions of the regenerated bath and at the post evaporation chamber reference temperature, *e.g.*, 78 °C.

Regarding the transient interpretation for the solid phase, Figures 26a and 26b present, respectively, the conversion and thermal profiles along the stages. Due to the fact that the arrangement of the pickling tanks, especially with regard to the liquid phase, presents a behavior with a concentrated parameter outside the reactor, slight discontinuities can be

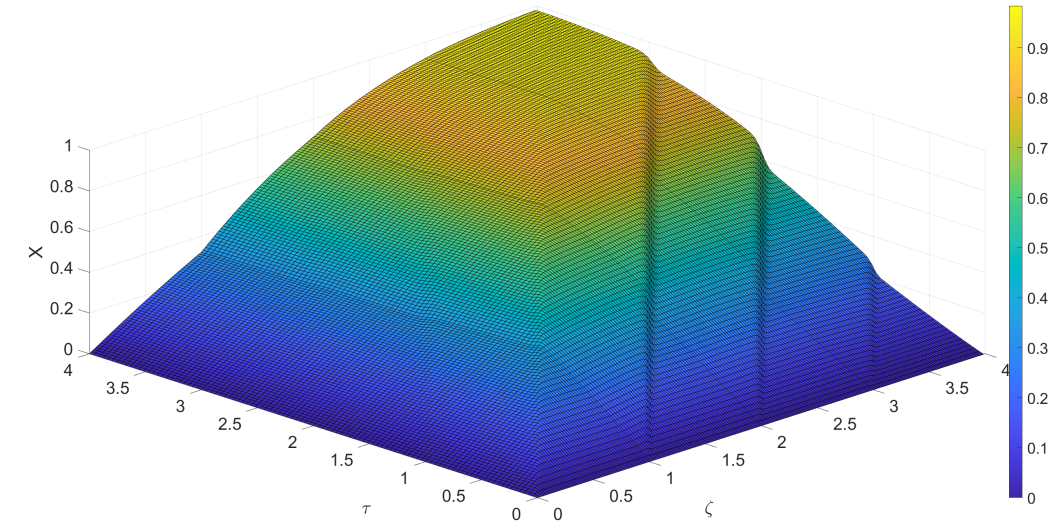

(a)

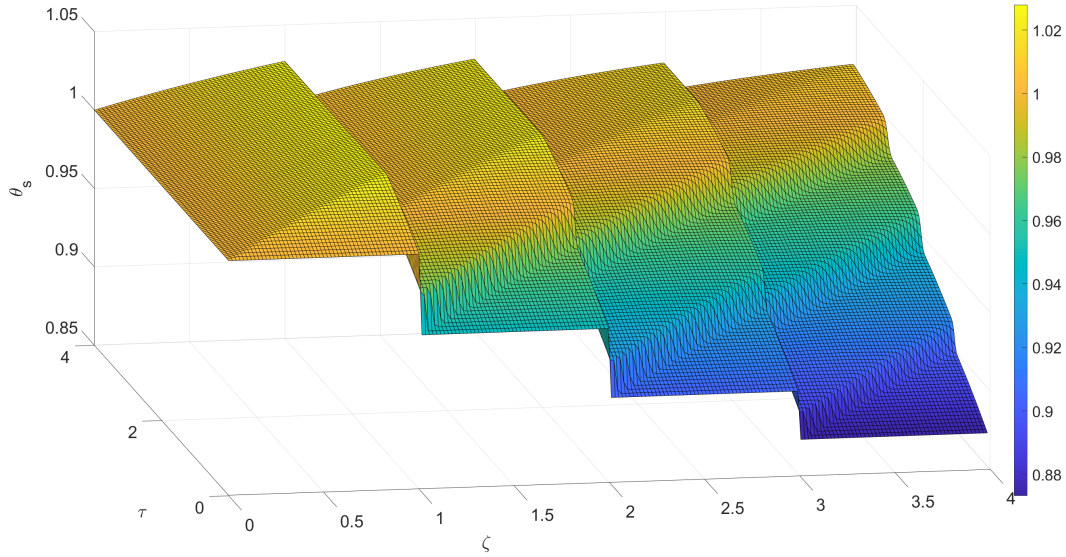

(b)

Figure 26 – Transient behavior in solid phase applied to the Base Case for a pickling speed of 3.55 m·s^{-1}. Figure 26a shows the conversion behavior along the four pickling tanks. In approximately four residence times the system reached the steady state. Figure 26b shows the dimensionless thermal behavior of the system. For each reactor (ζ) there is a discontinuity due to the temperature reference being different for each tank.

noted in the conversion profile at the end of the domains between one tank and another. The main point is that, according to the idealized theoretical model, the system should consist of a single reactor where the concentrated bath enters at one end, and the metallic strip to be pickled at the other. As this ideal arrangement does not exist, discontinuities are observed.

The discontinuity becomes more evident when observing the thermal behavior of the

solid phase in Figure 26b. It should be emphasized that the reference for the dimensionless solution is always based on the inlet temperatures of the solid in steady state. As at instant zero the plate is in the ambient condition, and, in addition, the last tank has a stationary condition with a higher temperature, this resulted in the highest level of thermal variation. By the same logic, the first tank resulted in the smallest variation.

With respect to the dynamic behavior of the fluid phase, Figures 27a and 27b show the solution surfaces of HCl consumption and temperature of the liquid phase between the different pickling baths. By first evaluating Figure 27a, it can be seen that the first tank has a high concentration gradient in relation to time zero and the fourth time. This result is due the countercurrent effect of the system. In TK-00 minimum acid concentrations are expected, around 3% in the steady state; while in TK-03 concentrations close to the regenerated bath are expected. In this case, it is clear why the mass gradient is greater in the TK-00 and almost imperceptible in the TK-03.

Regarding the thermal condition of the liquid phase, the scenario is different from that observed for the solid phase. In the case of the solid phase, the boundary conditions between the tanks showed continuity. That is, the temperature of the strip that leaves one stage is the boundary condition for the next one. In the case of the liquid phase, due to the fact that there is a heat exchanger in the recycle of the baths, always at the boundary of the baths the temperature is forced to a reference condition. For example, in the Base Case there is the condition of 80 °C minus the evaporation loss. This behavior is observed in Figure 27b. The key point is that there is a more abrupt thermal reduction in the initial times due to the metallic surface inside the tanks being in the ambient condition.

4.3.4 Thermal demand of heat exchangers

The mathematical model computed the heat consumption required for each heat exchanger in order to assess the needs in terms of utilities. Figure 28 presents a bar graph showing the thermal consumption of each heat exchanger according to the cases studied.

Figure 28 shows that regardless of the chosen situation, the most requested heat exchanger is for the TK-00 tank due to the metallic strip being at ambient temperature. In this scenario, the values are in the order of 275 to 285 kW. For the other scenarios, the parameters are identical in terms of consumption: ranging from 220 to 230 kW. Attention is attracted to the *best case* scenario. Note that in it the thermal needs along the stages tend to lessen. This is connected to the fact that the steel capacity is substantially reduced when compared to the other possibilities, approximately 35% of the worst case. That instance, knowing that the principal consumer of heat in the system is the heating of the metallic strip, then it is apparent that, with lesser steel capacity, the heat load is likewise lowered. Because of this incompatibility due to the poor operating capacity of the *best case*, the *base case* and *worst case* displayed identical values in terms of heat consumption. Respectively, the total consumptions were: 768, 902 and 972 kW. This information is useful for sizing the heat

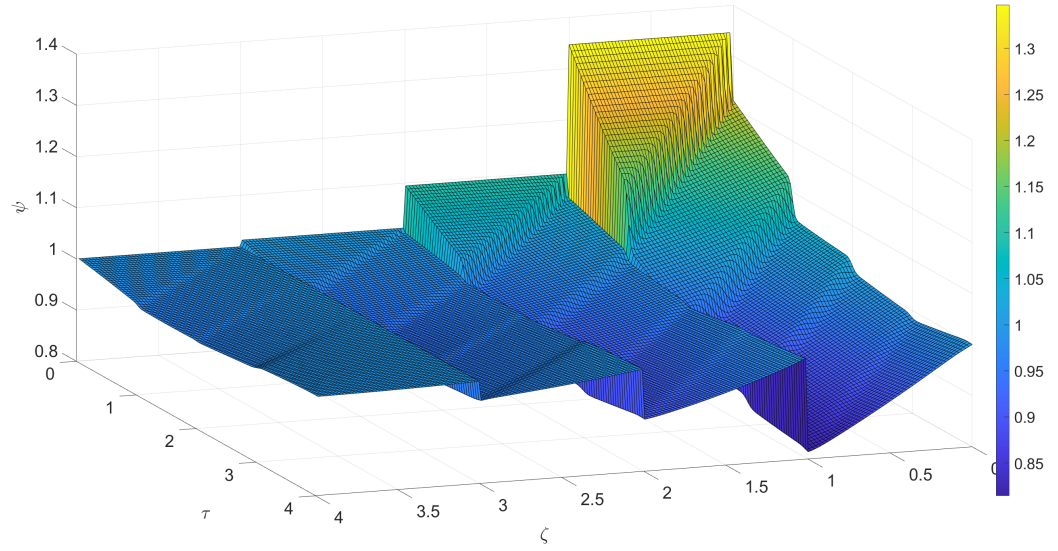

(a)

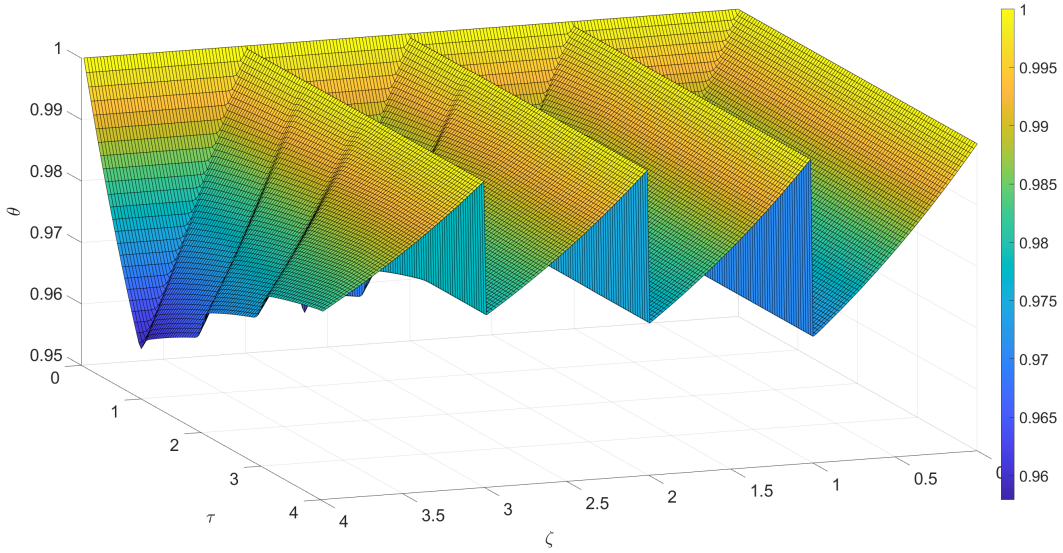

(b)

Figure 27 – Transient behavior in liquid phase applied to the Base Case for a pickling speed of 3.55 m·s^{-1}. Figure 27a shows the behavior of reagent consumption (ψ) along the four pickling tanks. In approximately four residence times the system reached the steady state. Figure 27b shows the dimensionless thermal behavior of the system. For each reactor (ζ) a discontinuity is observed due to the reference temperature and concentration of HCl being different for each tank.

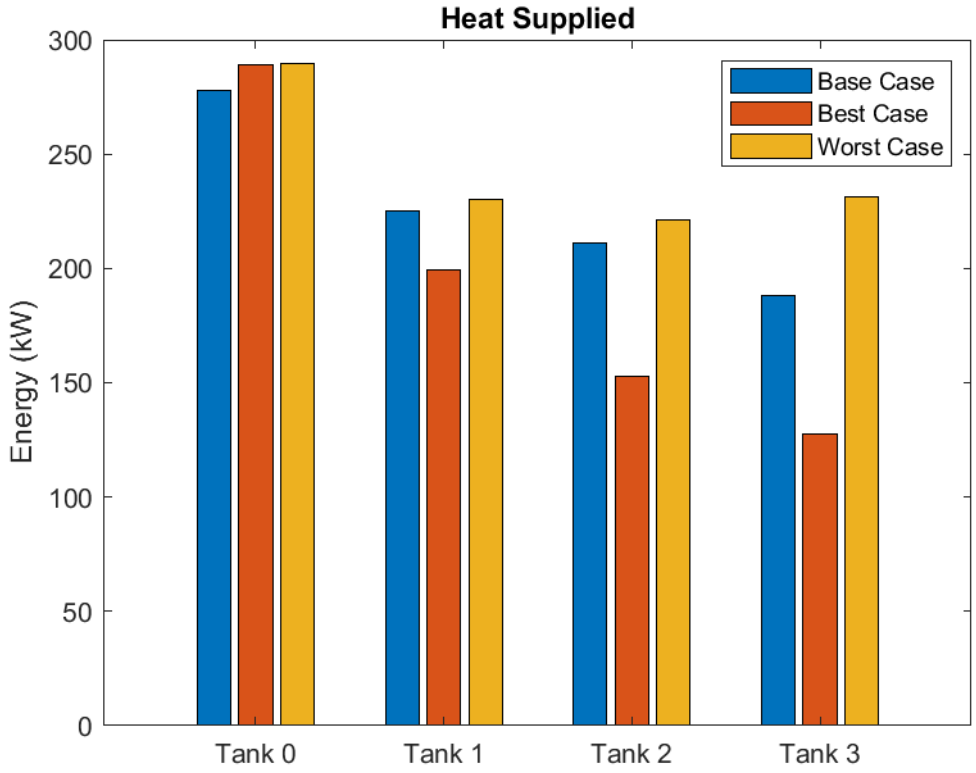

Figure 28 – Individual thermal consumption for each pickling tank. A total of 3 scenarios were simulated - Base Case, Worst Case and Best Case. The behavior in terms of total thermal energy consumption for the tanks ranges from 972 to 768 kW. The highest consumption was applied to the Worst Case and the lowest consumption was applied to the Best Case. The difference in terms of consumption is explained by the fact that the Best Case has a smaller nominal amount of metallic material going through the system. The opposite occurs for the Worst Case.

exchangers.

4.3.5 Comparison between the different study scenarios

Simulations were performed for three different operating conditions. The idea of the study was to compare the productive performance to a Baseline condition, that is, normally operated in the plant. An advantageous condition for the operation of the unit, *i.e.*, high bath temperatures, low material flow rate, high recirculation rate and regenerated bath with the highest possible acid concentration was considered. And a condition of great disadvantage was also evaluated, that is the opposite of the advantageous condition. The advantageous condition is called *best case*, the disadvantageous condition *worst case* and the normal operating condition *base case*.

In order to be able to compare the performance between the cases, the following prerogative was assumed: the system output conversions must be the same - 99.2%. Then, it is evaluated the speed that satisfies this conversion condition. Figure 29 shows this behavior.

Figure 29 presents a lot of information. It shows the fractions of $FeCl_2$ and HCl by

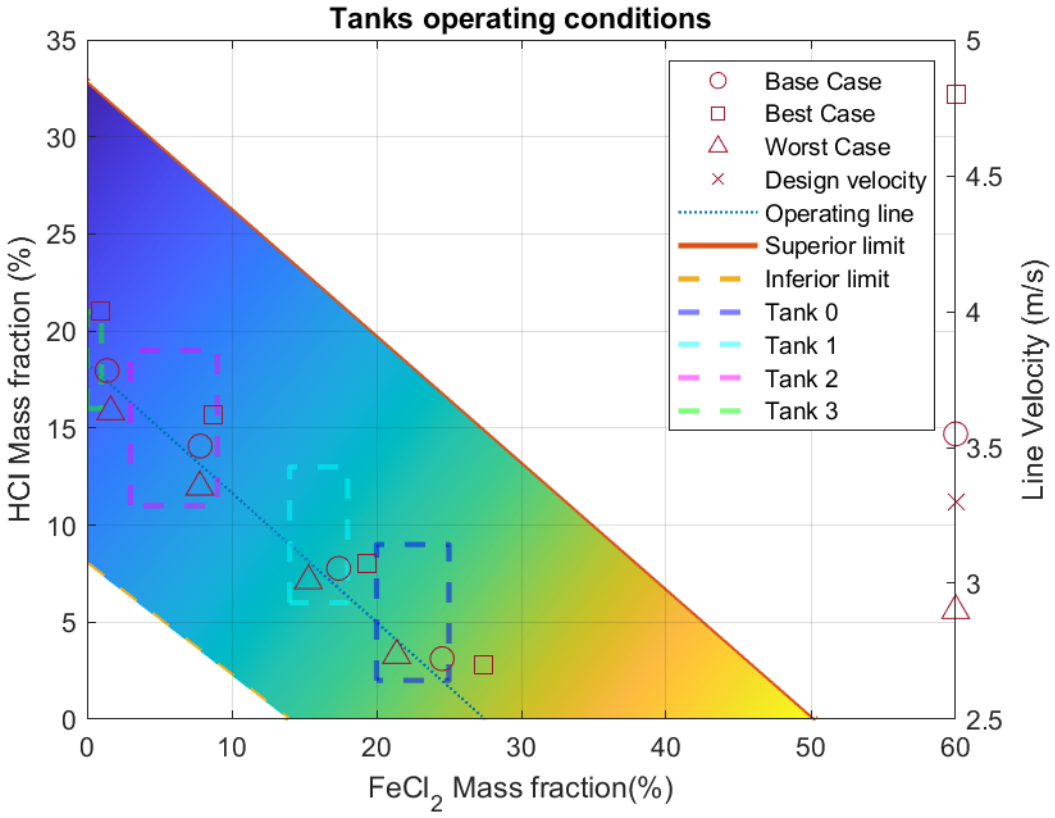

Figure 29 – Pickling bath concentrations along the different process tanks. Three scenarios were studied with the objective of evaluating the consistency of the results with the expected concentration ranges in the plant. Additional information on the ordinate axis, on the right, shows the speed of the metallic strip for each case studied. In addition, the reference speed is indicated on this axis. In the graph, three transversal lines are presented: Upper, Lower and Operating Limits of Concentration. The operating line is defined by the stoichiometric condition between ferrous chloride and hydrochloric acid. Rectangular boxes arranged in the operational area indicate the expected operational concentration range in each tank..

weight on the abscissa and ordinate axis, respectively. A new axis of ordinates was included, on the right, in order to indicate the linear speed of the system. Rectangles represent the concentration ranges of baths applicable in the industrial plant. A theoretical operating line, based on stoichiometry, is indicated. The upper and lower limits of operation are detailed in the authors' previous work (SIERRA FERNANDEZ et al., 2023b). Evaluating the results obtained, the concentration points found for the pickling baths in each scenario were indicated in the graphs. Note that, with the exception of the advantageous case, the points found are within the rectangles of each tank. Only the TK-03 tank indicated a limiting condition in terms of concentration, the rest stayed on track.

With regard to speeds, the industrial unit was sized and certified to operate with a nominal capacity of 3.33 $m{\cdot}s^{-1}$. It can be seen from the figure that in the base case the resulting speed value found was 3.55 $m{\cdot}s^{-1}$, presenting a difference of 7% in relation to the design reference. When comparing the *worst case*, a velocity of 2.9 $m{\cdot}s^{-1}$ is found, that is,

13% below the reference condition. The *best case* scenario resulted in a speed limit of 4.8 $m \cdot s^{-1}$, 44% more than the reference condition.

The results found for the base and pessimistic cases indicate an excellent consistency with the design operational ranges practiced in the studied industrial unit. The case that diverged significantly, *best case*, demonstrates both in the composition of the liquid streams and in the flow velocity of the material a certain inconsistency. It is believed that the main point, when analyzed it in terms of the hourly quantity of steel processed, is:

- *Base case*: 592 $ton \cdot h^{-1}$;
- *Worst case*: 768 $ton \cdot h^{-1}$;
- *Best case*: 232 $ton \cdot h^{-1}$.

Evaluating in terms of the resulting data, there is an average value of 531 $ton \cdot h^{-1}$ of processed material. Furthermore, the results show an amplitude of $\pm$ 268 $ton \cdot h^{-1}$. That is, in terms of control, it would be feasible to find values in a range of 531 $\pm$ 268 $ton \cdot h^{-1}$. Therefore, the upper processing limit would be 799 $ton \cdot h^{-1}$; the lower would be 263 $ton \cdot h^{-1}$. In other words, the *best case* condition would be outside the expected range. It can be said that a reasonable variation range for this process configuration is $\pm$ 50%. In the case of the *best case*, the processing value would be even below the minimum reference (263 *vs.* 232). Therefore, the mentioned scenario is only hypothetical and in industrial practice it is not feasible.

4.4 Conclusions

In this work, a heterogeneous phenomenological model applied to the industrial acid pickling process using HCl was developed. The phenomenological approach took into account typical aspects of the industrial process, such as the recirculation of the pickling baths in the tanks, as well as the effect of evaporation.

In terms of tool performance, for evaluation purposes with the industrial process, data from an industrial plant located in southern Brazil was used. Three operational scenarios were evaluated in order to verify the consistency of the simulated results and compare them with the plant data. As a result, the concentrations of HCl and $FeCl_2$ were analyzed along the pickling baths, as well as the nominal speed of the steel strips. Among the analyzed scenarios, two scenarios showed good consistency with real operating conditions - Base Case and Worst Case. The Best Scenario behaved as an *outlier* of the process.

In addition to the preliminary validation of the results, the process simulator made it possible to verify the influence of evaporation on the maximum feed speed of the metallic strips. On average, simulating the process with and without the evaporation module resulted in reductions in the linear velocity of the strips of up to approximately 5%. Which indicates this as a relevant factor for the process.

The central idea of the industrial use of this simulator is to serve as a pilot for a digital

twin for turbulent pickling systems using HCl. Some small advances are required to be able to consider all the details of the real process. In particular, it can be mentioned: 1) a detailed thermal model of the heat exchangers, 2) application of momentum balances in the bath transport lines and acid fume flow (pumping and venting systems), and 3) inclusion of work tanks in the system. It is important to note that the simulator, in future stages, must undergo field validation considering more specific material and process data. That is, it is considered that this work presents a preliminary validation, validating the simulator for characteristic operating ranges in which the process works. It is suggested that future works evaluate in detail the concentration behaviors of the baths and the residual scale thickness for a given operation campaign in order to compare with the results obtained by the model.

5 CONCLUDING REMARKS

This thesis aimed to contribute to the industrial process of acid pickling using HCl as a chemical agent. The contributions, as mentioned in Chapter 1, were segmented into three areas of chemical engineering knowledge: 1) Thermodynamics; 2) Chemical kinetics; and 3) Phenomenological mathematical modeling. Specifically, as presented in Section 1.1, this work sought to answer the following questions:

1. How does the temperature and concentration of $FeCl_2$ and HCl interfere with the main physicochemical properties of pickling baths?
2. Based on the dependency level, is it possible to create a criterion to define which of the parameters are more prevalent in relation to the other?
3. Is there any number or group of dimensionless numbers capable of characterizing the rate law or pickling kinetic of different materials?
4. Could the models that have been developed as a function of these dimensionless groups demonstrate reliability in accordance with the existing literature?
5. Can a PDE system be applied, and is it consistent with the operating conditions of an industrial pickling line using HCl as a pickling agent?
6. Based on the mathematical model, what is the level of interference of the evaporation of HCl on the performance of the maximum operating speed of an industrial line?

Questions 1 and 2, listed above, were answered in Chapter 2 of this thesis. To answer the first question, a calculation methodology was developed to estimate the main physicochemical properties of pickling baths. In this way, surface maps were generated in order to evaluate the behavior of each property, seven in total. Altogether 35 maps were generated. The seven studied properties were organized for five different operating temperatures. Such operating conditions adopted are typical of an industrial acid pickling unit. In addition to developing the methodology for the calculation and contributing with a graphical solution, the author proposed an approach to assess the level of dependence of a given variable as a function of temperature and its composition throughout the baths. The idea of the classification is to present a criterion for simplifying the calculation of physical properties with respect to their dependence on the intensive variables. In this way, this contribution seeks to allow the reader, in future works and in a conscious way, to simplify the constitutive equations in order to gain computational performance, for example.

Although the methodology for calculating the physicochemical properties has a theoretical character, it clearly contributes to scientists and professionals in the steel industry as a guide for estimating the usual physical parameters in process engineering applications involving hydrochloric acid and ferrous chloride solutions. Previously in the literature there was no contribution dedicated to this purpose. The information was dispersed in textbooks and

scientific papers. Furthermore, the suggested semi-quantitative analysis criterion provides an opportunity for additional researchers to employ this methodology in the examination of complex liquid solutions. For example, in the food and beverage industry it would be interesting to apply the strategy for the physical properties of miscella [1] or even in the sugar and alcohol industry along the mills.

It is important to keep in mind that every study in Chapter 2 has not been experimentally validated. Despite the results being consistent with what was observed in the industrial routine, and corroborated by the simulations, it is recommended that future works seek to experimentally validate the evaluated properties. In addition, another important point to evolve the work would be to also consider the influence of $FeCl_3$ in the calculations and, thus, investigate the level of interference in the quantified values. Among the estimated parameters, it is important that readers are aware that the mass diffusion of HCl was estimated without considering the influence of iron ions, a significant parameter in quantitative terms. Thus, although in practice this parameter presents orders of magnitude compatible with other solutes, *e.g.* NaCl, it is recommended that the reader be aware that it may have a significant impact on its application.

Questions 3 and 4 were answered by Chapter 3. This part of the thesis focused on developing a kinetic expression capable of representing the speed of acid pickling. As already mentioned, in previously published articles, authors always emphasized empirical approaches and only a few dedicated themselves to using traditional methods of chemical kinetics, considering the process as homogeneous and, in some cases, the JMA method, as a function of time. Those approaches does not allow, for example, to simulate the pickling phenomenon in a phenomenological computational tool. The reaction speeds could not be extrapolated to other configurations: either because they were time-dependent or because they were based on statistical expressions.

To solve this problem, a theoretical study of experimental pickling curves was carried out and it was proposed to apply the shrinking core model (SCM) to model the phenomenon. As a result, a kinetic expression compatible with other applications already tested was presented and validated with data from the literature. The main highlight was that the parameters were a function of the material's physical properties and not a "black box" parameter. As a result, in addition to the application of the SCM, the author applied a material balance in the solid phase in order to verify the application of the kinetic model. A classic chemical reactor - PFR model was chosen to compute the scale pickling along four tanks in series. The application of the reactor model together with the developed rate law gave rise to a dimensionless number: Pickling Number, which has an order of magnitude of 10^5, and which singularizes the pickling kinetic. That is, the higher the number, the shorter the residence times required for pickling. Therefore, it is proposed that, in future works, this dimensionless number found be named as *Pickling Number*.

1. solution of vegetable oil and organic solvent, typically n-hexane.

Questions 5 and 6 were answered in chapter 4 of this thesis. In this chapter a model of Partial Differential Equations was created taking into account phenomenological aspects of the pickling process. The simulation evaluated the heterogeneous behavior of an industrial acid pickling system. Aspects such as evaporation, recycle rate and material composition dynamics between pickling baths were evaluated.

Regarding question 5, the developed PDEs model was preliminarily validated with industrial data from a plant located in the south of Brazil. The concentration ranges of $FeCl_2$ and HCl were used to analyze whether the results obtained from the model are coherent with the operation of the unit. As a result, there was good consistency with two of the three cases evaluated. Another evaluated parameter was the speed of the resulting strips applied to the model. In practical terms, the speed calculated for a standard operational situation exhibited a deviation of 7% when compared to the designated speed. An additional case was assessed, taking into account an unfavorable operational circumstance, and was subsequently compared to the designated speed, revealing a deviation of 12%. Both evaluated aspects are indicators that the phenomenological model can be used to simulate acid pickling system.

Still using the analyzes developed by the phenomenological model, question 6, regarding the interference of evaporation in the pickling system, was answered by simulating the model with and without the evaporation balance for the same reference case. For the reference case, 5 different operating temperatures of baths from 65 to 85 °C were analyzed. As a result of the study, it was observed that evaporation negatively impacts the pickling speed, which varies from 2.8% to 4.8%. The factor that drew attention was the fact that the influence of evaporation does not linearly depend on the increase in operating temperature: the conditions at 70 and 85 °C had the lowest influence on evaporation, whereas the condition at 80 °C is the condition most affected by evaporation in the studied range. This investigation opens up a prerogative to evaluate the best configuration of pickling bath temperatures for a given operational condition.

Despite questions 5 and 6 having been satisfactorily answered, it is fundamental that future works seek to validate the temperature and concentration results of the pickling baths with a larger range of operational data. Furthermore, it is recommended to develop mathematical approaches for parts of the pickling line currently simplified by the current PDE model. For example, system flow effects of pumping and *venting*, working tanks and heat exchangers. With this development, in terms of unit operations, it is believed that future work will be able to implement and validate a true digital twin with the pickling process.

Finally, the main contributions of this thesis are summarized in the chart below:

Original Contributions

1. Methodology to compute physicochemical properties of pickling baths with HCl;
2. Criterion for classifying the level of variation in the physical properties of the pickling solution over the pickling baths;
3. Kinetic expression to compute the acid pickling rate using the SCM approach;
4. Identification of a Dimensionless Number called Pickling or Modified Damkohler Number;
5. Mathematical model of PDEs capable of simulating a turbulent acid pickling line.

References

BASCONE, D.; CIPOLLINA, A.; MORREALE, M.; RANDAZZO, S.; SANTORO, F.; MICALE, G. Simulation of a regeneration Bascone, D., Cipollina, A., Morreale, M., Randazzo, S., Santoro, F., & Micale, G. (2016). Simulation of a regeneration plant for spent pickling solutions via spray roasting. Desalination and Water Treatment, 57(48–49), 23405–2. **Desalination and Water Treatment**, v. 57, n. 48-49, p. 23405–23419, 2016. ISSN 19443986.

BECK, Marcus; WIRTZ, Siegmar; SCHERER, Viktor; BÄRHOLD, Frank. Numerical calculations of spray roasting reactors of the steel industry with special emphasis on Fe2O3-particle formation. **Chem. Eng. Technol.**, v. 30, n. 10, p. 1347–1354, 2007. ISSN 09307516.

BENINTENDI, Renato. **Process safety calculations**. [S.l.]: Elsevier, 2021.

BERGMAN, Theodore L; INCROPERA, Frank P; DEWITT, David P; LAVINE, Adrienne S. **Fundamentals of heat and mass transfer**. [S.l.]: John Wiley & Sons, 2011.

BORNMYR, Anders; HOLMBERG, Björn. **Handbook for the pickling and cleaning stainless steel**. [S.l.: s.n.], 1995.

CAO, Guang ming; LIU, Xiao jiang; SUN, Bin; LIU, Zhen yu. Morphology of oxide scale and oxidation kinetics of low carbon steel. **Journal of Iron and Steel Research International**, v. 21, n. 3, p. 335–341, 2014. ISSN 1006706X.

CHEN, R. Y.; YUEN, W. Y.D. Examination of oxide scales of hot rolled steel products. **ISIJ International**, v. 45, n. 1, p. 52–59, 2005. ISSN 09151559.

CREMASCO, Marco Aurélio. **Difusão mássica**. [S.l.]: Editora Blucher, 2019.

CROWL, Daniel A; LOUVAR, Joseph F. **Chemical process safety: fundamentals with applications**. [S.l.]: Pearson Education, 2001.

CUSSLER, Edward Lansing. **Diffusion: mass transfer in fluid systems**. [S.l.]: Cambridge university press, 2009.

DENG, G. Y.; TIEU, A. K.; SU, L. H.; ZHU, H. T.; ZHU, Q.; ZAMRI, W. F.H.; KONG, C. Characterizing deformation behaviour of an oxidized high speed steel: Effects of nanoindentation depth, friction and oxide scale porosity. **International Journal of Mechanical Sciences**, v. 155, February, p. 267–285, 2019. ISSN 00207403.

FELDER, Richard M; ROUSSEAU, Ronald W; BULLARD, Lisa G. **Elementary Principles of Chemical Processes**. [S.l.]: Wiley-Blackwell, 2010.

FENG-I, Wei. The effect of scale microstructure on the pickling of hot-rolled steel strip. **Anti-Corrosion Methods Mater.**, v. 35, n. 12, p. 4–9, 1988. ISSN 00035599.

FOGLER, H. Scott. **Elements of Chemical Reaction Engineering**. [S.l.: s.n.], 2016.

GINES, M. J L; BENITEZ, G. J.; PEREZ, T.; MERLI, E.; FIRPO, M. A.; EGLI, W. Study of the picklability of 1.8 mm hot-rolled steel strip in hydrochloric acid. **Lat. Am. Appl. Res.**, v. 32, n. 4, p. 281–288, 2002. ISSN 03270793.

GREEN, Don W.; PERRY, Robert H. **Perry's Chemical Engineers' HANDBOOK**. 8. ed. [S.l.]: MC Graw Hill, 2007. ISBN 0071422943.

GUAN, Chuang; LI, Jun; TAN, Ning; HE, Yong Quan; ZHANG, Shu Guang. Reduction of oxide scale on hot-rolled steel by hydrogen at low temperature. **Int. J. Hydrogen Energy**, Elsevier Ltd, v. 39, n. 27, p. 15116–15124, 2014. ISSN 03603199.

HEMMELMANN, Jan C.; XU, Hao; KRUMM, Wolfgang. Empirical modeling of iron oxide dissolution in sulphuric and hydrochloric acid. **Metall. Mater. Trans. B Process Metall. Mater. Process. Sci.**, v. 44, n. 5, p. 1232–1235, 2013. ISSN 10735615.

HUDSON, R M; BROWN, D W; WARNING, C J. Factors Influencing the Pickling Time Required for Hot-Rolled Steel Strip. **Journal of Metals**, p. 9–13, 1967.

HUDSON, R. M.; WARNING, C. J. Effect of Strip Velocity on Pickling Rate of Hot-Rolled Steel in Hydrochloric Acid. **JOM: Journal of The Minerals, Metals & Materials Society**, v. 34, n. 2, p. 65–70, 1982. ISSN 15431851.

HUDSON, RM. **ASM Handbook, Volume 5: Surface Engineering**. [S.l.]: ASM International, 1994.

ISOPESCU, L.; FRANK, P. M.; GONSIOR, G. Modelling of a turbulence pickling line for adaptive control. **European Control Conference, ECC 1999 - Conference Proceedings**, IEEE, p. 4014–4019, 2015.

JATUPHAKSAMPHAN, Yubonrat; PHINICHKA, Natthapong; PRAPAKORN, Kritsada; SUPRADIST, Mawin. Pickling Kinetics of Tertiary Oxide Scale Formed on Hot-Rolled Steel Strip. **Journal of Metals, Materials, and Minerals**, v. 20, n. 1, p. 33–39, 2010.

JAWORSKI, Zdzisław; CZERNUSZEWICZ, Małgorzata; GRALLA, Łukasz. A comparative study of thermodynamic electrolyte models applied to the Solvay soda system. **Chemical and Process Engineering**, v. 32, n. 2, p. 135–154, 2011.

KELL, George S. Density, thermal expansivity, and compressibility of liquid water from 0. deg. to 150. deg.. Correlations and tables for atmospheric pressure and saturation reviewed and expressed on 1968 temperature scale. **Journal of Chemical and Engineering Data**, ACS Publications, v. 20, n. 1, p. 97–105, 1975.

KLADNIG, W. F. New Development of Acid Regeneration in Steel Pickling Plants. English. **Journal of iron and steel research, international.**, v. 15, p. 1–6, 2008.

LALIBERTE, Marc; COOPER, W Edward. Model for calculating the density of aqueous electrolyte solutions. **Journal of Chemical & Engineering Data**, ACS Publications, v. 49, n. 5, p. 1141–1151, 2004.

LALIBERTÉ, Marc. A model for calculating the heat capacity of aqueous solutions, with updated density and viscosity data. **Journal of Chemical and Engineering Data**, v. 54, n. 6, p. 1725–1760, 2009. ISSN 00219568.

LALIBERTÉ, Marc. Model for calculating the viscosity of aqueous solutions. **Journal of Chemical and Engineering Data**, v. 52, n. 2, p. 321–335, 2007. ISSN 00219568.

LEVENSPIEL, Octave. **Chemical Reaction Engineering**. [S.l.: s.n.], 1998.

LI, Lian Fu; CAENEN, Peter; DAERDEN, Mathieu; VAES, David; MEERS, Guido; DHONDT, Caroline; CELIS, Jean Pierre. Mechanism of single and multiple step pickling of 304 stainless steel in acid electrolytes. **Corrosion Science**, v. 47, n. 5, p. 1307–1324, 2005. ISSN 0010938X.

MAANONEN, Mika. Steel pickling in challenging conditions. **thesis, Metropolia Ammattikorkeakoulu**, 2014.

MCKINLEY, Caitlyn; GHAHREMAN, Ahmad. Hydrochloric acid regeneration in hydrometallurgical processes: a review. **Mineral Processing and Extractive Metallurgy: Transactions of the Institute of Mining and Metallurgy**, Taylor & Francis, v. 127, n. 3, p. 157–168, 2018. ISSN 2572665X.

MCLAUGHLIN, E. The thermal conductivity of liquids and dense gases. **Chemical Reviews**, ACS Publications, v. 64, n. 4, p. 389–428, 1964.

OLIVEIRA, José Augusto Furtado de. Modelagem e Simulação da Solubilidade de Sais em Sistemas Aquosos com Monoetilenoglicol, 2014. ISSN 1098-6596. arXiv: arXiv:1011.1669v3.

OMEIRI, Hanane; INNAL, Fares; HAMAIDI, Brahim. safety integrity evaluation of a butane tank overpressure evacuation system according to IEC 61508 standard. **Journal of Failure Analysis and Prevention**, Springer, v. 15, p. 892–905, 2015.

ÖZDEMIR, T.; ÖZTIN, C.; KINCAL, N. Suzan. Treatment of waste pickling liquors: Process synthesis and economic analysis. **Chemical Engineering Communications**, v. 193, n. 5, p. 548–563, 2006. ISSN 00986445.

REGEL-ROSOCKA, Magdalena. A review on methods of regeneration of spent pickling solutions from steel processing. **Journal of Hazardous Materials**, v. 177, p. 57–69, 2010.

ROBINSON, RA; STOKES, RH. Solutions of electrolytes and diffusion in liquids. **Annual Review of Physical Chemistry**, Annual Reviews 4139 El Camino Way, PO Box 10139, Palo Alto, CA 94303-0139, USA, v. 8, n. 1, p. 37–54, 1957.

ROBSON, John. Steel Pickling: A Profile. n. 68, 1993.

RUZICKA, M. C. On dimensionless numbers. **Chemical Engineering Research and Design**, v. 86, n. 8, p. 835–868, 2008. ISSN 02638762.

SEBORG, Dale E; MELLICHAMP, Duncan A; EDGAR, Thomas F; DOYLE III, Francis J. **Process dynamics and control**. [S.l.]: John Wiley & Sons, 2010.

SHREVE, R. Norris; JR., Joseph A. Brink. **Indústria de Processos Químicos**. Quarta. [S.l.: s.n.], 1997.

SIERRA FERNANDEZ, Jose O.; GUEBERT, Diogo A. M.; PORTO, Luismar Marques; DE NONI JR., Agenor. Kinetic and phenomenological model to estimate maximum speeds of pickling lines using dimensionless numbers: a typical chemical reactor engineering approach, 2023.

SIERRA FERNANDEZ, Jose O.; GUEBERT, Diogo A. M.; PORTO, Luismar Marques; DE NONI JR., Agenor. Semi-quantitative method for categorizing the effect of composition and temperature on HCl solutions used in acid pickling processes, 2023.

TURKDOGAN, E. T.; VINTERS, J. V. Gaseous reduction of iron oxides: Part I. Reduction of hematite in hydrogen. **Metall. Mater. Trans. B**, v. 2, n. 11, p. 3175–3188, 1971. ISSN 1073-5615.

TURTON, Richard; BAILIE, Richard C; WHITING, Wallace B; SHAEIWITZ, Joseph A. **Analysis, synthesis and design of chemical processes**. [S.l.]: Pearson Education, 2008.

WEN, C. Y. Noncatalytic heterogeneous solid-fluid reaction models. **Industrial and Engineering Chemistry**, v. 60, n. 9, p. 34–54, 1968. ISSN 00197866.

YAMAGUCHI, Susumu; YOSHIDA, Teruo; SAITO, Takaho. Improvement in Descaling of Hot Strip by Hydrochloric Acid. **ISIJ Int.**, v. 34, n. 8, p. 670–678, 1994. ISSN 0915-1559.

APPENDIX A – Surface plots for physicochemical properties

A.1 Density

This subsection presents density surfaces plots applied to temperatures other than those shown in the results and discussion section of chapter 2. Figures A.1, A.2, A.3 and A.4 presents the density plots for pickling solution bath at 65, 70, 75 and 80 °C, respectively.

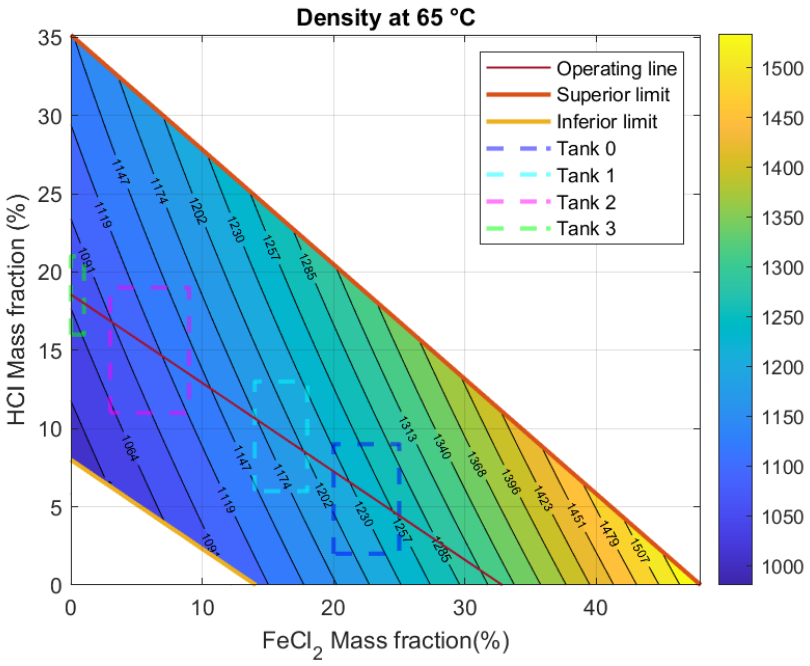

Figure A.1 – Surface plot for density in feasible operational region for HCl pickling solution at 65°C. The operating line it is based on a regenerated pickling solution with 18% of HCl and 1% of $FeCl_2$. Each pickling tank region is represented by rectangles delimited by the concentration ranges.

A.2 Vapor pressure

This subsection presents vapor pressure surface plots applied to temperatures other than those shown in the results and discussion section of chapter 2. Figures A.5, A.6 and A.7 presents the vapor pressure plots for pickling solution bath at 70, 75 and 80 °C, respectively.

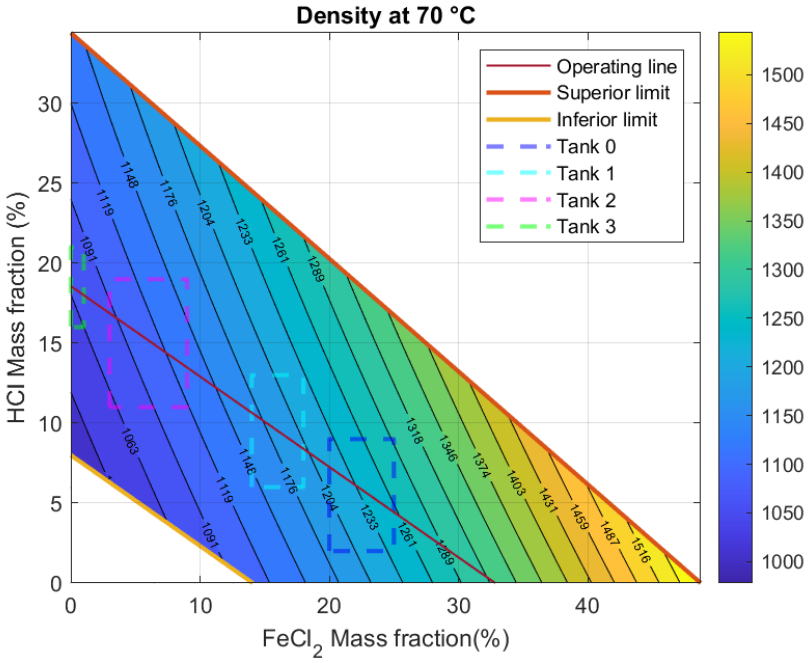

Figure A.2 – Surface plot for density in feasible operational region for HCl pickling solution at 70°C. The operating line it is based on a regenerated pickling solution with 18% of HCl and 1% of $FeCl_2$. Each pickling tank region is represented by rectangles delimited by the concentration ranges.

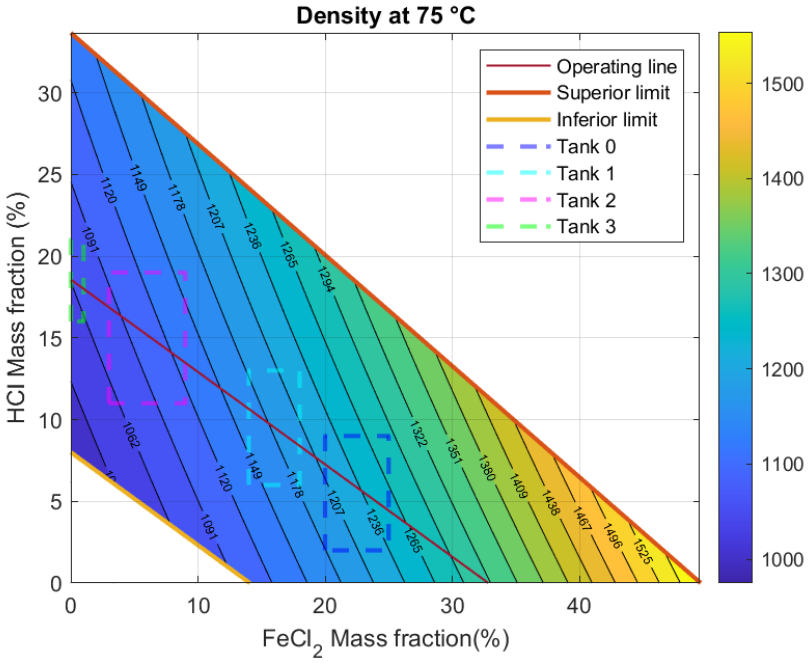

Figure A.3 – Surface plot for density in feasible operational region for HCl pickling solution at 75°C. The operating line it is based on a regenerated pickling solution with 18% of HCl and 1% of $FeCl_2$. Each pickling tank region is represented by rectangles delimited by the concentration ranges.

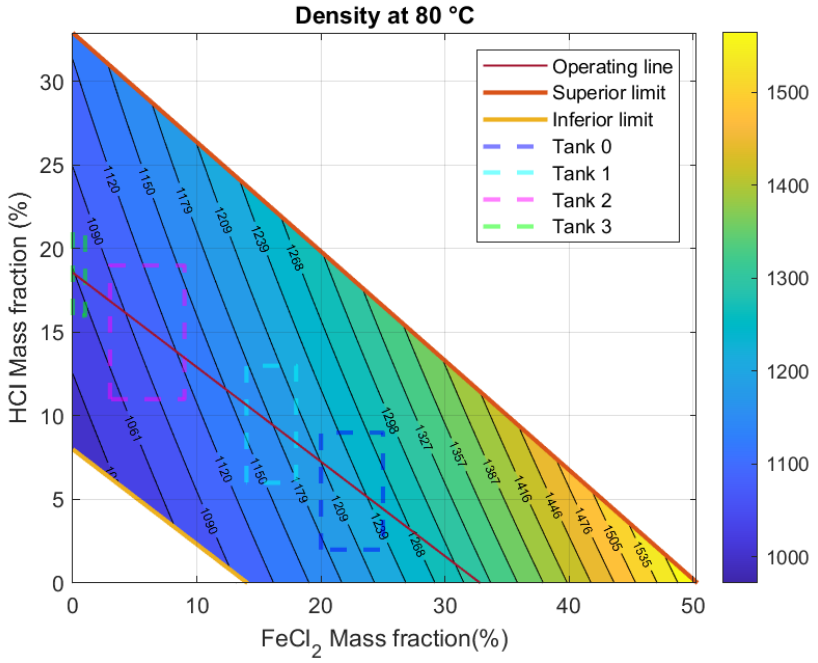

Figure A.4 – Surface plot for density in feasible operational region for HCl pickling solution at 80°C. The operating line it is based on a regenerated pickling solution with 18% of HCl and 1% of $FeCl_2$. Each pickling tank region is represented by rectangles delimited by the concentration ranges.

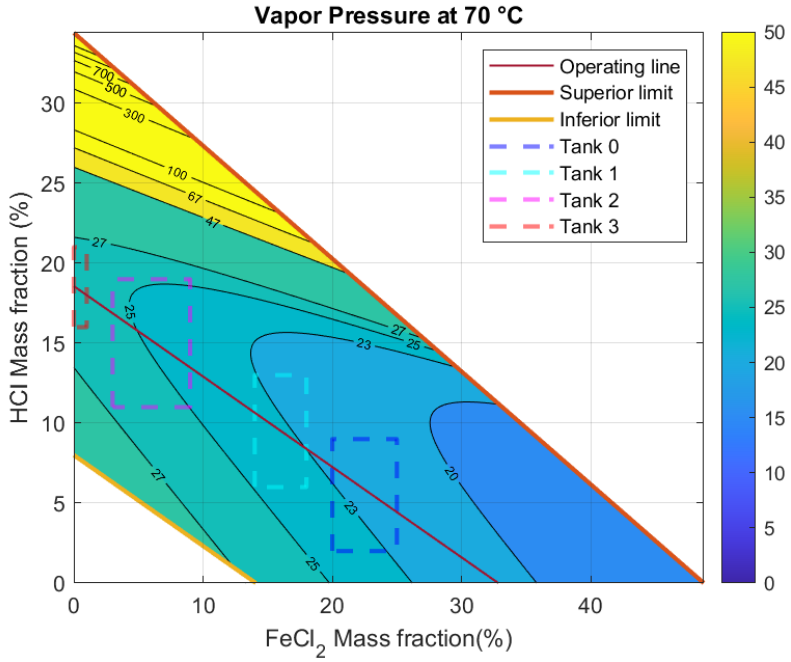

Figure A.5 – Surface plot for vapor pressure in feasible operational region for HCl pickling solution at 70°C. The operating line it is based on a regenerated pickling solution with 18% of HCl and 1% of $FeCl_2$. Each pickling tank region is represented by rectangles delimited by the concentration ranges.

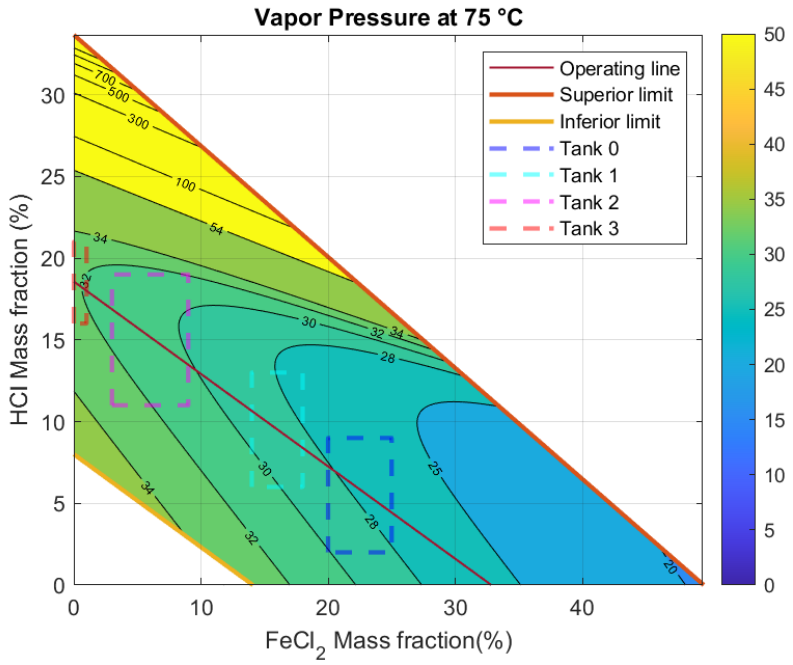

Figure A.6 – Surface plot for vapor pressure in feasible operational region for HCl pickling solution at 75°C. The operating line it is based on a regenerated pickling solution with 18% of HCl and 1% of $FeCl_2$. Each pickling tank region is represented by rectangles delimited by the concentration ranges.

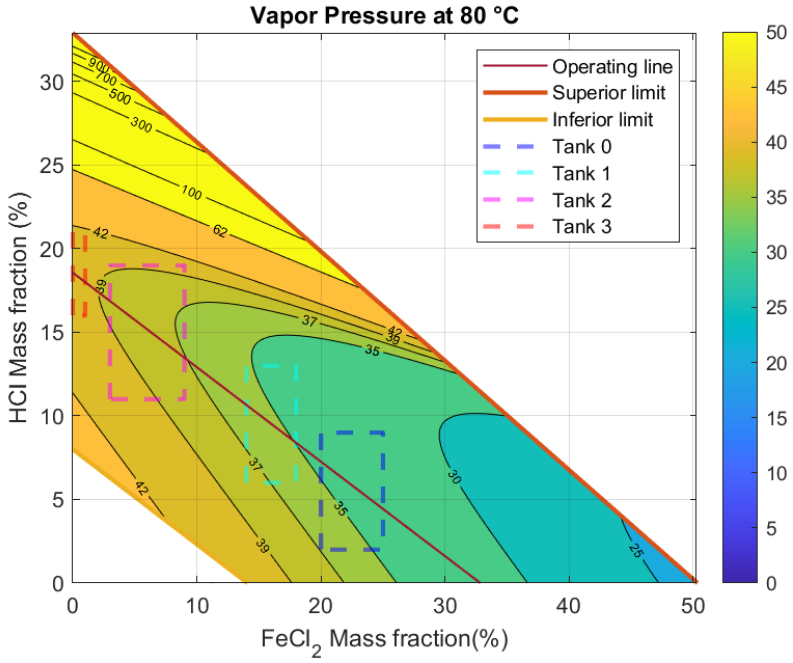

Figure A.7 – Surface plot for vapor pressure in feasible operational region for HCl pickling solution at 80°C. The operating line it is based on a regenerated pickling solution with 18% of HCl and 1% of $FeCl_2$. Each pickling tank region is represented by rectangles delimited by the concentration ranges.

A.3 Heat of vaporization

This subsection presents evaporation heat surfaces plots applied to temperatures other than those shown in the results and discussion section of chapter 2. Figures A.8, A.9, A.10 and A.11 presents the evaporation heat plots for pickling solution bath at 65, 70, 75 and 80 °C, respectively.

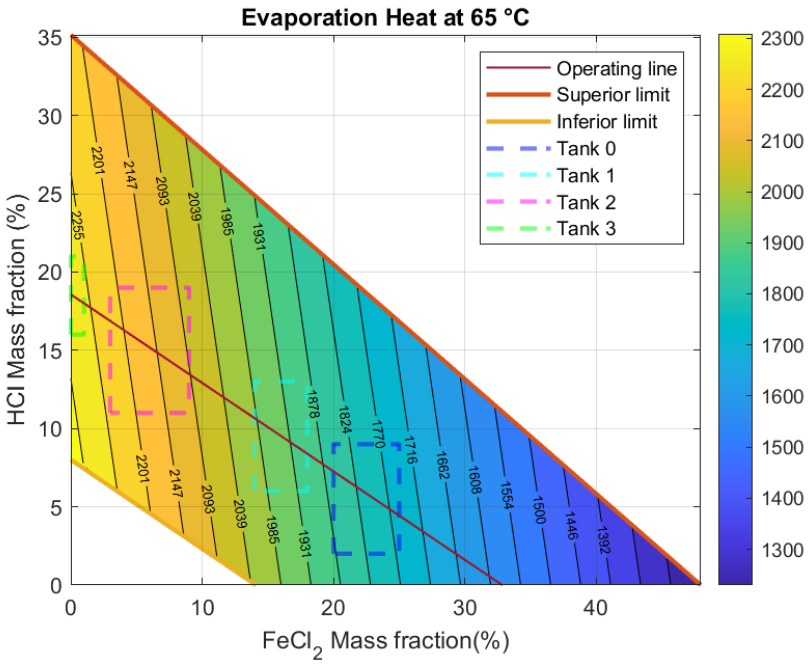

Figure A.8 – Surface plot for evaporation heat in feasible operational region for HCl pickling solution at 65°C. The operating line it is based on a regenerated pickling solution with 18% of HCl and 1% of $FeCl_2$. Each pickling tank region is represented by rectangles delimited by the concentration ranges.

A.4 Specific heat capacity

This subsection presents specific heat capacity surfaces plots applied to temperatures other than those shown in the results and discussion section of chapter 2. Figures A.12, A.13, A.14 and A.15 presents the specific heat plots for pickling solution bath at 65, 70, 75 and 80 °C, respectively.

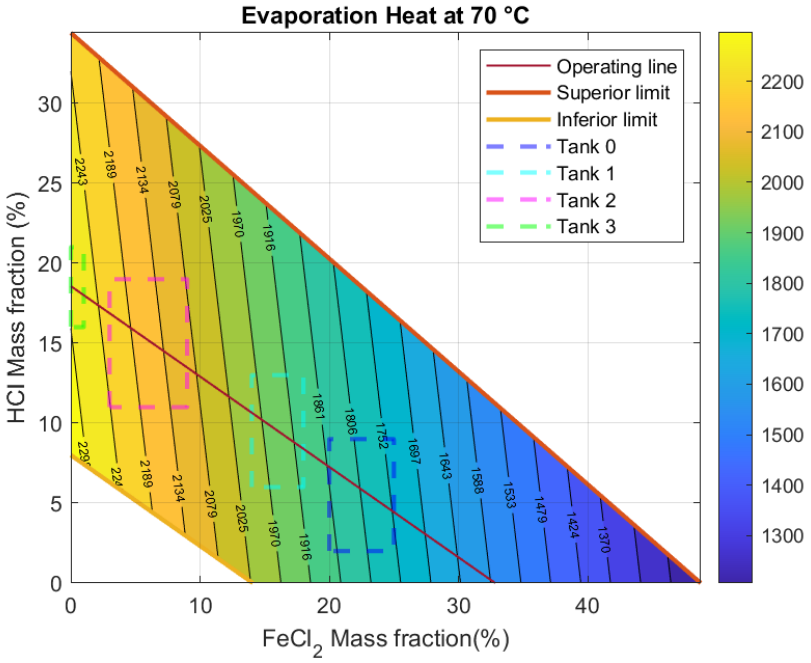

Figure A.9 – Surface plot for evaporation heat in feasible operational region for HCl pickling solution at 70°C. The operating line it is based on a regenerated pickling solution with 18% of HCl and 1% of $FeCl_2$. Each pickling tank region is represented by rectangles delimited by the concentration ranges.

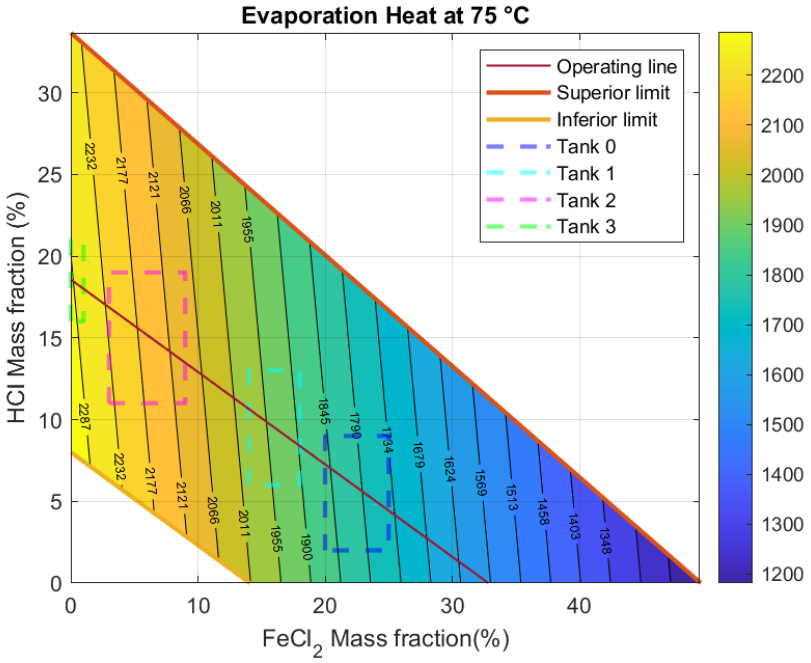

Figure A.10 – Surface plot for evaporation heat in feasible operational region for HCl pickling solution at 75°C. The operating line it is based on a regenerated pickling solution with 18% of HCl and 1% of $FeCl_2$. Each pickling tank region is represented by rectangles delimited by the concentration ranges.

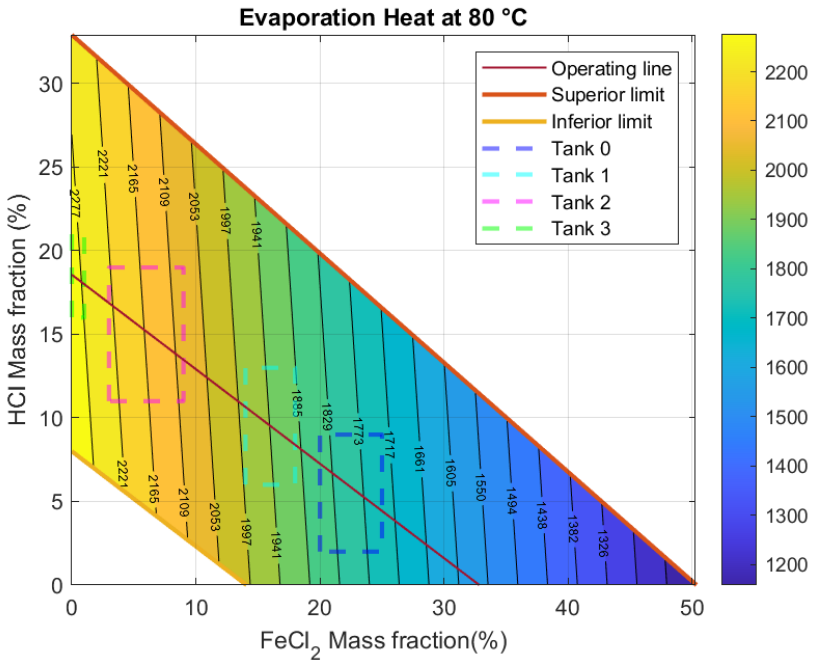

Figure A.11 – Surface plot for evaporation heat in feasible operational region for HCl pickling solution at 80°C. The operating line it is based on a regenerated pickling solution with 18% of HCl and 1% of $FeCl_2$. Each pickling tank region is represented by rectangles delimited by the concentration ranges.

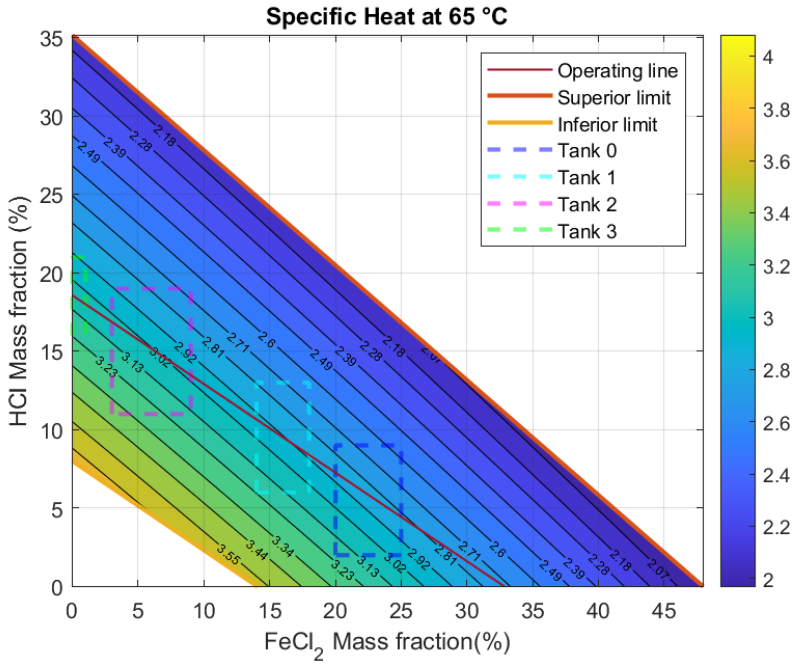

Figure A.12 – Surface plot for specific heat in feasible operational region for HCl pickling solution at 65°C. The operating line it is based on a regenerated pickling solution with 18% of HCl and 1% of $FeCl_2$. Each pickling tank region is represented by rectangles delimited by the concentration ranges.

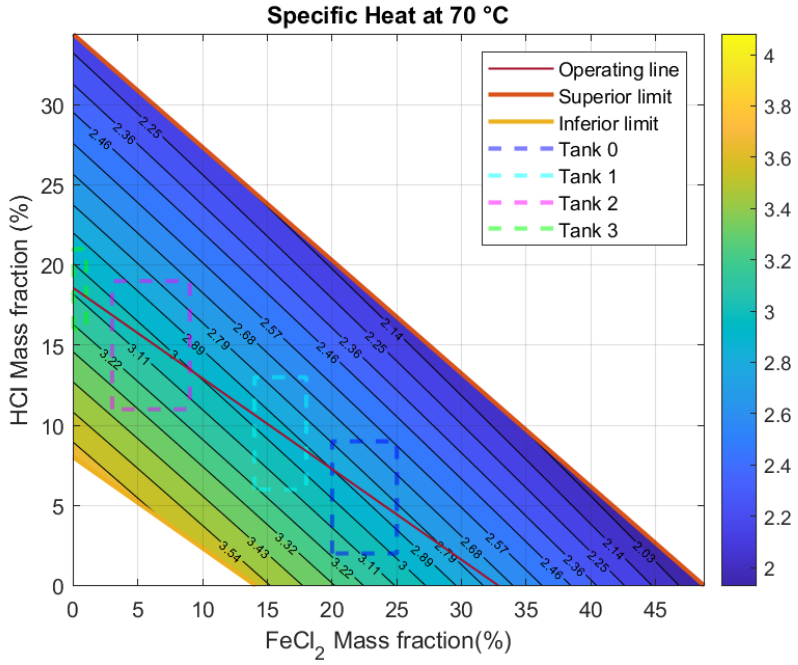

Figure A.13 – Surface plot for specific heat in feasible operational region for HCl pickling solution at 70°C. The operating line it is based on a regenerated pickling solution with 18% of HCl and 1% of $FeCl_2$. Each pickling tank region is represented by rectangles delimited by the concentration ranges.

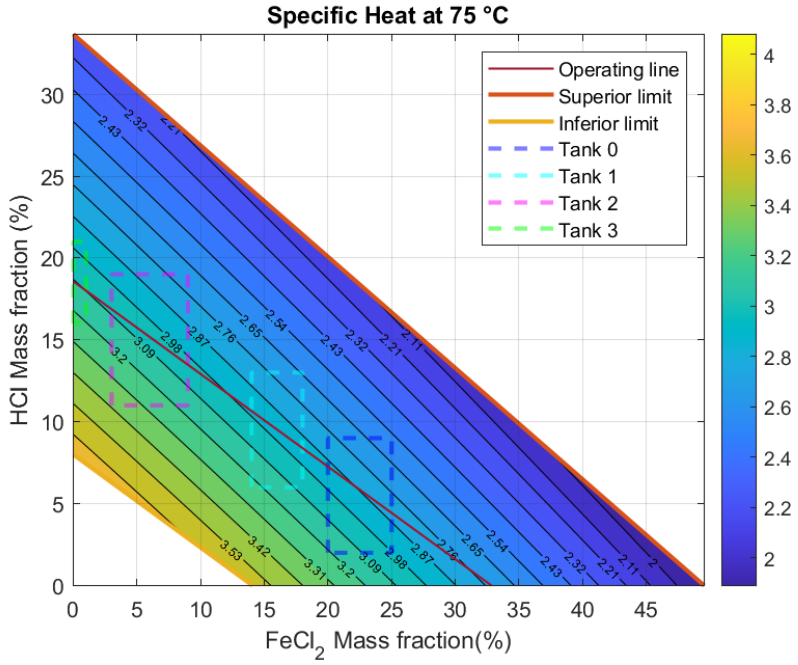

Figure A.14 – Surface plot for specific heat in feasible operational region for HCl pickling solution at 75°C. The operating line it is based on a regenerated pickling solution with 18% of HCl and 1% of $FeCl_2$. Each pickling tank region is represented by rectangles delimited by the concentration ranges.

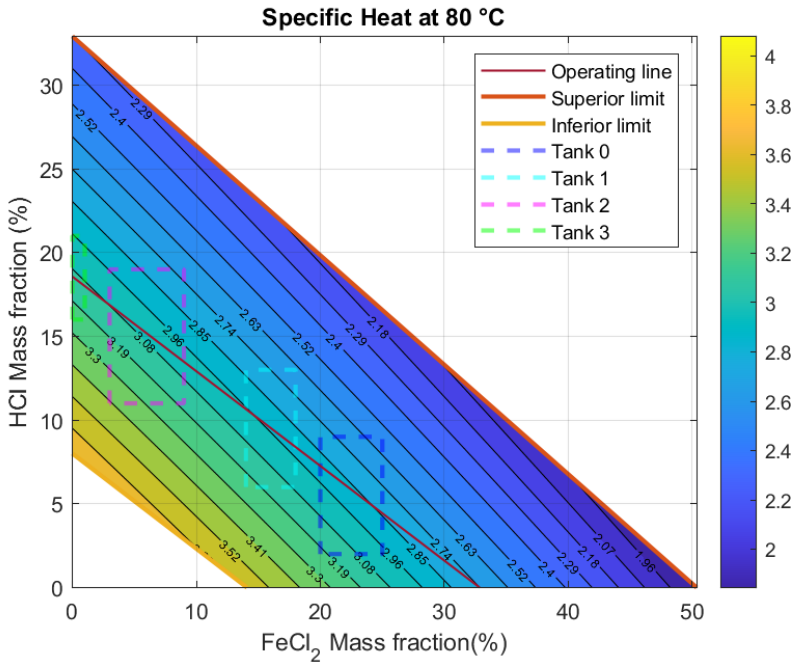

Figure A.15 – Surface plot for specific heat in feasible operational region for HCl pickling solution at 80°C. The operating line it is based on a regenerated pickling solution with 18% of HCl and 1% of $FeCl_2$. Each pickling tank region is represented by rectangles delimited by the concentration ranges.

A.5 Viscosity

This subsection presents dynamic viscosity surfaces plots applied to temperatures other than those shown in the results and discussion section of chapter 2. Figures A.16, A.17 and A.18 presents the viscosity plots for pickling solution bath at 70, 75 and 80 °C, respectively.

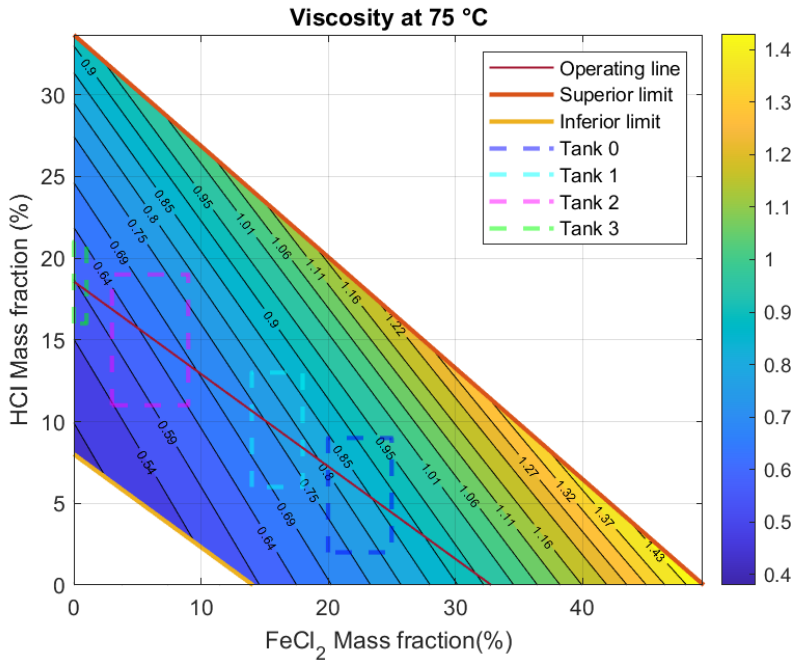

Figure A.17 – Surface plot for dynamic viscosity in feasible operational region for HCl pickling solution at 75°C. The operating line it is based on a regenerated pickling solution with 18% of HCl and 1% of $FeCl_2$. Each pickling tank region is represented by rectangles delimited by the concentration ranges.

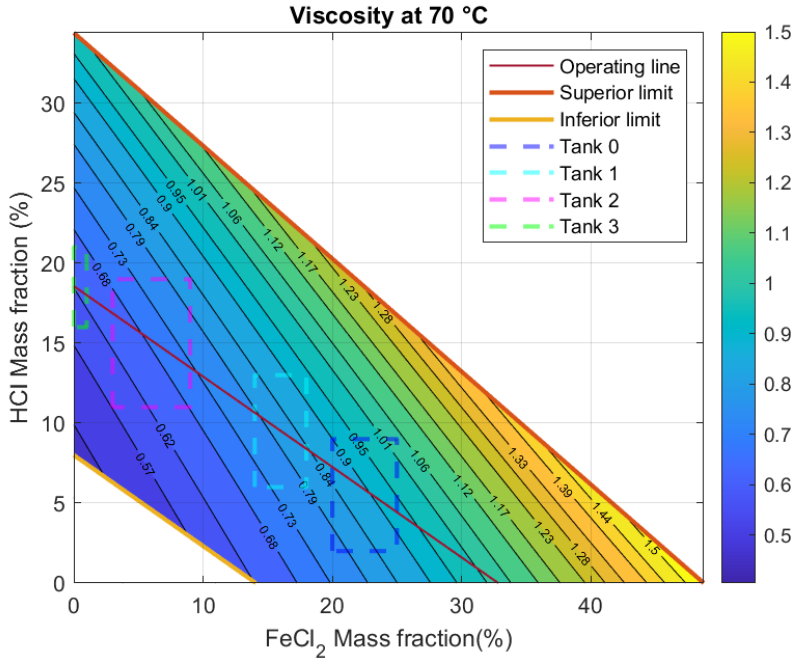

Figure A.16 – Surface plot for dynamic viscosity in feasible operational region for HCl pickling solution at 70°C. The operating line it is based on a regenerated pickling solution with 18% of HCl and 1% of $FeCl_2$. Each pickling tank region is represented by rectangles delimited by the concentration ranges.

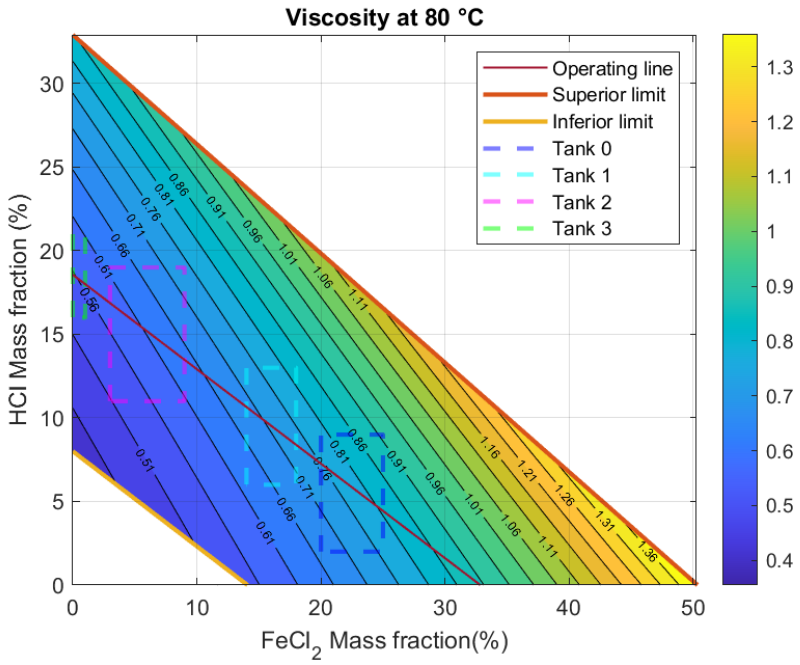

Figure A.18 – Surface plot for dynamic viscosity in feasible operational region for HCl pickling solution at 80°C. The operating line it is based on a regenerated pickling solution with 18% of HCl and 1% of $FeCl_2$. Each pickling tank region is represented by rectangles delimited by the concentration ranges.

A.6 Thermal conductivity

This subsection presents thermal conductivity surfaces plots applied to temperatures other than those shown in the results and discussion section of chapter 2. Figures A.19, A.20, A.21 and A.22 presents the evaporation heat plots for pickling solution bath at 65, 70, 75 and 80 °C, respectively.

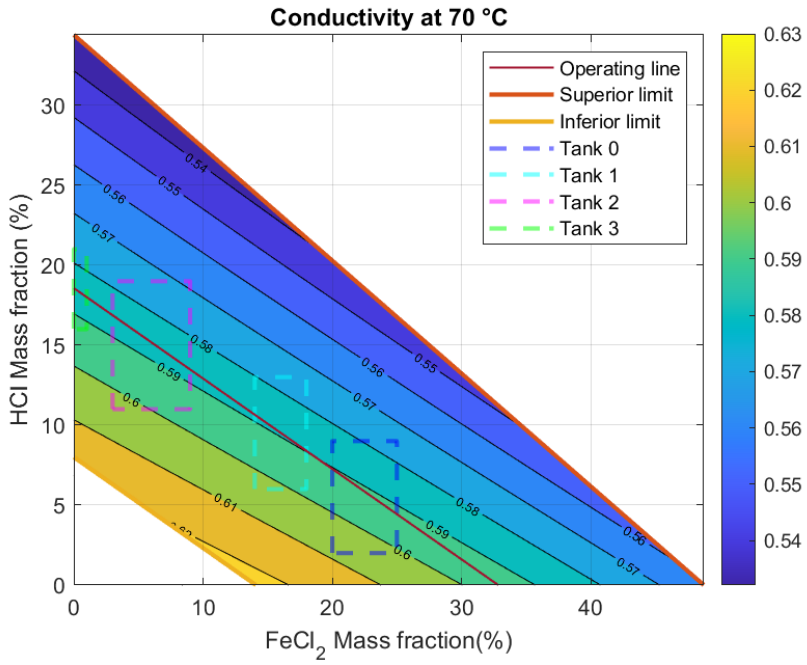

Figure A.20 – Surface plot for thermal conductivity in feasible operational region for HCl pickling solution at 70°C. The operating line it is based on a regenerated pickling solution with 18% of HCl and 1% of $FeCl_2$. Each pickling tank region is represented by rectangles delimited by the concentration ranges.

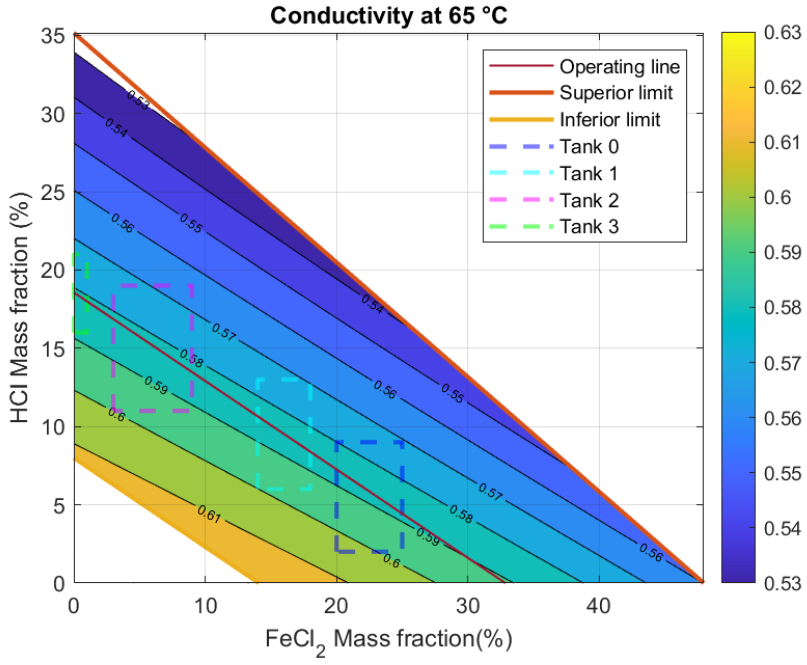

Figure A.19 – Surface plot for thermal conductivity in feasible operational region for HCl pickling solution at 65°C. The operating line it is based on a regenerated pickling solution with 18% of HCl and 1% of $FeCl_2$. Each pickling tank region is represented by rectangles delimited by the concentration ranges.

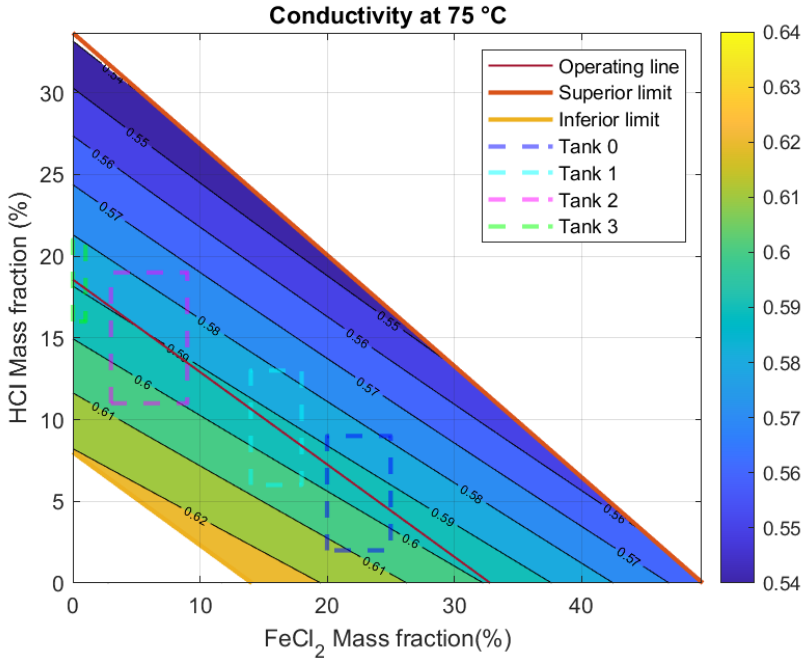

Figure A.21 – Surface plot for thermal conductivity in feasible operational region for HCl pickling solution at 75°C. The operating line it is based on a regenerated pickling solution with 18% of HCl and 1% of $FeCl_2$. Each pickling tank region is represented by rectangles delimited by the concentration ranges.

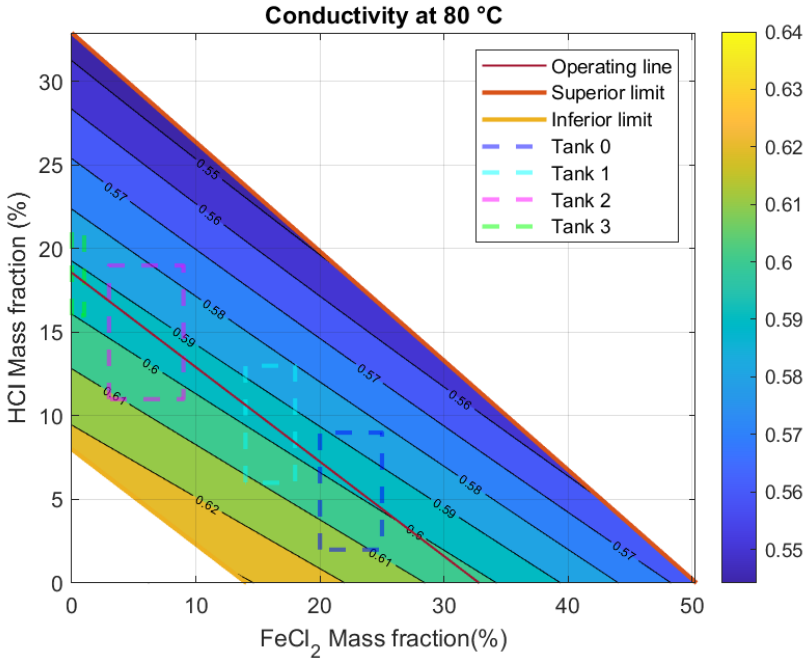

Figure A.22 – Surface plot for thermal conductivity in feasible operational region for HCl pickling solution at 80°C. The operating line it is based on a regenerated pickling solution with 18% of HCl and 1% of $FeCl_2$. Each pickling tank region is represented by rectangles delimited by the concentration ranges.

A.7 HCl diffusion coefficient

This subsection presents HCl diffusion coefficient surfaces plots applied to temperatures other than those shown in the results and discussion section of chapter 2. Figures A.23, A.24, A.25 and A.26 presents the diffusion coefficient plots for pickling solution bath at 65, 70, 75 and 80 °C, respectively.

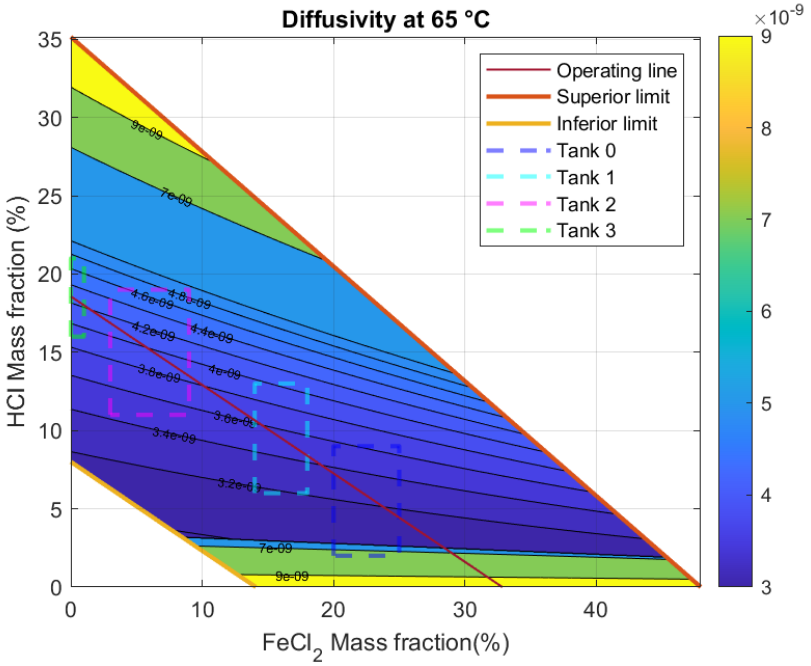

Figure A.23 – Surface plot for diffusion coefficient in feasible operational region for HCl pickling solution at 65°C. The operating line it is based on a regenerated pickling solution with 18% of HCl and 1% of $FeCl_2$. Each pickling tank region is represented by rectangles delimited by the concentration ranges.

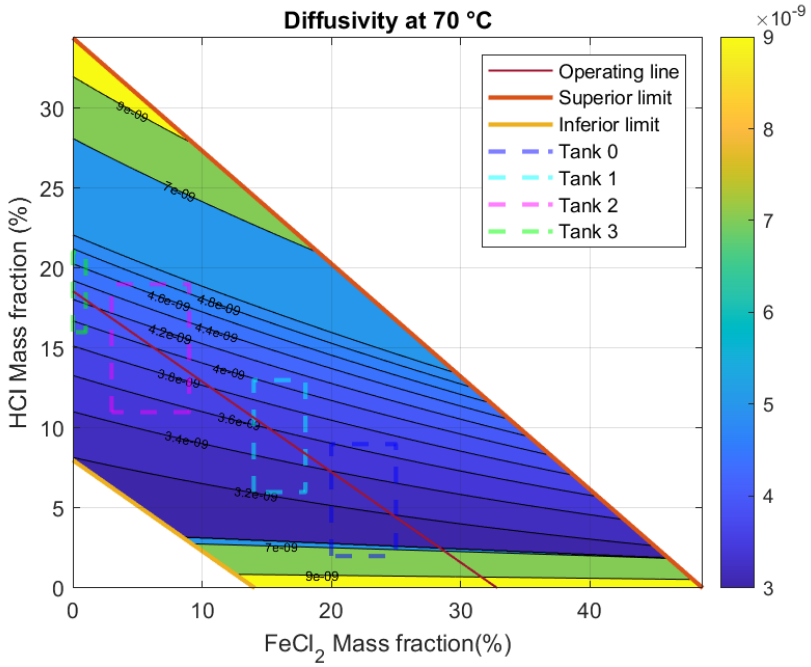

Figure A.24 – Surface plot for diffusion coefficient in feasible operational region for HCl pickling solution at 70°C. The operating line it is based on a regenerated pickling solution with 18% of HCl and 1% of $FeCl_2$. Each pickling tank region is represented by rectangles delimited by the concentration ranges.

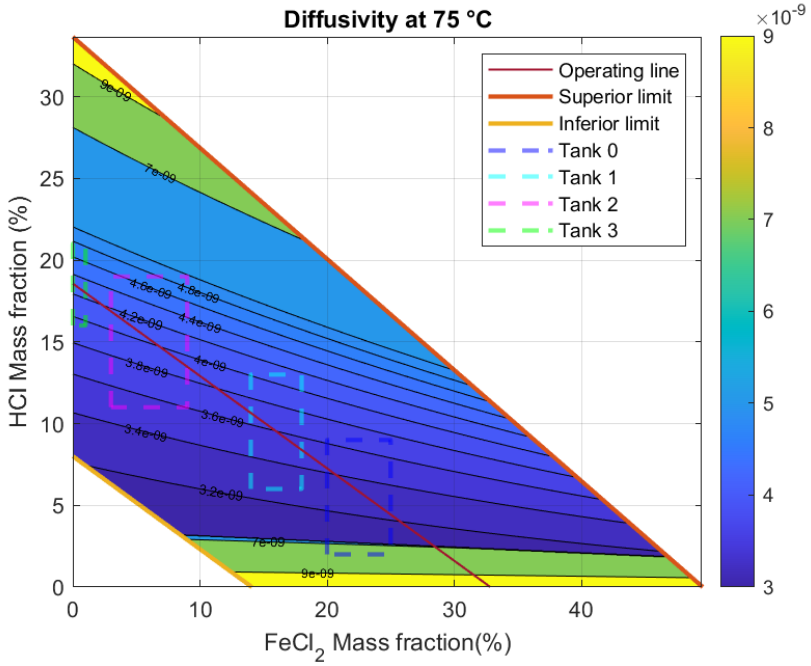

Figure A.25 – Surface plot for diffusion coefficient in feasible operational region for HCl pickling solution at 75°C. The operating line it is based on a regenerated pickling solution with 18% of HCl and 1% of $FeCl_2$. Each pickling tank region is represented by rectangles delimited by the concentration ranges.

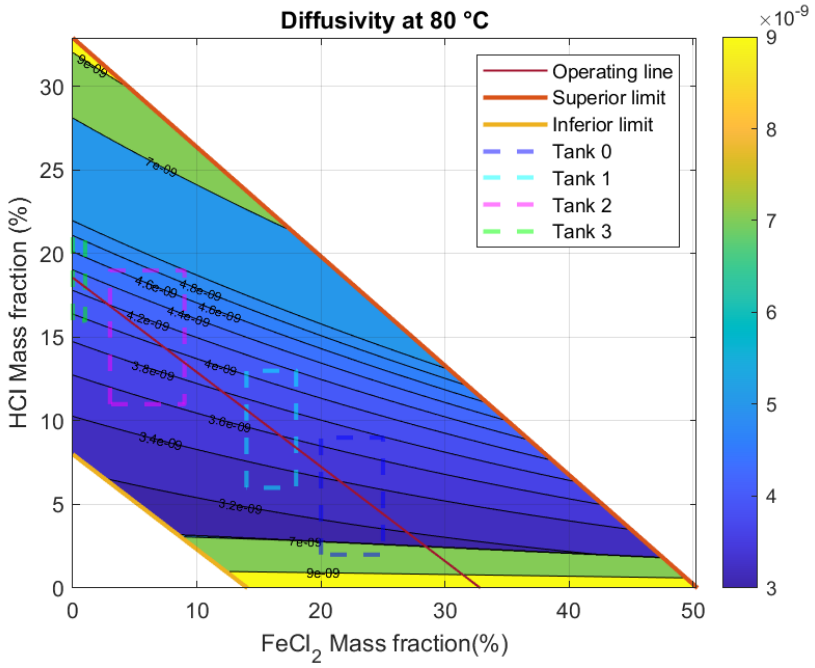

Figure A.26 – Surface plot for diffusion coefficient in feasible operational region for HCl pickling solution at 80°C. The operating line it is based on a regenerated pickling solution with 18% of HCl and 1% of $FeCl_2$. Each pickling tank region is represented by rectangles delimited by the concentration ranges.

APPENDIX B – Calculations example: density case

B.1 Concentration effect - MV

Table 27 presents the average density for each temperature and tank concentration range.

Table 27 – Average density values for each tank at different temperatures. The columns refer to the tank average mass fraction of $FeCl_2$, and the rows to temperature.

	$\overline{x}_0 = 0.225$	$\overline{x}_1 = 0.16$	$\overline{x}_2 = 0.06$	$\overline{x}_3 = 0.005$
$T_1 = 65$	1238	1188	1111	1073
$T_2 = 70$	1235	1185	1108	1070
$T_3 = 75$	1231	1181	1105	1067
$T_4 = 80$	1227	1178	1102	1064
$T_5 = 85$	1223	1174	1099	1061

In Table 27, each row represents a temperature and each columns the tank average mass fraction of $FeCl_2$. *e.g.* for Tank 0, the maximum value for $FeCl_2$ mass fraction is 25%, and the minimum 20%, resulting in a average value of 22.5%.

Using the density data from Table 27, the average density ($\overline{\rho}$) value for all 20 points is calculated using equation ((153)):

$$\overline{\rho} = \frac{\Sigma_{n=1}^{n=20} \rho_i}{n} \tag{153}$$

In this case, $\overline{\rho}$ equals to 1146 kg·m^{-3}. A table is then created to evaluate the density derivative with respect to $FeCl_2$ concentration.

Table 28 – Parameters of the concentration indicators (MV) referring to the derivative of the density in relation to the concentration of $FeCl_2$.

	$\Delta x_0 = (0.225 - 0.16)$	$\Delta x_1 = (0.16 - 0.06)$	$\Delta x_2 = (0.06 - 0.005)$
$T_1 = 65$	$MV_{1,0}$	$MV_{1,1}$	$MV_{1,2}$
$T_2 = 70$	$MV_{2,0}$	$MV_{2,1}$	$MV_{2,2}$
$T_3 = 75$	$MV_{3,0}$	$MV_{3,1}$	$MV_{3,2}$
$T_4 = 80$	$MV_{4,0}$	$MV_{4,1}$	$MV_{4,2}$
$T_5 = 85$	$MV_{5,0}$	$MV_{5,1}$	$MV_{5,2}$

Table 28, presents the values for the ratio between property variation and concentration variation for each temperature and adjacent tanks in 27, according to the equations below.

Table 29 – Results of MV values for the density case.

	$\Delta x_0 = (0.225 - 0.16)$	$\Delta x_1 = (0.16 - 0.06)$	$\Delta x_2 = (0.06 - 0.005)$
$T_1 = 65$	761	772	705
$T_2 = 70$	766	765	699
$T_3 = 75$	764	762	691
$T_4 = 80$	756	760	688
$T_5 = 85$	753	755	680

$$
\begin{aligned}
MV_{1,0} &= \frac{1238 - 1188}{0.225 - 0.16} = 761 \\
MV_{1,1} &= \frac{1188 - 1111}{0.16 - 0.06} = 772 \\
MV_{1,2} &= \frac{1111 - 1073}{0.06 - 0.005} = 705 \\
&\vdots \\
MV_{5,0} &= \frac{1223 - 1178}{0.225 - 0.16} = 753 \\
MV_{5,1} &= \frac{1178 - 1099}{0.16 - 0.06} = 755 \\
MV_{5,2} &= \frac{1099 - 1061}{0.06 - 0.005} = 680
\end{aligned}
\tag{154}
$$

The resulting matrix is presented in Table 29.

The Material Variation mean ($\overline{MV}$) is calculated as:

$$
\overline{MV} = \frac{\Sigma_{n=1}^{n=15} MV_i}{n} \tag{155}
$$

The resulting Material Variation mean $\overline{MV}$ value is 739. The Material Variation indicator is calculated multiplying $\overline{MV}$ by the concentration range of the system over the property overall average:

$$
MV = \frac{739 \cdot (0.25 - 0)}{1146} = 0.161 \quad \text{or} \quad 16\%. \tag{156}
$$

Note that MV depends on the minimum and maximum $FeCl_2$ mass fraction. The idea is to analyse the salt concentration influence on the property across the tanks.

B.2 Temperature effect (TV)

The temperature influence is calculated in the same manner as the concentration influence, but varying temperature, as shown in Table 30.

Table 30 presents the values for the ratio between property variation and temperature variation for each tank in Table 27, according to the equations below.

Table 30 – Parameters of the temperature indicators (TV) referring to the derivative of the density in relation to the temperature.

	$\overline{x}_0 = 0.225$	$\overline{x}_1 = 0.16$	$\overline{x}_2 = 0.06$	$\overline{x}_3 = 0.005$
$\Delta T_1 = (65-70)$	$TV_{1,0}$	$TV_{1,1}$	$TV_{1,2}$	$TV_{1,3}$
$\Delta T_2 = (70-75)$	$TV_{2,0}$	$TV_{2,1}$	$TV_{2,2}$	$TV_{2,3}$
$\Delta T_3 = (75-80)$	$TV_{3,0}$	$TV_{3,1}$	$TV_{3,2}$	$TV_{3,3}$
$\Delta T_4 = (80-85)$	$TV_{4,0}$	$TV_{4,1}$	$TV_{4,2}$	$TV_{4,3}$

Table 31 – Results of TV values for the case of density.

	$\overline{x}_0 = 0.225$	$\overline{x}_1 = 0.16$	$\overline{x}_2 = 0.06$	$\overline{x}_3 = 0.005$
$\Delta T_1 = (65-70)$	-0.7	-0.7	-0.6	-0.5
$\Delta T_2 = (70-75)$	-0.7	-0.7	-0.6	-0.5
$\Delta T_3 = (75-80)$	-0.8	-0.7	-0.6	-0.6
$\Delta T_4 = (80-85)$	-0.8	-0.7	-0.6	-0.6

$$
\begin{aligned}
TV_{1,0} &= \frac{1238-1235}{65-70} = -0.7 \\
TV_{2,0} &= \frac{1235-1231}{70-75} = -0.7 \\
TV_{3,0} &= \frac{1231-1227}{75-80} = -0.8 \\
TV_{4,0} &= \frac{1227-1223}{80-85} = -0.8 \\
&\vdots \\
TV_{1,3} &= \frac{1073-1070}{65-70} = -0.5 \\
TV_{2,3} &= \frac{1070-1067}{70-75} = -0.5 \\
TV_{3,3} &= \frac{1067-1064}{75-80} = -0.6 \\
TV_{4,3} &= \frac{1064-1061}{80-85} = -0.6
\end{aligned}
\tag{157}
$$

The resulting matrix is presented in Table 31.

The Temperature Variation mean ($\overline{TV}$) is calculated using:

$$
\overline{TV} = \frac{\Sigma_{n=1}^{n=16} MV_i}{n} \tag{158}
$$

The resulting $\overline{TV}$ value is -0.7. The Temperature Variation indicator is calculated multiplying $\overline{TV}$ by the temperature range of the system over the property overall average:

$$TV = \frac{-0.7 \cdot (65 - 85)}{1146} = 0.012 \quad \text{or} \quad 1.2\%. \tag{159}$$

Note that TV depends on the minimum and maximum temperature. The idea is to assess the temperature influence on property.

APPENDIX C – Numerical equations

This appendix present the details of each mass and energy balance equations utilized in the Reactor Modelling system. Including the solid and fluid phase balances. Below each PDE is provided using the finite difference discretization utilizing the Forward Time-Centered Space (FTCS) method.

1. **Solid phase mass balance:**

$$X_{[t,i]} = \Delta\tau[Da.exp(-\frac{Arr}{\theta_{s,[t-1,i]}}).\psi^{m}_{[t-1,i]}.(1-X_{[t-1,i]}) + \frac{X_{[t-1,i]} - X_{[t-1,i-1]}}{\Delta\zeta} + \frac{X_{[t-1,i]}}{\Delta\tau}] \quad (160)$$

$$\text{I.C.:} \quad X_{[0,i]} = X_i \quad (161)$$

$$\text{B.C.:} \quad X_{[t,0]} = X_0 \quad (162)$$

2. **Solid phase energy balance:**

$$\begin{aligned}\theta_{s,[t,i]} = \Delta\tau \Bigg[& Da \cdot Da_T \cdot \gamma \cdot s \cdot exp\left(-\frac{Arr}{\theta_{s,[t-1,i]}} \right) \cdot \psi^{m}_{[t-1,i]} \cdot (1 - X_{[t-1,i]}) + \\ & -St \cdot \gamma \cdot \varphi \cdot (\theta_{s,[t-1,i]} - \Gamma\theta_{[t-1,i]}) - \frac{\theta_{s,[t-1,i]} - \theta_{s,[t-1,i-1]}}{\Delta\zeta} + \frac{\theta_{s,[t-1,i]}}{\Delta\tau} \Bigg]\end{aligned} \quad (163)$$

$$\text{I.C.:} \quad \theta_{s,[0,i]} = \frac{T_{si}}{T_{s0}} \quad (164)$$

$$\text{B.C.:} \quad \theta_{s,[t,0]} = 1 \quad (165)$$

3. **Liquid phase mass balance:**

$$\begin{aligned}\psi_{[t,i]} = \Delta\tau \Bigg[& - Da \cdot \kappa \cdot \varphi^{-1} \cdot (1 - X_{[t-1,i]}) \cdot exp(-\frac{Arr}{\theta_{s,[t-1,i]}}) \cdot \psi^{m}_{[t-1,i]} + \\ & + \frac{\psi_{[t-1,i]} - \psi_{[t-1,i-1]}}{\Delta\zeta} + \frac{\psi_{[t-1,i]}}{\Delta\tau} + \frac{\psi_{[t-1,i+1]} - 2\psi_{[t-1,i]} + \psi_{[t-1,i-1]}}{Pe \cdot \Delta\zeta^2} \Bigg]\end{aligned} \quad (166)$$

$$\text{I.C.:} \quad \psi_{[0,i]} = \frac{C_{HCl,i}}{C_{HCl,0}} \quad (167)$$

$$\text{B.C.I.:} \quad \psi_{[t,0]} = 1 \quad (168)$$

$$\text{B.C.II.:} \quad \psi_{[t,n]} = \psi_{[t,n-1]} \quad (169)$$

4. **Liquid phase energy balance:**

$$\theta_{[t,i]} = \Delta\tau \Bigg[- St \cdot (\theta_{[t-1,i]} - \frac{1}{\Gamma}\theta_{s,[t-1,i]}) + \frac{\theta_{[t-1,i]} - \theta_{[t-1,i-1]}}{\Delta\zeta} + \\ + \frac{\theta_{[t-1,i]}}{\Delta\tau} + \frac{\theta_{[t-1,i+1]} - 2\theta_{[t-1,i]} + \theta_{[t-1,i-1]}}{Pe_T \cdot \Delta\zeta^2} \Bigg] \tag{170}$$

$$\text{I.C.:} \quad \theta_{[0,i]} = \frac{T_i}{T_0} \tag{171}$$

$$\text{B.C.I.:} \quad \theta_{[t,0]} = 1 \tag{172}$$

$$\text{B.C.II.:} \quad \theta_{[t,n]} = \theta_{[t,n-1]} \tag{173}$$